

THE UNIVERSITY OF MICHIGAN
INDUSTRY PROGRAM OF THE COLLEGE OF ENGINEERING

THE FLOW DUE TO A ROTATING DISC WITH A CENTER SINK

Charles G. Richards

A dissertation submitted in partial fulfillment
of the requirements for the degree of
Doctor of Philosophy in the
University of Michigan
Department of Engineering Mechanics
1964

December, 1964

IP-688

Doctoral Committee:

Associate Professor William P. Graebel, Chairman
Professor Samuel K. Clark
Associate Professor Walter R. Debler
Professor Arthur G. Hansen
Assistant Professor James O. Wilkes

ACKNOWLEDGEMENT

The author wishes to express his gratitude for the assistance and advice of the members of his Doctoral Thesis Committee. A special expression of gratitude is due to Associate Professor William P. Graebel, Chairman of the Committee.

The author is also grateful for the technical assistance given him by Mr. William G. Huizenga and Mr. Milo W. Kaufman.

TABLE OF CONTENTS

		<u>Page</u>
	ACKNOWLEDGEMENT.....	ii
	LIST OF TABLES.....	v
	LIST OF FIGURES.....	vi
CHAPTER		
1	INTRODUCTION.....	1
2	THE DIFFERENTIAL EQUATIONS GOVERNING THE FLOW DUE TO A ROTATING DISC WITH A CENTER SINK.....	5
	2.1 Statement of the Problem.....	5
	2.2 Dimensionless Form.....	12
3	THE FINITE DIFFERENCE FORM OF THE EQUATIONS GOVERN- ING THE PROBLEM OF THE ROTATING DISC WITH A CENTER SINK.....	17
	3.1 Introduction.....	17
	3.2 System of Grid Points.....	19
	3.3 Finite Difference Approximations to the Equa- tions of Motion.....	20
	3.4 Finite Difference Approximations to the Bound- ary Conditions.....	26
	3.5 Stability of the Method.....	29
4	NUMERICAL RESULTS.....	31
	4.1 The Dividing Streamline.....	31
	4.2 Preservation of Circulation.....	33
	4.3 Influence of the Sink at Large Z	34
	4.4 Influence of the Parameter β	38
	4.5 Technique of Solution.....	46
	4.6 The Rotating Disc with a Center Source.....	50
5	EXPERIMENTAL PROGRAM.....	51
	5.1 Apparatus.....	51
	5.2 Procedure.....	52
	5.3 Results.....	54

TABLE OF CONTENTS (CONT'D)

CHAPTER		<u>Page</u>
6	CONCLUSIONS.....	60
7	SUGGESTIONS FOR FUTURE WORK.....	61
APPENDIX A - GRAPHS OF STREAMLINES AND VELOCITY PROFILES.....		63
APPENDIX B - COMPUTER PROGRAMS.....		79
BIBLIOGRAPHY.....		98

LIST OF TABLES

<u>Table</u>		<u>Page</u>
4.1	Comparison of the Computed Values of U with the Quasi-Potential Values of U at the Point $R = 6.0$, $Z = 6.0$	37
4.2	The Location of the Radial Distance R_0 from the Origin of the Point of Intersection of the Dividing Streamline with the Disc.....	43
4.3	Computed Values for α and C for Use in Equation (4.31)	44
4.4	Computed Values for the Coefficients in the Power Series Given in Equation (4.41).....	46

LIST OF FIGURES

<u>Figure</u>		<u>Page</u>
2.1	Plot of w vs. r Across the Axis of Symmetry.....	9
4.1	Pressure Gradient on the Disc as a Function of Radial Position.....	42
4.2	Simplified Flow Diagram for the Computer Program.....	47
5.1	Experimental Apparatus.....	53
5.2	Superposition of the Streamlines (Experimental).....	56
5.3	Photograph of the Streamlines for $\omega = 2.5$ rad/sec and $Q_0 = 5.0$ scfm.....	59
A-1	Streamlines for $\beta = 1.0$	64
A-2	Streamlines for $\beta = 2.0$	65
A-3	Streamlines for $\beta = 3.0$	66
A-4	Streamlines for $\beta = 4.0$	67
A-5	Streamlines for $\beta = 5.0$	68
A-6	Streamlines for $\beta = 6.0$	69
A-7	Streamlines for $\beta = 7.0$	70
A-8	Streamlines for $\beta = 12.0$	71
A-9	Tangential Velocities (V) for $\beta = 3.0$	72
A-10	Vertical Velocities (W) for $\beta = 3.0$	73
A-11	Radial Velocities (U) for $\beta = 3.0$	74
A-12	Axial Velocity (W) Profiles for Various Values of β at $Z = 7.2$	75
A-13	Axial Velocity (W) Profiles for Various Values of β at $Z = 3.0$	76
A-14	Radial Velocity (U) Profiles for Various Values of β at $R = 0.6$	77
A-15	Streamlines for $\beta = - 2.0$	78

CHAPTER 1

INTRODUCTION

A number of studies dealing with rotational motion have been conducted in the field of fluid mechanics. In many of these studies, the flow outside of the boundary layer had circulation. Taylor⁽¹³⁾ considered the problem of a liquid tangentially entering a chamber a distance R_1 from the center of rotation and emerging through an orifice of radius R_2 ($R_1 \gg R_2$) after passing down a converging cone with vertex angle 2α . Rosenblat⁽⁹⁾ investigated the viscous flow between two parallel infinite discs which were torsionally oscillating. Stewartson⁽¹¹⁾ studied the effect on a viscous fluid between infinite parallel discs rotating steadily with the same speeds in opposite directions. Stewartson⁽¹²⁾ also studied the flow between two parallel coaxial discs rotating almost as if solid as well as the flow inside a circular cylinder which is almost rotating like a solid body. Long⁽⁷⁾ worked on the problem of a vortex in an infinite viscous fluid and obtained both numerical and experimental results. Earlier, Long⁽⁸⁾ had obtained the solution for the flow of a rotating, frictionless, incompressible fluid due to a strong source or sink at the axis of rotation. The experimental and analytical results which he obtained were for a tall cylinder. Boewadt⁽⁴⁾ handled the problem for the flow of a viscous fluid in solid body rotation over a stationary flat disc. Barua⁽¹⁾ studied the case of a source in a fluid which is rotating with solid body rotation.

The second type of problem dealing with rotational motion, for which there is no circulation outside of the boundary layer, is illustrated by the problem of a rotating disc in an infinite fluid which was solved by von Kármán⁽¹⁴⁾ and Cochran.⁽⁵⁾ In von Kármán's work, which appears to be the most closely related to the present work, it was assumed that the radial and tangential velocities near the disc were linearly proportional to the radial distance from the axis of symmetry and that the axial velocity and the pressure were functions of the vertical distance above the disc. Making this similarity transformation, von Kármán was able to reduce the set of partial differential equations governing the flow to a set of four coupled ordinary differential equations with the dimensionless vertical coordinate as the independent variable.

The Navier-Stokes equations for axially symmetric flow, which arise for the present case of the rotating disc with a center sink, rarely can be solved analytically in closed form. For this reason, the partial differential equations governing this flow in the present work have been solved using finite-difference methods. A very impressive demonstration of the power of finite-difference techniques has been given by Fromm in various publications (Physics of Fluids, IASL Reports) and at various meetings. At the July, 1964, International Union of Theoretical and Applied Mechanics Symposium on Concentrated Vortex Motions in Fluids held in Ann Arbor, Fromm showed motion pictures of the development of the Kármán vortex street as predicted by his numerical results and as photographed experimentally.

The agreement was generally excellent, except far downstream where the computer results began to break down after long periods of time. This was due to the fact that he made the computation assuming a series of cylinders which were spaced far apart upstream and downstream from the cylinder under consideration and waves from the cylinder downstream finally arrived at the downstream boundary of the region under consideration. At first, one was able to observe the symmetrical pair of eddies form behind the cylinder. Then after the application of a small disturbance (to accelerate the formation of the vortex street and thus save machine time) to the vortex field, the wake lost its symmetry, and the vortex street was formed. Grid space size naturally precluded any fine structure details, but large scale agreement for the time duration was remarkably good.

The present work, in which the flow is due to a disc rotating in an infinite fluid with a sink at the center of the disc, differs from previous efforts in that in previous work if a sink was present, the fluid far away was in solid body rotation, or if the fluid was not rotating far away from the solid surface considered, there was not a sink. For the present work, the computation was carried out on the IBM 7090 at The University of Michigan. In addition to the steady state solutions, the transient solutions were also obtained for various values of a parameter $\beta (= \frac{Q_0}{2\pi} \sqrt{\omega/\nu^3})$ relating sink, rotational, and viscous forces. An experimental program was carried out in conjunction with the computer study in the hope of obtaining experimental evidence to support the numerical results. Unfortunately,

the experimental flow regime did not coincide with the flow regime studied numerically. This was due to the fact that the experimental value of β had to be sufficiently large so that the effects of the sink could be observed, while the value of β for the numerical study had to be sufficiently small so as to not require excess computer time. However, the extrapolated experimental results appear to support the computational results, as is discussed in Section 5.3.

CHAPTER 2

THE DIFFERENTIAL EQUATIONS GOVERNING THE FLOW DUE TO A ROTATING DISC WITH A CENTER SINK

2.1 Statement of the Problem

The formulation of the problem is as follows - An infinite disc is assumed to be rotating at a constant speed in an infinite fluid. The conditions are taken to be the solution as given by von Kármán for the rotating disc without the sink. The sink is suddenly "turned on", and the resulting flow studied. It is natural to assume axial symmetry about the axis of rotation of the disc, so one chooses a cylindrical coordinate system (r, θ, z) in the usual manner with the origin at the center of the disc and the z -axis coincident with the axis of rotation.

The Navier-Stokes equations in cylindrical coordinates for unsteady axi-symmetric flow are

$$\frac{\partial u}{\partial t} + u \frac{\partial u}{\partial r} + w \frac{\partial u}{\partial z} - \frac{v^2}{r} = - \frac{1}{\rho} \frac{\partial p}{\partial r} + \nu \left[\frac{\partial^2 u}{\partial r^2} + \frac{\partial^2 u}{\partial z^2} + \frac{1}{r} \frac{\partial u}{\partial r} - \frac{u}{r^2} \right] \quad (2.1a)$$

$$\frac{\partial v}{\partial t} + u \frac{\partial v}{\partial r} + w \frac{\partial v}{\partial z} + \frac{uv}{r} = \nu \left[\frac{\partial^2 v}{\partial r^2} + \frac{\partial^2 v}{\partial z^2} + \frac{1}{r} \frac{\partial v}{\partial r} - \frac{v}{r^2} \right] \quad (2.1b)$$

$$\frac{\partial w}{\partial t} + u \frac{\partial w}{\partial r} + w \frac{\partial w}{\partial z} = - \frac{1}{\rho} \frac{\partial p}{\partial z} + \nu \left[\frac{\partial^2 w}{\partial r^2} + \frac{\partial^2 w}{\partial z^2} + \frac{1}{r} \frac{\partial w}{\partial r} \right] \quad (2.1c)$$

while the continuity equation is

$$\frac{\partial u}{\partial r} + \frac{u}{r} + \frac{\partial w}{\partial z} = 0 \quad (2.2)$$

where u , v , and w are the radial, tangential, and axial components of the velocity, respectively, ρ is the fluid density, ν the kinematic viscosity, and p the pressure of the fluid. Differentiating the first of Equations (2.1) with respect to z and the third with respect to r , subtracting the results and using

$$\eta = \frac{\partial u}{\partial z} - \frac{\partial w}{\partial r} \quad (2.3)$$

one obtains the tangential vorticity equation

$$\frac{\partial \eta}{\partial t} + u \frac{\partial \eta}{\partial r} + w \frac{\partial \eta}{\partial z} - \frac{u\eta}{r} - \frac{2v}{r} \frac{\partial v}{\partial z} = \nu \left[\frac{\partial^2 \eta}{\partial r^2} + \frac{\partial^2 \eta}{\partial z^2} + \frac{1}{r} \frac{\partial \eta}{\partial r} - \frac{\eta}{r^2} \right] \quad (2.4)$$

The continuity Equation (2.2) permits an axisymmetric stream function, ψ , to be defined such that

$$u = \frac{1}{r} \frac{\partial \psi}{\partial z} \quad \text{and} \quad w = -\frac{1}{r} \frac{\partial \psi}{\partial r} \quad (2.5)$$

Substituting (2.5) into (2.3) yields

$$\eta = \frac{1}{r} \frac{\partial^2 \psi}{\partial z^2} + \frac{1}{r} \frac{\partial^2 \psi}{\partial r^2} - \frac{1}{r^2} \frac{\partial \psi}{\partial r} \quad (2.6)$$

The system of equations which were used in obtaining the solution is then given by (2.1b), (2.4), (2.5), and (2.6) and repeated here for convenience is

$$\frac{\partial v}{\partial t} + u \frac{\partial v}{\partial r} + w \frac{\partial v}{\partial z} + \frac{uv}{r} = \nu \left[\frac{\partial^2 v}{\partial r^2} + \frac{\partial^2 v}{\partial z^2} + \frac{1}{r} \frac{\partial v}{\partial r} - \frac{v}{r^2} \right] \quad (2.1b)$$

$$\frac{\partial \eta}{\partial t} + u \frac{\partial \eta}{\partial r} + w \frac{\partial \eta}{\partial z} - \frac{u\eta}{r} - \frac{2v}{r} \frac{\partial v}{\partial r} = \nu \left[\frac{\partial^2 \eta}{\partial r^2} + \frac{\partial^2 \eta}{\partial z^2} + \frac{1}{r} \frac{\partial \eta}{\partial r} - \frac{\eta}{r^2} \right] \quad (2.4)$$

$$\eta = \frac{1}{r} \frac{\partial^2 \psi}{\partial z^2} + \frac{1}{r} \frac{\partial^2 \psi}{\partial r^2} - \frac{1}{r^2} \frac{\partial \psi}{\partial r} \quad (2.6)$$

and

$$u = \frac{1}{r} \frac{\partial \psi}{\partial z} \quad ; \quad w = - \frac{1}{r} \frac{\partial \psi}{\partial r} \quad (2.5)$$

The boundary conditions for the problem are the following -
On the disc, the no-slip condition must be satisfied, i.e., the fluid must move with the disc. Hence, on the disc

$$v = r\omega \quad \text{and} \quad u = 0 \quad (2.7)$$

Also, fluid must not penetrate the solid boundary; thus the disc must be a streamline, i.e.,

$$\psi = \text{constant for } z = 0 \quad (2.8)$$

This ensures that

$$\text{at } z = 0 \quad : \quad w = 0 \quad (2.9)$$

Along the axis of symmetry, one requires that the axis be a stream-line since the radial velocity must vanish there. Hence

$$\text{at } r = 0 \quad : \quad \psi = 0 \quad (2.10)$$

Also,

$$\text{at } r = 0 \quad : \quad v = 0 \quad (2.11)$$

Along the axis of symmetry, a minor difficulty is encountered with the velocity definitions in terms of the stream functions. For instance, the second of Equations (2.5) must be taken as

$$w(0,z) = \lim_{r \rightarrow 0} \left[-\frac{1}{r} \frac{\partial \psi}{\partial r} \right] \quad (2.12)$$

Using l'Hospital's rule, (2.12) becomes

$$\text{at } r = 0 \quad : \quad w = -\frac{\partial^2 \psi}{\partial r^2} \quad (2.13)$$

This expression must be used then in computing w on the line $r = 0$.

The vorticity, η , on the axis of symmetry due to (2.7) is given by

$$\text{at } r = 0 \quad : \quad \eta = \lim_{r \rightarrow 0} \left[-\frac{\partial w}{\partial r} \right] \quad (2.14)$$

Now if $\frac{\partial w}{\partial r}$ were not zero at $r = 0$, then the velocity profile would have a cusp at the axis of symmetry. If one were then to transfer

the system to rectangular Cartesian coordinates, $\frac{\partial w}{\partial x}$ would not be

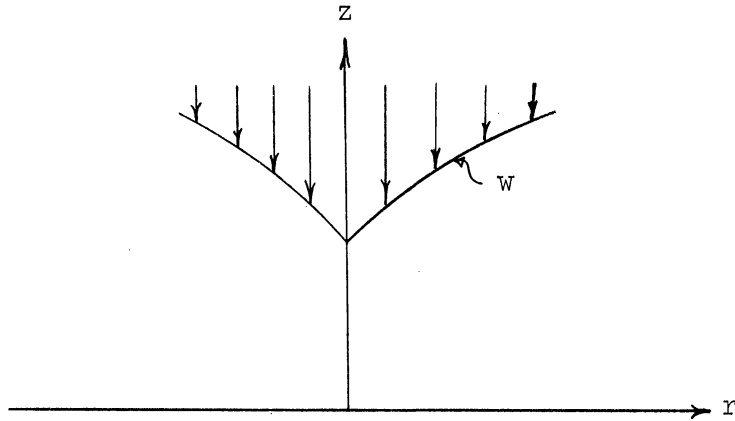


Figure 2.1. Plot of w vs. r Across the Axis of Symmetry.

continuous at $x = 0$, and hence the shear stress, which is proportional to the first derivative of the velocity, would also be discontinuous. This cannot happen in a physical system, so an additional requirement is that

$$\frac{\partial w}{\partial r} = 0 \quad \text{at } r = 0 \quad (2.15)$$

with the direct result that

$$\text{at } r = 0 : \quad \eta = 0 \quad (2.16)$$

The boundary conditions far from the disc are not as obvious. It would seem that the effects of the sink should decay at least

algebraically with increasing z ; thus it would appear natural to require that the radial and tangential velocities be zero as in the von Kármán problem, i.e.,

$$u = v = 0 \quad \text{at} \quad z = \infty \quad (2.17)$$

From these and also the continuity equation, (2.2), it follows that

$$\frac{\partial w}{\partial z} = 0 \quad \text{at} \quad z = \infty \quad (2.18)$$

Therefore

$$w = w(r) \quad \text{at} \quad z = \infty \quad (2.19)$$

The vorticity Equation (2.4) for steady state then gives

$$\frac{\partial^2 \eta}{\partial r^2} + \frac{1}{r} \frac{\partial \eta}{\partial r} - \frac{\eta}{r^2} = 0 \quad (2.20)$$

or

$$\eta = Ar + \frac{B}{r} = - \frac{\partial w}{\partial r} \quad (2.21)$$

Thus

$$w = - \frac{1}{2} Ar^2 - B \ln r + C \quad (2.22)$$

If it is required that w be bounded for large as well as small r ,

$$A = B = 0 \quad (2.23)$$

Then from (2.21)

$$\eta = 0 \quad \text{at} \quad z = \infty \quad (2.24)$$

Finally, for large values of r , it again seems natural to require that the flow approach that given for the von Kármán problem of the rotating disc without a sink because the sink is very far away and its influence is negligible. Hence, the requirement is that the downward velocity component, w , is independent of its radial position and that the tangential velocity component, v , is a linear function of its radial position, i.e.,

$$\text{for large } r : \quad \frac{\partial w}{\partial r} = 0 \quad (2.25)$$

and

$$\frac{\partial(\frac{v}{r})}{\partial r} = 0 \quad (2.26)$$

These are the radiation conditions used by von Kármán. Their use is suggested here since the influence of the sink should not be felt near the disc for large r .

The difference between the value of the stream function on the axis of symmetry and its value on the disc is proportional to the discharge, Q_0 , of the sink. For cylindrical coordinates, in this case,

$$Q_0 = 2 \Pi [\psi_{\text{disc}} - \psi_{\text{axis of symmetry}}] \quad (2.27)$$

Using (2.10)

$$\psi_{\text{disc}} = \frac{Q_0}{2\pi} \quad (2.28)$$

2.2 Dimensionless Form

Solving the equations can be simplified significantly by a suitable dimensionless form of the system of partial differential equations and associated boundary conditions. A natural length in the present problem is related to the thickness of the boundary layer as used by von Kármán. This yields

$$\begin{aligned} Z &= z \sqrt{\frac{\omega}{\nu}} ; & R &= r \sqrt{\frac{\omega}{\nu}} ; & \beta &= \frac{Q_0}{2\pi} \sqrt{\frac{\omega}{\nu^3}} \\ \Gamma &= \frac{\eta}{\omega} ; & \tau &= t\omega ; & \Psi &= \frac{1}{\nu} \sqrt{\frac{\omega}{\nu}} \psi \\ U &= \frac{u}{\sqrt{\nu\omega}} ; & V &= \frac{v}{\sqrt{\nu\omega}} ; & W &= \frac{w}{\sqrt{\nu\omega}} \end{aligned} \quad (2.29)$$

where ω is the rotational speed of the disc. U , V , W , and Γ are functions of R , Z , and τ , and Ψ is a function of R and Z .

Substitution of (2.29) into the system of Equations (2.1b), (2.4), (2.5), and (2.6) produces the dimensionless system

$$\frac{\partial \Gamma}{\partial \tau} + U \frac{\partial \Gamma}{\partial R} + W \frac{\partial \Gamma}{\partial Z} - \frac{U\Gamma}{R} - \frac{2V}{R} \frac{\partial V}{\partial Z} = \left[\nabla^2 - \frac{1}{R^2} \right] \Gamma \quad (2.30)$$

$$\frac{\partial V}{\partial \tau} + U \frac{\partial V}{\partial R} + W \frac{\partial V}{\partial Z} + \frac{UV}{R} = \left[\nabla^2 - \frac{1}{R^2} \right] V \quad (2.31)$$

$$\Gamma = \frac{\partial U}{\partial Z} - \frac{\partial W}{\partial R} = \frac{1}{R} \frac{\partial^2 \Psi}{\partial R^2} - \frac{1}{R^2} \frac{\partial \Psi}{\partial R} + \frac{1}{R} \frac{\partial^2 \Psi}{\partial Z^2} \quad (2.32)$$

and

$$U = \frac{1}{R} \frac{\partial \Psi}{\partial Z} \quad ; \quad W = - \frac{1}{R} \frac{\partial \Psi}{\partial R} \quad (2.33)$$

where

$$\nabla^2 \equiv \frac{\partial^2}{\partial R^2} + \frac{1}{R} \frac{\partial}{\partial R} + \frac{\partial^2}{\partial Z^2} \quad (2.34)$$

In a similar manner the boundary conditions are transformed into the following dimensionless forms:

on the disc at $Z = 0$

$$V = R \quad (2.35)$$

$$\Psi_{\text{disc}} = \beta \quad (2.36)$$

$$U = 0 \quad (2.37)$$

on the axis of symmetry at $R = 0$

$$\Psi = 0 \quad (2.38)$$

$$U = V = 0 \quad (2.39)$$

$$\Gamma = 0 \quad (2.40)$$

and

$$W = - \frac{\partial^2 \Psi}{\partial R^2} \quad (2.41)$$

is used as means of calculating W here so that these values of W will be on hand.

Far above the disc at $Z = \infty$

$$U = V = 0 \quad (2.42)$$

$$\Gamma = 0 \quad (2.43)$$

For large radii at $R = \infty$

$$\frac{\partial W}{\partial R} = 0 \quad (2.44)$$

$$\frac{\partial(\frac{V}{R})}{\partial R} = 0 \quad (2.45)$$

The dimensionless system of partial differential equations with its associated boundary conditions is the form used in obtaining a numerical solution. Note that no Reynolds number or other dimensionless parameter is present in the system of differential equations. The only dimensionless parameter is β which enters through the boundary conditions. One also notes that the values of β need not be restricted to positive values, but may be given negative values as in the case of a point source at the origin. A physical interpretation of β is that it is the ratio of sink and rotation forces to viscous forces.

There are three simultaneous partial differential equations, (2.30) - (2.32), in the three unknowns, Γ , V , and Ψ . Inspection of the boundary conditions indicates that on the boundaries $Z = \infty$ and $R = \infty$ there does not appear to be sufficient information. This will be discussed in Section 3.4. The foregoing dimensionless form is suitable if the only length scale present is the boundary layer thickness. If, however, there is a characteristic length, L , present,

such as in vortex chamber problems, then a more suitable transformation is

$$R = \frac{r}{L} \quad ; \quad Z = \frac{z}{L} \quad (2.46)$$

and

$$U = \frac{u}{\omega L} \quad ; \quad V = \frac{v}{\omega L} \quad ; \quad W = \frac{w}{\omega L} \quad (2.47)$$

along with the remaining relations of (2.29) to transform the system of partial differential equations into the form

$$\frac{\partial \Gamma}{\partial \tau} + U \frac{\partial \Gamma}{\partial R} + W \frac{\partial \Gamma}{\partial Z} - \frac{U\Gamma}{R} - \frac{2V}{R} \frac{\partial V}{\partial Z} = R_e \left[\frac{\partial^2 \Gamma}{\partial R^2} + \frac{\partial^2 \Gamma}{\partial Z^2} + \frac{1}{R} \frac{\partial \Gamma}{\partial R} - \frac{\Gamma}{R^2} \right] \quad (2.48)$$

$$\frac{\partial V}{\partial \tau} + U \frac{\partial V}{\partial R} + W \frac{\partial V}{\partial Z} + \frac{UV}{R} = R_e \left[\frac{\partial^2 V}{\partial R^2} + \frac{\partial^2 V}{\partial Z^2} + \frac{1}{R} \frac{\partial V}{\partial R} - \frac{V}{R^2} \right] \quad (2.49)$$

and

$$\Gamma = R_e^{3/2} \left[\frac{1}{R} \frac{\partial^2 \Psi}{\partial Z^2} + \frac{1}{R} \frac{\partial^2 \Psi}{\partial R^2} - \frac{1}{R^2} \frac{\partial \Psi}{\partial R} \right] \quad (2.50)$$

where R_e is the inverse of the Reynolds number and is given by

$$R_e = \frac{\nu}{\omega L^2} \quad (2.51)$$

Likewise (2.33) becomes

$$U = \frac{R_e^{3/2}}{R} \frac{\partial \Psi}{\partial Z} \quad ; \quad W = - \frac{R_e^{3/2}}{R} \frac{\partial \Psi}{\partial R} \quad (2.52)$$

and (2.41) becomes

at $R = 0$:

$$W = - R_e^{3/2} \frac{\partial^2 \Psi}{\partial R^2} \quad (2.53)$$

The boundary conditions either remain unchanged or must be modified in order to consider other problems with walls, etc.

CHAPTER 3

THE FINITE DIFFERENCE FORM OF THE EQUATIONS GOVERNING THE PROBLEM OF THE ROTATING DISC WITH A CENTER SINK

3.1 Introduction

The partial differential equations that govern the problem of the rotating disc with a center sink were given in the previous chapter as

$$\frac{\partial \Gamma}{\partial \tau} + U \frac{\partial \Gamma}{\partial R} + W \frac{\partial \Gamma}{\partial Z} - \frac{U\Gamma}{R} - \frac{2V}{R} \frac{\partial V}{\partial Z} = \left[\nabla^2 - \frac{1}{R^2} \right] \Gamma \quad (3.1)$$

$$\frac{\partial V}{\partial \tau} + U \frac{\partial V}{\partial R} + W \frac{\partial V}{\partial Z} + \frac{UV}{R} = \left[\nabla^2 - \frac{1}{R^2} \right] V \quad (3.2)$$

and

$$\Gamma = \frac{1}{R} \frac{\partial^2 \Psi}{\partial R^2} - \frac{1}{R^2} \frac{\partial \Psi}{\partial R} + \frac{1}{R} \frac{\partial^2 \Psi}{\partial Z^2} \quad (3.3)$$

along with the boundary conditions and the two equations yielding the radial and axial velocities from the stream functions.

The problem considered by Wilkes⁽¹⁵⁾ (two dimensional convective flow in a cavity), while physically different, bears a high degree of mathematical similarity to the present problem. His vorticity equation and energy equation compare with (3.1) and (3.2), V being analogous to temperature in his case and the Coriolis and centripetal forces to internal energy and bouyancy force. This suggests a similar mathematical approach. The form of the equations in cylindrical coordinates presents difficulties for values of R approaching the axis of

symmetry ($R = 0$) which are not present in the cavity well problem, while the infinite domain presents difficulties for large values of R , as well as Z , which are also not present in Wilkes' problem. Nevertheless, the methods developed by Wilkes⁽¹⁵⁾ and Fromm⁽⁶⁾ prove quite useful in the numerical solution of the present problem.

Equations (3.1) and (3.2) give the relationship of the first order time derivatives of the circumferential vorticity and circumferential velocity to the space derivatives of the same quantities. These two equations are of the parabolic type. On the other hand, Equation (3.3) gives the vorticity as a function of the stream function and does not contain a time derivative. This equation is of the elliptic type. Different methods of solution are indicated by this fundamental mathematical difference.

The equations are next put into finite difference form. The finite difference forms for (3.1) and (3.2) are used to predict the new values of vorticity and tangential velocity after an increment of time, $\Delta\tau$. Using this new value of the vorticity, the finite difference form of (3.3) is used to compute the new stream function. This process, along with the application of the boundary conditions, is repeated until steady state conditions are reached. This method was chosen in preference to other methods - say a relaxation method or a non-transient alternating direction method - because it was felt to be more economical with regard to computer time than these other methods.

The methods used for obtaining the finite difference approximation to the solutions of the partial differential equations are essentially the same as given by Wilkes⁽¹⁵⁾ and Fromm,⁽⁶⁾ but are included since there are some minor differences.

3.2 System of Grid Points

For the von Kármán problem, the solution given by Cochran⁽⁴⁾ indicates that the boundary conditions at $Z = \infty$ are very closely approached by the values of the solution at $Z = 4.4$. With this in mind, it was felt that for use on the computer a value of $Z = 7.2$ was sufficiently large to use as the location of the infinite boundary in the vertical direction. For small values of β , i.e., sink strength, this was felt to be sufficient. However, one can see from the results shown in Figure A-12 that the distance should be increased for the larger values of β . The location of the radial infinite boundary had to be at least as far away, if not farther. For a square region with grid spacings of 0.6, the total number of grid points is thus 169. With the present form of the program the time required to reach steady-state conditions for a grid of this size is 14 minutes on the IBM 7090. An increase of R at infinity to a value of 10.8 yields a square grid of 247 points and an increase in computer time to at least 20.5 minutes in order to reach steady-state conditions.

In using finite difference methods, one usually truncates the infinite series at the point for which the truncation error is

of the order of the square of the change in the independent variable, which in this case is the grid spacing. Hence the finer the grid spacing, the better the accuracy. However, there is a limit as to how fine the spacing can be made in practical computation, since eventually round-off error becomes larger than the improvement due to a finer grid, and the computer time required is at least linearly proportional to the number of grid points. It is shown in Section 4.4 that the radial position of the dividing streamline is of the order of $\beta^{1/3}$ for small β . Thus a crude estimate of computer time would be of the order of $15(0.5\beta)^{1/3}$ minutes for a grid spacing of $\Delta R = \Delta Z = 0.6$ using the present program, a minimum number of grid points, and small β . As β becomes large, it is reasonable to suppose that the time will depend on an even higher power of β . Thus economics and computer capabilities limit the range of β values. For this study, it was felt that $\beta = 12$ was economically the maximum feasible value, since these values exhibit all of the basic physical aspects of the problem.

3.3 Finite Difference Approximations to the Equations of Motion

The finite difference forms of the equations of motion, (3.1) - (3.3) and of the equations giving U and W , i.e., (2.33),

are obtained in the usual manner using a Taylor's series expansion. For the vorticity and tangential velocity equations, i.e., (3.1) and (3.2), the equations are put into a form suitable for the implicit alternating direction (I.A.D.) method (for instance, see Birkhoff⁽³⁾). In the method, one considers two successive half-time steps, each of length $\Delta\tau/2$. Over the first half-step, all derivatives in the R-direction are approximated implicitly (i.e., at the half-step) while all derivatives in the Z-direction are approximated explicitly (i.e., at the present value). During the second half-step the procedure is reversed. In the following finite difference equations an asterisk(*) superscript denotes the value of the function computed at the end of the half-step in time while a prime(') superscript denotes the value at the end of the full time step. Variables with no superscript are evaluated at the beginning of the time step. The subscripts i and j denote the grid coordinates of the point in the R- and Z-directions, respectively. Thus for given values of i and j, say I and J, the space coordinates are

$$R = I\Delta R$$

$$Z = J\Delta Z \tag{3.4}$$

where ΔR and ΔZ are the sizes of the grid spacing in the R- and Z-directions, respectively.

In practice, (3.2) was first evaluated, and then, using these results, (3.1) was evaluated. Thus, for the first half-step

in time, (3.2) is written

$$\begin{aligned}
 & \frac{V_{i,j}^* - V_{i,j}}{\Delta\tau/2} + U_{i,j} \frac{V_{i+1,j}^* - V_{i-1,j}^*}{2\Delta R} + W_{i,j} \frac{V_{i,j+1} - V_{i,j-1}}{2\Delta Z} + \frac{U_{i,j}V_{i,j}}{(i\Delta R)} \\
 &= \frac{V_{i,j+1} - 2V_{i,j} + V_{i,j-1}}{(\Delta Z)^2} + \frac{V_{i+1,j}^* - 2V_{i,j}^* + V_{i-1,j}^*}{(\Delta R)^2} \\
 & \quad + \frac{1}{i\Delta R} \frac{V_{i+1,j}^* - V_{i-1,j}^*}{2\Delta R} - \frac{V_{i,j}}{(i\Delta R)^2} \tag{3.5}
 \end{aligned}$$

and for the second half-step in time, (3.2) becomes

$$\begin{aligned}
 & \frac{V'_{i,j} - V_{i,j}^*}{\Delta\tau/2} + U_{i,j} \frac{V_{i+1,j}^* - V_{i-1,j}^*}{2\Delta R} + W_{i,j} \frac{V'_{i,j+1} - V'_{i,j-1}}{2\Delta Z} + \frac{U_{i,j}V_{i,j}}{i\Delta R} \\
 &= \frac{V'_{i,j+1} - 2V'_{i,j} + V'_{i,j-1}}{(\Delta Z)^2} + \frac{V_{i+1,j}^* - 2V_{i,j}^* + V_{i-1,j}^*}{(\Delta R)^2} \\
 & \quad + \frac{1}{i\Delta R} \frac{V_{i+1,j}^* - V_{i-1,j}^*}{2\Delta R} - \frac{V_{i,j}}{(i\Delta R)^2} \tag{3.6}
 \end{aligned}$$

In (3.6) some V 's appear without superscripts due to the fact that they do not appear as derivatives in (3.2), and hence are evaluated at the beginning of the time step, as are U and W .

For the first half-step in time, (3.1) is written

$$\begin{aligned}
 & \frac{\Gamma_{i,j}^* - \Gamma_{i,j}}{\Delta\tau/2} + U_{i,j} \frac{\Gamma_{i+1,j}^* - \Gamma_{i-1,j}^*}{2\Delta R} + W_{i,j} \frac{\Gamma_{i,j+1} - \Gamma_{i,j-1}}{2\Delta Z} - \frac{U_{i,j}\Gamma_{i,j}}{i\Delta R} \\
 & \quad - \frac{2V'_{i,j}}{i\Delta R} \frac{V'_{i,j+1} - V'_{i,j-1}}{2\Delta Z} = \frac{\Gamma_{i+1,j}^* - 2\Gamma_{i,j}^* + \Gamma_{i-1,j}^*}{(\Delta R)^2} \\
 & \quad + \frac{1}{i\Delta R} \frac{\Gamma_{i+1,j}^* - \Gamma_{i-1,j}^*}{2\Delta R} + \frac{\Gamma_{i,j+1} - 2\Gamma_{i,j} + \Gamma_{i,j-1}}{(\Delta Z)^2} - \frac{\Gamma_{i,j}}{(i\Delta R)^2} \tag{3.7}
 \end{aligned}$$

For the second half-step in time, (3.1) becomes

$$\begin{aligned}
 & \frac{\Gamma'_{i,j} - \Gamma^*_{i,j}}{\Delta\tau/2} + U_{i,j} \frac{\Gamma^*_{i+1,j} - \Gamma^*_{i-1,j}}{2\Delta R} + W_{i,j} \frac{\Gamma'_{i,j+1} - \Gamma'_{i,j-1}}{2\Delta Z} - \frac{U_{i,j}\Gamma_{i,j}}{i\Delta R} \\
 & - \frac{2V'_{i,j}}{i\Delta R} \frac{V'_{i,j+1} - V'_{i,j-1}}{2\Delta Z} = \frac{\Gamma^*_{i+1,j} - 2\Gamma^*_{i,j} + \Gamma^*_{i-1,j}}{(\Delta R)^2} \\
 & + \frac{1}{i\Delta R} \frac{\Gamma^*_{i+1,j} - \Gamma^*_{i-1,j}}{2\Delta R} + \frac{\Gamma'_{i,j+1} - 2\Gamma'_{i,j} + \Gamma'_{i,j-1}}{(\Delta Z)^2} \\
 & - \frac{\Gamma_{i,j}}{(i\Delta R)^2} \tag{3.8}
 \end{aligned}$$

Since no time derivative is explicitly stated in (3.3), the finite difference approximation is given by

$$\begin{aligned}
 \Gamma_{i,j} = & \frac{1}{i\Delta R} \frac{\Psi_{i+1,j} - 2\Psi_{i,j} + \Psi_{i-1,j}}{(\Delta R)^2} - \frac{1}{(i\Delta R)^2} \frac{\Psi_{i+1,j} - \Psi_{i-1,j}}{2\Delta R} \\
 & + \frac{1}{i\Delta R} \frac{\Psi_{i,j+1} - 2\Psi_{i,j} + \Psi_{i,j-1}}{(\Delta Z)^2} \tag{3.9}
 \end{aligned}$$

(3.9) could be solved for $\Psi_{i,j}$ and a relaxation procedure used to solve it, but the successive over-relaxation method (S.O.R.) converges more rapidly, thus saving computer time. Using the S.O.R. method, one modifies and rearranges (3.9) to the form

$$\begin{aligned}
 \Psi_{i,j}^{(s+1)} = & \Psi_{i,j}^{(s)} + \frac{A}{2(1+D)} \left[-i(\Delta R)^3 \Gamma_{i,j} + \Psi_{i+1,j}^{(s)} \left(1 - \frac{1}{2i}\right) \right. \\
 & + \Psi_{i-1,j}^{(s)} \left(1 + \frac{1}{2i}\right) + D(\Psi_{i,j+1}^{(s)} + \Psi_{i,j-1}^{(s)}) \\
 & \left. - 2(1+D)\Psi_{i,j}^{(s)} \right] \tag{3.10}
 \end{aligned}$$

where the relaxation parameter, A , lies between 1.0 and 2.0 and is best evaluated using a trial and error method on the computer, and where

$$D \equiv \left(\frac{\Delta R}{\Delta Z}\right)^2 \quad (3.11)$$

The superscript (s) is the number of the iteration. Thus in (3.10) one sees that the new value of $\Psi_{i,j}$ is computed using the present values of the Ψ 's and of $\Gamma_{i,j}$. It was found by trial and error for $\beta = 5$ that the optimum value of A was 1.720 and that 50 iterations were sufficient to reduce the magnitude of the change in the stream function to the order of 10^{-7} of the value of the stream function at that point.

All of the finite difference forms given above are used only at the interior points of the grid, i.e., i and j always lie between their minimum and maximum values - never at these values. The values at the boundary are computed using formulas given later.

The forms for (2.33) are slightly more involved, due to the differing information available on the various boundaries. Thus if the maximum values of i and j are M and N , respectively, one has

for $i \neq 0$, $N - 2 \geq j \geq 2$,

$$U_{i,j} = \frac{1}{i\Delta R} \frac{\Psi_{i,j-2} - 8\Psi_{i,j-1} + 8\Psi_{i,j+1} - \Psi_{i,j+2}}{12 \Delta Z} \quad (3.12)$$

for $i \neq 0$, $j = 1$ (adjacent to the disc),

$$U_{i,1} = \frac{1}{i\Delta R} \frac{-2\Psi_{i,0} - 3\Psi_{i,1} + 6\Psi_{i,2} - \Psi_{i,3}}{6 \Delta Z} \quad (3.13)$$

for $i \neq 0$, $j = N - 1$,

$$U_{i,N-1} = \frac{1}{i\Delta R} \frac{2\Psi_{i,N} + 3\Psi_{i,N-1} - 6\Psi_{i,N-2} + \Psi_{i,N-3}}{6 \Delta Z} \quad (3.14)$$

for $M - 2 \geq i \geq 2$,

$$W_{i,j} = \frac{-1}{i\Delta R} \frac{\Psi_{i-2,j} - 8\Psi_{i-1,j} + 8\Psi_{i+1,j} - \Psi_{i+2,j}}{12 \Delta R} \quad (3.15)$$

for $i = 1$,

$$W_{1,j} = \frac{-1}{\Delta R} \frac{-2\Psi_{0,j} - 3\Psi_{1,j} + 6\Psi_{2,j} - \Psi_{3,j}}{6 \Delta R} \quad (3.16)$$

for $i = M - 1$,

$$W_{M-1,j} = \frac{-1}{(M-1)\Delta R} \frac{2\Psi_{M,j} + 3\Psi_{M-1,j} - 6\Psi_{M-2,j} + \Psi_{M-3,j}}{6 \Delta R} \quad (3.17)$$

No expressions are given for U and W on the boundary $j = N$ or for W on the boundary $i = 0$. The values of U and W are needed in their explicit forms only at interior grid points since they are used in Equations (3.5) - (3.10) which involve values of U and W at interior grid points only, as mentioned above. The forms

for U and W on these boundaries were constructed and used in the program for completeness, but will not be given here, since they did not interact with any other part of the solution.

3.4 Finite Difference Approximations to the Boundary Conditions

Having given the finite difference forms of the equations of motion, it is now necessary to prescribe the boundary conditions in a similar manner.

Thus on the disc, at $Z = 0$, one has
for $j = 0$:

$$V_{i,0} = i\Delta R \quad (3.18)$$

$$\Psi_{i,0} = \beta \quad (3.19)$$

$$U_{i,0} = 0 \quad (3.20)$$

Here, an explicit condition for $\Gamma_{i,0}$ is missing. It is supplied by computing the value using the condition which arises from (2.9), i.e., at $Z = 0$:

$$\frac{\partial W}{\partial R} = 0 \quad (3.21)$$

so

$$\Gamma_{Z=0} = \frac{\partial U}{\partial Z} \Big|_{Z=0} = \frac{1}{R} \frac{\partial^2 \Psi}{\partial Z^2} \Big|_{Z=0} \quad (3.22)$$

or in finite difference form

$$\Gamma_{i,0} = \frac{1}{i\Delta R} \frac{8\Psi_{i,1} - 7\Psi_{i,0} - \Psi_{i,2}}{2(\Delta Z)^2} \quad (3.23)$$

Next, on the axis of symmetry, $R = 0$, one has
for $i = 0$:

$$\Psi_{0,j} = 0 \quad (3.24)$$

$$U_{0,j} = V_{0,j} = 0 \quad (3.25)$$

$$\Gamma_{0,j} = 0 \quad (3.26)$$

and for completeness

$$W_{0,j} = - \frac{\Psi_{3,j} - 2\Psi_{2,j} - 11\Psi_{1,j}}{5(\Delta R)^2} \quad (3.27)$$

Far above the disc at large Z , one has
at $j = N$:

$$U_{i,N} = 0 \quad (3.28)$$

$$V_{i,N} = 0 \quad (3.29)$$

$$\Gamma_{i,N} = 0 \quad (3.30)$$

Here one notes that no condition is given for the stream function.
Again, one makes use of (2.33) and constructs the finite difference
form

$$\Psi_{i,N} = \frac{4\Psi_{i,N-1} - \Psi_{i,N-2}}{3} \quad (3.31)$$

Also, it was desired to see if the vorticity would go to zero on this boundary if its value were not fixed at zero. Here, the vorticity was computed using (3.32),

$$\Gamma_{i,N} = \frac{\Psi_{i+1,N} - 2\Psi_{i,N} + \Psi_{i-1,N}}{i(\Delta R)^3} - \frac{\Psi_{i+1,N} - \Psi_{i-1,N}}{2i^2(\Delta R)^3} + \frac{8\Psi_{i,N-1} - 7\Psi_{i,N} - \Psi_{i,N-2}}{2i(\Delta R)(\Delta Z)^2} \quad (3.32)$$

and the result used to check that the vorticity does indeed tend toward zero far above the disc. The check proved satisfactory. However, Equation (3.30) was used in the final computations.

Finally, the boundary at large R must be considered. Equation (2.44) is replaced using (2.33) in finite difference form. Thus (2.44) becomes

$$\Psi_{M,j} = \frac{5\Psi_{M-1,j} - 4\Psi_{M-2,j} + \Psi_{M-3,j}}{2} + \frac{3\Psi_{M,j} - 4\Psi_{M-1,j} + \Psi_{M-2,j}}{4M} \quad (3.33)$$

where (3.33) was obtained from the form

$$\frac{\partial^2 \Psi}{\partial R^2} = \frac{1}{R} \frac{\partial \Psi}{\partial R} \quad (3.34)$$

Equation (2.45) is first written as

$$\frac{\partial V}{\partial R} = \frac{V}{R} \quad (3.35)$$

and then put into the finite difference form

$$V_{M,j} = \frac{\sum_{M=3}^3 V_{M,j} + 9V_{M-1,j} - 4.5V_{M-2,j} + V_{M-3,j}}{5.5} \quad (3.36)$$

The value for the vorticity at this boundary was simply that computed from

$$\Gamma_{M,j} = \frac{1}{i\Delta R} \frac{\Psi_{M,j+1} - 2\Psi_{M,j} + \Psi_{M,j-1}}{(\Delta Z)^2} \quad (3.37)$$

where use has been made of (2.44).

3.5 Stability of the Method

All of the finite difference approximations neglect terms at least of order $(\Delta R)^2$, $(\Delta Z)^2$, or $\Delta\tau$ and higher. It was found that only when the ratio of the time increment to the square of the grid spacing was less than or equal to one-half was the process numerically stable, i.e.,

$$\frac{\Delta\tau}{(\text{grid spacing})^2} \leq \frac{1}{2} \quad (3.38)$$

for stability. Otherwise large meaningless numbers were generated with the result that the computer "dumped" the program. The values used in this study were

$$\Delta\tau = 0.15, \quad \Delta R = \Delta Z = 0.6 \quad (3.39)$$

giving a ratio of 5/12.

No criterion for the stability of the implicit alternating direction method has yet been developed. An attempt was made by Wilkes,⁽¹⁵⁾ but his analysis which is based on Fourier analysis, is valid only in the small,* according to Birkhoff,⁽²⁾ and does not involve the boundary conditions. The conclusion one may draw from Wilkes' analysis is that instability was not proved, but neither was stability. Also, the original system of differential equations is non-linear, and his stability analysis is performed on a system that, in a sense, has been linearized.

*i.e., near some fixed value of time; although this value can be any arbitrary value of time, it is not allowed to change by more than an amount $\Delta\tau$.

CHAPTER 4

NUMERICAL RESULTS

4.1 The Dividing Streamline

One notes that in all the plots of the streamlines (see Figures A-1 to A-8 in the appendix) there is a streamline which intersects the disc and upon which the stream function has the same value as on the disc. The streamlines between it and the axis of symmetry all enter the point sink at the origin while the remaining streamlines all tend to infinity in the direction of large R . This streamline which intersects the disc divides the flow into two parts and hereafter will be referred to as the dividing streamline.

The vorticity on the disc is given by

$$\Gamma = \frac{\partial U}{\partial Z} \quad (4.1)$$

since $W = 0$ everywhere on the plate. Just above the disc, between the origin (sink) and the dividing streamline, the radial velocity component is negative while on the disc it is zero. Hence in this region the vorticity is negative, i.e.,

$$0 < R < R_0 - \epsilon: \quad \Gamma < 0 \quad (4.2)$$

where R_0 is the location of the dividing streamline on the disc and ϵ is some positive number. On the other side of the dividing streamline, just above the disc, the radial velocity component is

positive. Thus the vorticity here is positive, i.e.,

$$R_0 + \epsilon < R < \infty : \quad \Gamma > 0 \quad (4.3)$$

Therefore, the vorticity becomes zero somewhere along the disc. If the vorticity is not zero at the point of intersection, then it must be zero elsewhere. Now if $\Gamma = 0$ elsewhere, then from (4.1), $\frac{\partial U}{\partial Z} = 0$ at this other point. But if $\frac{\partial U}{\partial Z} = 0$ at this other point, then another streamline must intersect the disc at this other point since the velocity on the disc is zero and the velocity profile starts out normal to the disc. But since two streamlines which intersect have the same value, this second intersecting streamline can only be the dividing streamline itself, i.e., they are one and the same. Hence, the conclusion is that the dividing streamline must be normal to the plate at the point of intersection. A consequence of this is that the shear stress component, τ_{zr} , is also zero at this point since it is proportional to the vorticity along the disc.

Inspection of the plots of the streamlines shows that the dividing streamline for large values of Z slopes toward the origin, and becomes more vertical as it approaches the disc. The latter is due to the centrifugal force being greater than the sink force in this region, and the former is due to the reverse of this. This influence of the sink on the flow far away is discussed in more detail in Section 4.3.

4.2 Preservation of Circulation

In viewing the plots of the tangential velocity component, V , (see Figure A-9 in the appendix) one notes that there is a bulge in the curves near the sink, i.e., the velocity increases with decreasing Z to a maximum value and then decreases to the value of the disc. If one looks at the streamline plots, one sees that near the axis of symmetry, a particle descends fairly vertically until it nears the disc (and the sink) at which time it begins to curve inward towards the sink and in so doing decreases its radial distance from the axis of symmetry. While descending, it had picked up a tangential velocity component due to the viscous effect of the rotating disc, and hence had a circulation about the axis of symmetry. Looking at the second Navier-Stokes equation, (2.1b), one sees that it can be rewritten as

$$\frac{\partial(rv)}{\partial t} + u \frac{\partial(rv)}{\partial r} + w \frac{\partial(rv)}{\partial z} = v \left[\frac{\partial^2(rv)}{\partial r^2} - \frac{1}{r} \frac{\partial(rv)}{\partial r} + \frac{\partial^2(rv)}{\partial z^2} \right] \quad (4.4)$$

Far above the disc u and v are both small, so for small values of r one may approximate (4.4) by

$$\frac{\partial(rv)}{\partial t} \sim v \left[\frac{\partial^2(rv)}{\partial r^2} - \frac{1}{r} \frac{\partial(rv)}{\partial r} + \frac{\partial^2(rv)}{\partial z^2} \right] \quad (4.5)$$

In (4.5) one sees that as a particle between the axis of symmetry and the dividing streamline descends, its circulation, rv , is slowly increasing due to the viscous effects, mentioned above, and that this

rate of increase is of the order of the viscous terms which are very small far away from the disc. Now as this particle nears the sink, it moves very rapidly inward, thus rapidly decreasing its radial distance, r , from the axis of rotation. This very rapid change in radial position is accompanied by a rapid increase in the particle's tangential velocity component. The viscous forces initially give the circulation. Then, as the particle nears the sink, the inertia forces dominate the motion. This then is the explanation for the bulge in the curves near the axis of symmetry. This effect was also observed experimentally when soap bubbles were used to trace the particle paths.

4.3 Influence of the Sink at Large Z

As mentioned previously and as can be seen from the plots of the streamlines, the streamlines far away from the disc, i.e., for large values of Z , curve slightly away from the vertical direction toward the sink. This can also be seen from pictures taken in the experimental phase of the program, although the effect is exaggerated by the three-dimensionality of the streamlines which were photographed. At first it seems as if the flow at large distances above the disc and at large radial distances should be entirely downward as in the problem solved by von Kármán. However, a little reflection on potential theory recalls that, for a three-dimensional sink flow, all the flow is directly toward the sink - even very far away. Hence in cylindrical coordinates, there is a

radial component. For a three-dimensional sink in cylindrical coordinates, if the disc is not present, the radial velocity at any point is given by

$$u = - \frac{Qr}{4\pi(r^2 + z^2)^{3/2}} \quad (4.6)$$

where Q is the sink discharge. In the rotating disc with a center sink, since only flow above the disc is considered

$$u = - \frac{Q_0 r}{2\pi(r^2 + z^2)^{3/2}} \quad (4.7)$$

Non-dimensionalizing (4.7) using (2.29) yields

$$U_{\text{sink}} = \frac{-\beta R}{(R^2 + Z^2)^{3/2}} \quad (4.8)$$

While these arguments are useful for a qualitative picture of the flow, they are limited by the fact that the centrifugal forces near the disc tend to confine the source, the amount of confinement being inversely dependent on β . However, general trends are indicated. For example, for a value of $\beta = 5.0$, $R = 6.0$, and $Z = 6.0$ one has from (4.8)

$$U_{\text{sink}} = -0.0494 \quad (4.9)$$

And from the von Kármán problem as run on the computer

$$U_{\text{vonK}} = 0.0215 \quad (4.10)$$

Then

$$U_{\text{sink}} + U_{\text{vonK}} = - 0.0279 \quad (4.11)$$

As given by the present computer program, the corresponding value was found to be

$$U = - 0.0243 \quad (4.12)$$

Recall that in von Kármán's problem, he used the transformation

$$u = r\omega F(Z) \quad (4.13)$$

while in the present work, the transformation is

$$u = \sqrt{v\omega} U(R,Z) \quad (4.14)$$

Thus for conversion from one set of values to the other, one uses

$$U = RF \quad (4.15)$$

Comparisons are shown for other values of β in Table 4.1. The signs of the second and third columns agree, and the magnitudes of the velocities in the two columns are of the same order. Thus

TABLE 4.1

COMPARISON OF THE COMPUTED VALUES OF U WITH THE
QUASI-POTENTIAL VALUES OF U AT THE POINT
R = 6.0, Z = 6.0

β	$U_{\text{sink}} + U_{\text{vonK}}$	U_{computed}	% difference
1	+ 0.01164	+ 0.00915	27
2	+ 0.00185	+ 0.00008	96
3	- 0.0081	- 0.00827	2
4	- 0.0178	- 0.0166	7
5	- 0.0279	- 0.0243	13
6	- 0.0375	- 0.02912	22
7	- 0.0475	- 0.0391	18

this model can be used to approximate the location and shape of the dividing streamline for β of such values that the confinement is not too severe (i.e., for sufficiently large β).

4.4 Influence of the Parameter β

Looking at the results for W , the axial component of the dimensionless velocity, one sees that the values of W near the axis of symmetry increase with increasing β , while the values of W away from this axis change very little.

For a given value of β , the dimensionless dividing streamline intersects the disc at some fixed R . However R and β are both dimensionless. As before

$$\beta = \frac{Q_0}{2\pi} \sqrt{\frac{\omega}{\nu}} \quad (4.16)$$

and

$$R = r \sqrt{\frac{\omega}{\nu}} \quad (4.17)$$

Experimentally, Q_0 and ω can be varied independently. Thus it is possible to obtain the same value of β with numerous sets of values for Q_0 and ω . Suppose one decreased Q_0 and increased ω in such a manner as to give a constant value of β . Then, since R

here is constant, from (4.17) one can see that the physical radial position, r_0 , of the dividing streamline moves inward toward the axis of symmetry, while from

$$w = \sqrt{v\omega} W \quad (4.18)$$

one can see that the downward physical velocity component, w , increases in magnitude. If, instead, ω were to be decreased and Q_0 increased, the equations would predict that the reverse occurs.

Now near the axis of symmetry, the sink dominates the flow. Since the dimensionless dividing streamline moves radially outward for increasing values of β , holding the rotational speed ω constant while increasing Q_0 means that more fluid flows into the sink. Thus near the sink the physical velocity components u and w should both increase. But if ω is constant, then from (4.18) and

$$u = \sqrt{v\omega} U \quad (4.19)$$

U and W must increase in order to give an increase to the physical velocities, u and w . The computer solutions show that this is indeed what happens. However, next suppose β is increased by increasing ω with Q_0 fixed. As before for increasing β , the computer shows that both U and W increase in this case. Then from (4.18) and (4.19) both u and w must increase due to the larger U and W in addition to the increase in ω .

Now from the computer data, the dividing streamline position, R_o , is some function of β , i.e.,

$$R_o = f(\beta) \quad (4.20)$$

and from (4.17) the physical position, r_o , of the dividing streamline is given by

$$r_o = \sqrt{\frac{v'}{\omega}} f(\beta) \quad (4.21)$$

or

$$r_o = \sqrt{\frac{v'}{\omega}} f \left(\frac{Q_o}{2\pi} \sqrt{\frac{\omega'}{v'}} \right) \quad (4.22)$$

From (4.22), one can see that if the function $f(\beta)$ is of any degree in β less than unity, then r_o will decrease with increasing ω . If this is true then the physical components, u and w , must increase with ω (Q_o fixed) as predicted above.

Now from the Navier-Stokes equation, (2.1a), when viscosity is neglected, one has for steady state

$$-\frac{\partial p}{\partial r} = \rho \left[u \frac{\partial u}{\partial r} + w \frac{\partial u}{\partial z} - \frac{v^2}{r} \right] \quad (4.23)$$

On the disc this reduces to

$$-\frac{\partial p}{\partial r} = \rho \left[u \frac{\partial u}{\partial r} - \frac{v^2}{r} \right] \quad (4.24)$$

If one now considers the potential flow of a fluid which is in solid body rotation with a sink on the axis of symmetry at the center of the disc, one finds that (4.24) may be written as

$$-\frac{\partial p}{\partial r} = \rho \left[\frac{-Q_0}{2\pi^2 r^4} - r\omega^2 \right] \quad (4.25)$$

If one plots the separate contributions of the sink and solid body rotations to the pressure gradient, as well as the total pressure gradient, versus the radial position on the disc, as is done in Figure 4.1, one sees that indeed the pressure gradient has a minimum which is non-zero. The minimum pressure gradient is found by differentiating (4.24). Now for the minimum pressure gradient, differentiating (4.24) with respect to r and setting the result equal to zero yields

$$\frac{\partial}{\partial r} \left[u \frac{\partial u}{\partial r} - \frac{v^2}{r} \right] = 0 \quad (4.26)$$

Using (2.29) this becomes

$$\left(\frac{\partial U}{\partial R} \right)^2 + U \frac{\partial^2 U}{\partial R^2} - \frac{2V}{R} \frac{\partial V}{\partial R} + \frac{V^2}{R} = 0 \quad (4.27)$$

Putting (4.8) and (2.35) into (4.27) yields

$$1 - \frac{10\beta^2}{R_0^6} = 0 \quad (4.28)$$

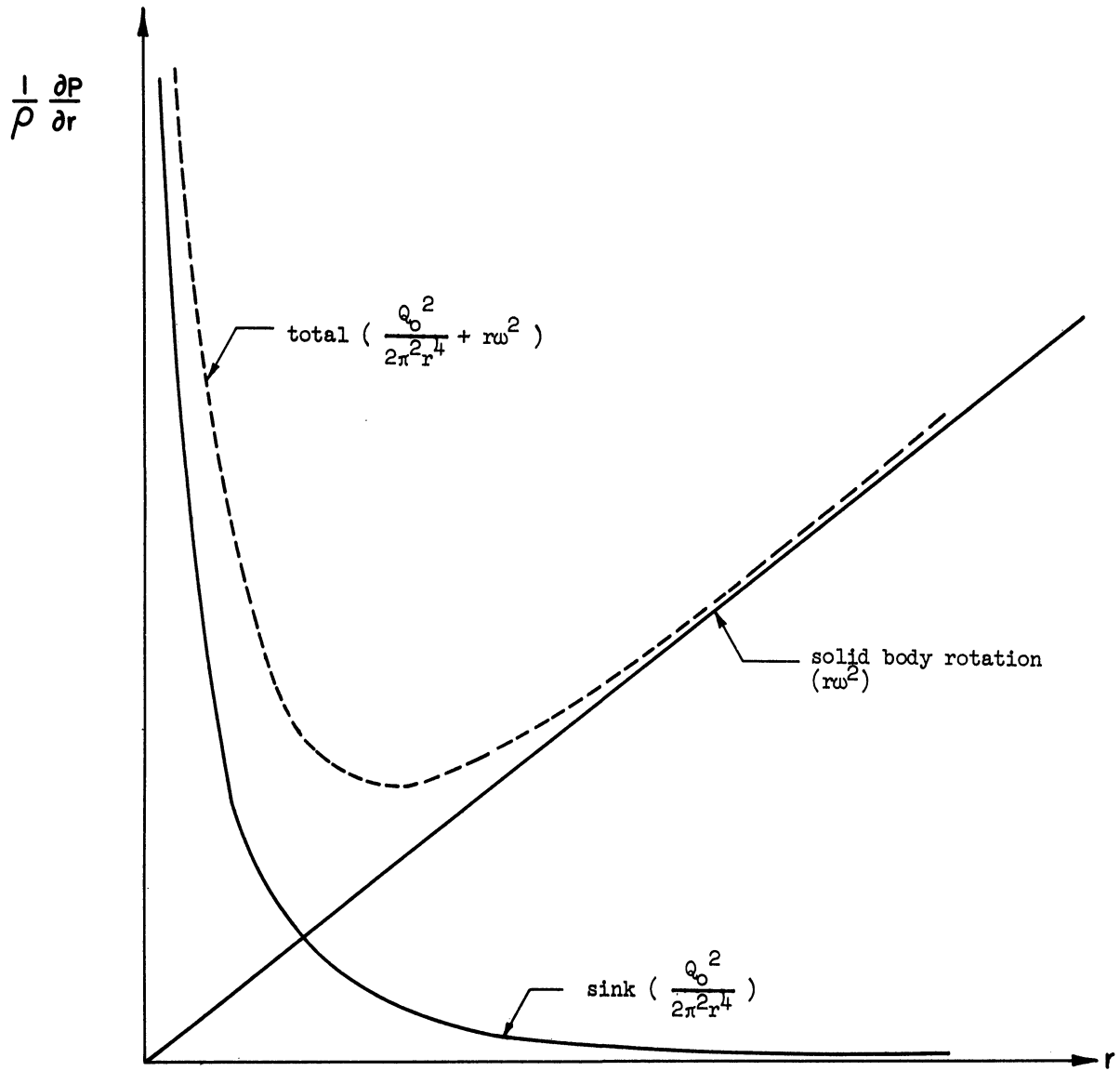


Figure 4.1. Pressure Gradient on the Disc as a Function of Radial Position for Inviscid Flow.

solving for R_o

$$R_o = \sqrt[6]{10} \beta^{1/3} \quad (4.29)$$

or

$$R_o = 1.468\beta^{1/3} \quad (4.30)$$

which approximates the location of the minimum pressure gradient on the disc. Looking at the data for the position of the dividing streamline and the corresponding values for β in Table 4.2, suppose one makes the simple assumption that

$$R_o = C\beta^\alpha \quad (4.31)$$

then

$$\ln R_o = \alpha \ln \beta + \ln C \quad (4.32)$$

TABLE 4.2

THE LOCATION OF THE RADIAL DISTANCE R_o FROM THE ORIGIN OF THE POINT OF INTERSECTION OF THE DIVIDING STREAMLINE WITH THE DISC

β	R_o
1	1.49992
2	1.83384
3	2.10654
4	2.30103
5	2.45902
6	2.62331

Then α is found from

$$\alpha = \frac{\ln (R_o)_2 - \ln (R_o)_1}{\ln (\beta)_2 - \ln (\beta)_1} \quad (4.33)$$

The range of α for the data obtained from the computer is given by Table 4.3 and is

$$0.28998 \leq \alpha \leq 0.354737 \quad (4.34)$$

So one may try

$$\alpha = 1/3 \quad (4.35)$$

Thus it appears that

$$R_o \sim \beta^{1/3} \quad (4.36)$$

is a reasonable approximation for small β , and hence the above conclusions based on the assumption that $\alpha < 1$ are substantiated.

TABLE 4.3

COMPUTED VALUES FOR α AND C FOR
USE IN EQUATION (4.31)

β	α	C
1	0.289980	1.49992
2	0.341917	1.44689
3	0.306958	1.50354
4	0.297597	1.52318
5	0.354737	1.38935
6	0.324893	1.46566

The values of R_0 , α , and C were found using the computer program EXPON.OO1. The location of R_0 was based on the data at $Z = 0.6$, i.e., it was assumed that the streamline intersected the disc in a vertical line which was straight for a distance of at least 0.6 above the disc. Similarly, C was found to be

$$C \simeq 1.47 \quad (4.37)$$

so that one has

$$R_0 \simeq 1.47\beta^{1/3} \quad (4.38)$$

In view of the above results, it is interesting to note that for an infinite, inviscid, incompressible fluid rotating with solid body rotation about an axis on which a sink was located, Long⁽⁸⁾ found that all the flow going into the sink came from within a region bounded by a cylinder of radius

$$r_0 = \left(\frac{Q_0}{4.6\pi\omega} \right)^{1/3} \quad (4.39)$$

In the same paper, Long quotes a personal communication from Sir Geoffrey Taylor in which Taylor gives

$$r_0 = \left(\frac{Q_0}{0.62\pi\omega} \right)^{1/3} \quad (4.40)$$

for a jet due to a source at the axis of a rotating fluid.

If now, instead, one tries to express β as a power series in R_0 , i.e.,

$$\beta = \sum_n a_n R_0^n \quad (4.41)$$

one finds that the coefficients a_n are as shown in Table 4.4. Thus the first seven terms in (4.41) are given by

$$\begin{aligned} \beta = & 1362.74 R_0 - 3962.5 R_0^2 + 4753.88 R_0^3 \\ & - 3012.45 R_0^4 + 1063.96 R_0^5 \\ & - 198.628 R_0^6 + 15.3175 R_0^7 \end{aligned} \quad (4.42)$$

TABLE 4.4

COMPUTED VALUES FOR THE COEFFICIENTS IN THE POWER SERIES GIVEN IN EQUATION (4.41)

n	a_n
1	1362.74
2	- 3962.5
3	4753.88
4	- 3012.45
5	1063.96
6	- 198.628
7	15.3175

4.5 Technique of Solution

As mentioned previously, the solution was carried out on the IBM 7090 computer at The University of Michigan. The program was broken down into the main program and five subroutines. A simplified program flow diagram is shown in Figure 4.2.

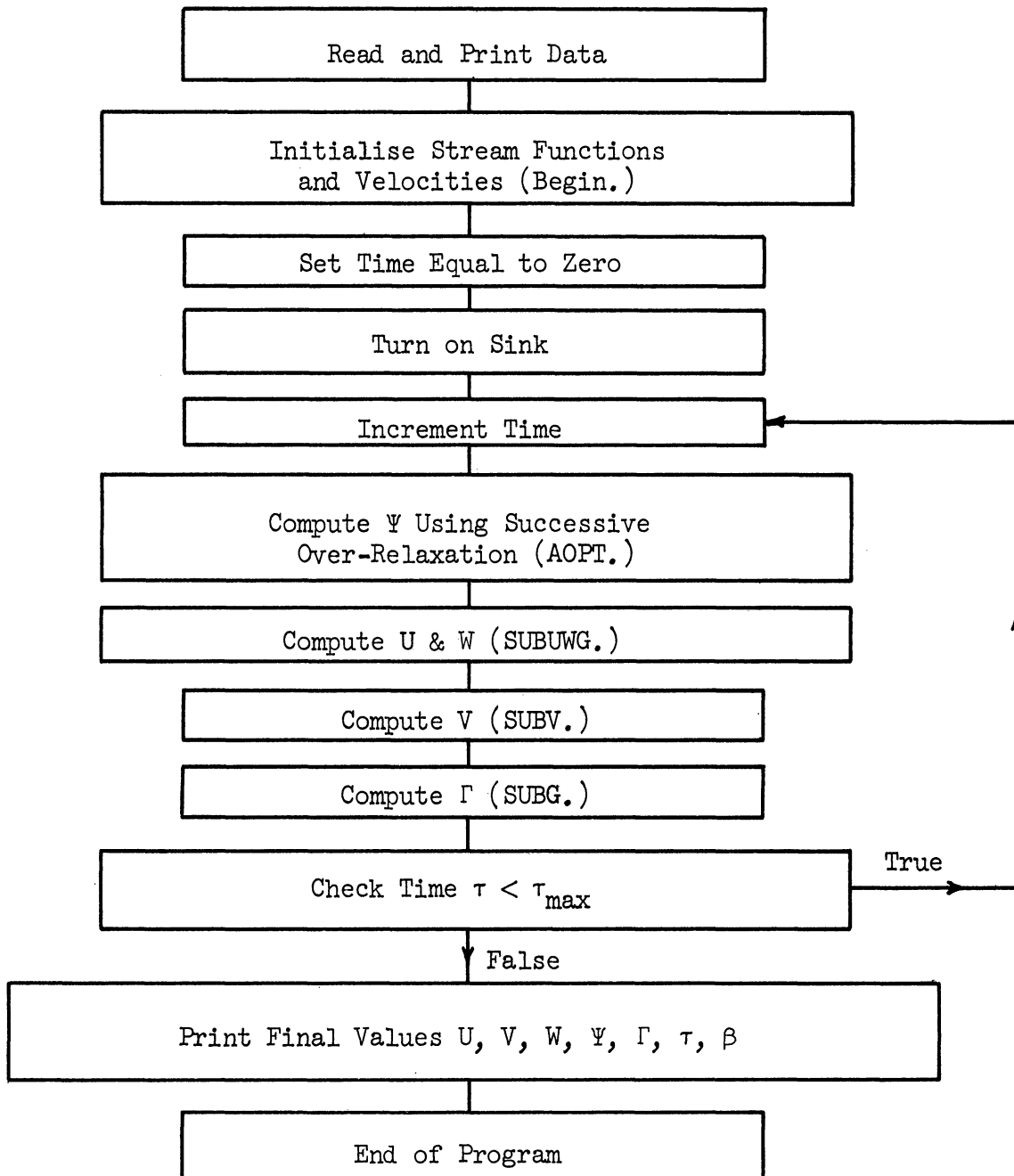


Figure 4.2. Simplified Flow Diagram for the Computer Program.

In more detail, the main program first, in the subroutine BEGIN., initializes the values of the stream function, i.e., the von Kármán stream functions are calculated. The main program then transfers to the subroutine SUBUWG. where all values of U and W are calculated as well as the vorticity on the disc. The program next "turns on" the sink and then moves to the subroutine AOPT. where the new stream functions are computed from Equation (3.10) using the successive over-relaxation technique mentioned earlier. Using these new values of the stream function, the program returns to SUBUWG. After computing the new values for U and W and for Γ on the disc, in SUBUWG., the program computes the new tangential velocities, V, using (3.5) and (3.6) in the subroutine SUBV. Finally, using (3.7) and (3.8) the new values of the vorticity, Γ , are computed in the subroutine SUBG. The program then computes the values for the variables on the boundaries which are allowed to change and returns to AOPT. to compute the new stream functions, and the cycle starts again. The process is repeated until a pre-set time is reached.

In applying the boundary conditions where the value was allowed to change with time, i.e., the stream function at $Z = \infty$ or at $R = \infty$, it was found that if the values were recomputed at the end of each iteration in the successive over-relaxation process (AOPT.) the process became unstable and large meaningless numbers were generated. If, however, the values were recomputed after each time step, then the process appeared to be stable with meaningful results.

Also, in applying the conditions at $Z = \infty$, three methods were tried. First, U was set equal to zero, and the corresponding stream function was calculated using (3.31). The values of Γ on this boundary were then computed on the basis of the stream functions. The second method was to set Γ equal to zero on this boundary and calculate the stream function here on this basis. The value of U here corresponding to the stream function derivatives was then computed. It was found that the first method was slightly superior to the second in that the values of both U and Γ were smaller adjacent to this boundary. However, a third method was the one used. This was simply to set $U = 0$ on this boundary and calculate the stream function using (3.31). In addition, Γ was set equal to zero here. This is the more rigorous approach, but the other two approaches were tried in order to see if less rigid boundary conditions would possibly result in a good approximation in a shorter time. The third approach gave the smallest values of U and Γ near this boundary for a given amount of computation time. Due to the fact that the grid spacing was large and the number of grid points was relatively small, the results obtained on the computer are only indicative of the flow behavior for the problem of the rotating disc with a center sink.

Better quantitative results would be obtained with a much finer grid spacing, many more grid points and longer runs on the computer.

4.6 The Rotating Disc with a Center Source

The case of a source in a fluid rotating with solid body rotation has been considered by Barua.⁽¹⁾ In his problem, the fluid is rotating about the x-axis and the source is replaced by a discharge through a sphere

$$x^2 + y^2 + z^2 = a^2 \quad (4.43)$$

located at the origin. However, the flow from the source is assumed to remain irrotational, thus giving rise to a discontinuity at the interface of the irrotational and rotational fluids.

In the present case of the rotating disc with a center source, no assumption of irrotationality is made.

As mentioned previously, the computer program was set up such that it could be used with a source instead of a sink. This is done simply by using a negative value for β . The result of using $\beta = -2.0$ is shown in Figure A-15 in the appendix.

CHAPTER 5
EXPERIMENTAL PROGRAM

5.1 Apparatus

The experimental program was carried out in the Fluids Laboratory Building at the North Campus. A room 12 feet long, 10 feet wide and 11-1/2 feet high was constructed using 2-inch x 4-inch beams covered with masonite on the sides and a thin polyethylene sheet 0.008 inch thick on the ceiling. All joints, cracks, and holes were then sealed using masking tape. The experimental work was done inside this room in order to eliminate any drafts.

Inside this room, a 1/4 inch thick piece of tempered masonite approximately 4 feet in diameter with a 3/8 inch hole at its center was mounted in a horizontal plane on a vertical hollow shaft which could be driven by a motor. The hollow shaft was connected to a vacuum pump located outside of the room. The connecting line between the disc hole and the vacuum pump contained two Cox flowmeters connected in parallel used to measure the discharge. The flow was controlled with metering valves mounted in series with the flow meters. The drive unit was a Servo-Tek thyatron regulated drive unit. Thus the disc speed could be varied as well as the sink discharge.

The streamlines were visualized using a smoke generator which fed smoke into the region above the disc through fifteen 1/8 inch diameter glass tubes spaced two inches apart. The smoke was generated by blowing air through a 1 inch diameter pyrex tube containing a burning oil-of-wintergreen-impregnated cigar.

A second method of visualizing the flow consisted of dipping eight 19 gage hypodermic needles, mounted in parallel at the end of the air line, into a glycerin-soap solution, raising the needles far above the disc, and blowing small bubbles into this region. The path lines of the bubbles were then observed. Tufts of wool were also tried, but even very fine threads were too heavy and too stiff to be of any value.

A cutaway drawing of the experimental set-up is shown in Figure 5.1.

5.2 Procedure

It was found that the experiments could be carried out only in the evening with the lights turned off above the room. If there was a strong breeze blowing outside, there was a noticeable effect inside the room. This was attributed to a cooling effect of the subsequent drafts inside the laboratory passing over the ceiling, which was only a thin plastic sheet, and to possible entry of these drafts into the room. The lights above the room caused a very noticeable convection current in the room when lit.

In order to obtain photographs, a spotlight was aimed from outside the room through a glass window. The spotlight beam was at right angles to the direction from which photographs were taken. To minimize the heating of the air inside the room from the spotlight, it was switched on only during the period when the camera was in use.

The procedure for making a run was to turn off the lights and blowers in the portion of the building near the room. Ten to

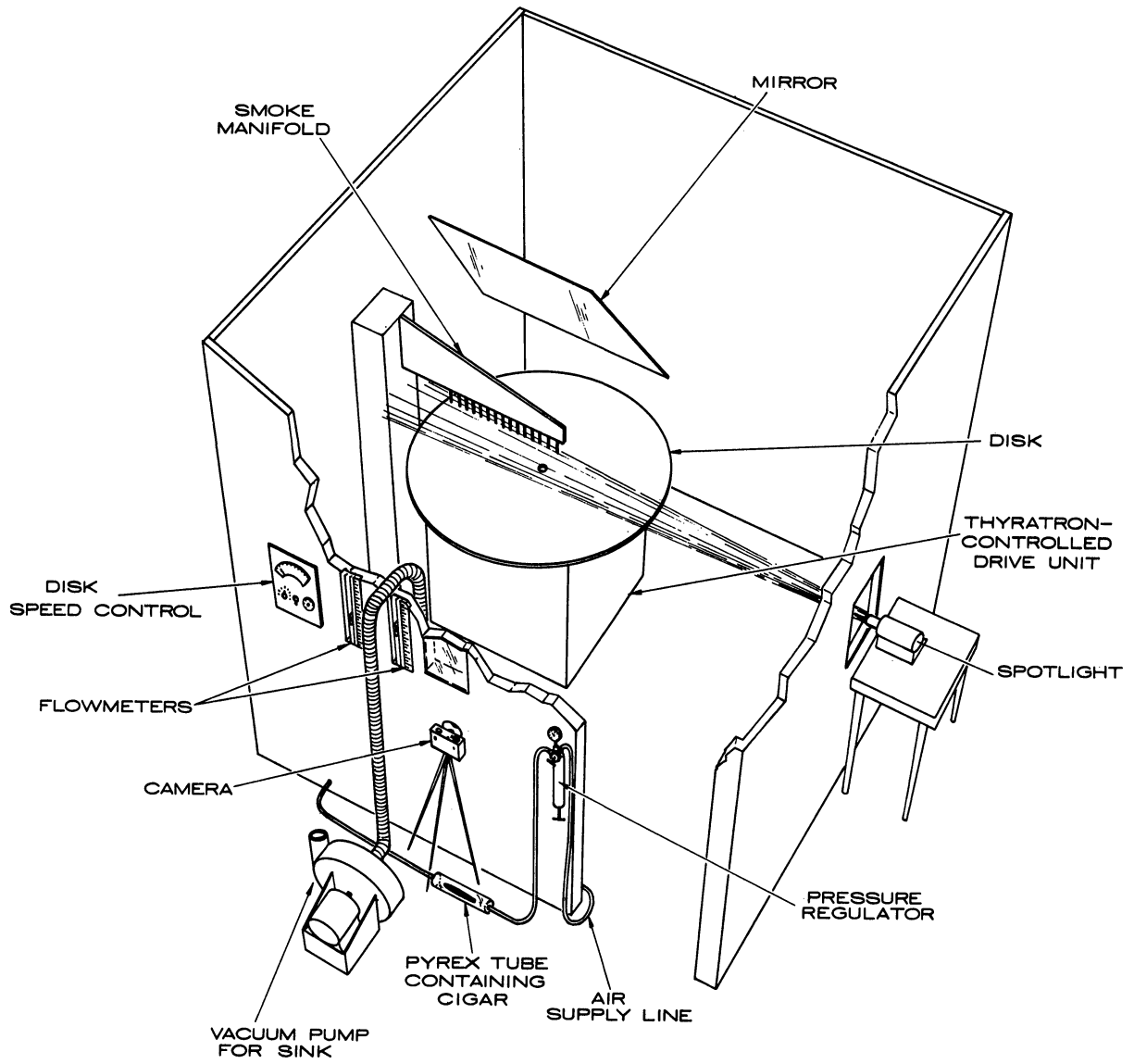


Figure 5.1. Experimental Apparatus.

fifteen minutes were then allowed for the air inside the room to become quiescent. The vacuum pump was then turned on along with the smoke generator. The smoke was introduced at a velocity comparable to that of the surrounding air so as not to disturb the flow. A short time later, the disc was set in motion and pictures were taken. After about a minute of running, the apparatus was turned completely off, and a period of ten to fifteen minutes allowed to pass before making another run. This was done to minimize turbulent effects due to the nearness of the walls of the room to the disc. This wall effect also limited the speeds at which the disc could be run for even short periods of time.

5.3 Results

Pictures taken of a vertical plane of the flow show some change in the streamlines with changes in the variables Q_0 and ω . These changes are indicative of what is happening but do not yield good quantitative results. This is due to the fact that the actual streamlines are three-dimensional while the photographs are plane. Photographs taken looking down on the disc gave little detail because the streamlines were fairly vertical until they neared the disc where they were quickly dissipated due to the increased velocity of the air in this region.

Actual observation, just as in the attempts made using soap bubbles, appears to be the best method at the present time. With the disc speed, ω , fixed at its minimum value one can see the dividing streamline move outward as the sink discharge, Q_0 , is

increased. It is more difficult to see the dividing streamline move inward when Q_0 is fixed at its maximum value (5 scfm) and ω increased. It is almost impossible to see the dividing streamline move when Q_0 is fixed at a value of 2.0 scfm or less and ω is varied. Actually, one does not "see" the dividing streamline at all; one only observes the streamlines in the vicinity change their slope near the disc as Q_0 or ω is varied. The effect is noticeable in the region $0 \leq r \leq 6$ inches. The streamlines farther away move so little that it is difficult to tell whether they are being affected by the changes in Q_0 and ω or by the little disturbances that are undoubtedly present in the room.

The fact that the disc was not perfectly plane could be seen at high rotational speeds (15-20 rad/sec) as pulses in the smoke streams that caused a wavy form.

When a large amount of smoke was present in the room, it was possible to see the air above the disc being pulled downward as the disc was started up from rest.

The readings taken directly from the flowmeters were felt to be sufficiently accurate for this work since the maximum pressure drop before entering the flowmeters was 0.55-inch of mercury. This coupled with a correction for changes in atmospheric pressure amounted to less than a 4 percent error in the sink discharge values.

The superposition of the streamlines for $\omega = 2.5$ rad/sec, $Q_0 = 5.0$ scfm on the streamlines for $\omega = 4.0$ rad/sec, $Q_0 = 2.5$ scfm is shown in Figure 5.2. Here one sees that due to the three-

— $\beta = 5470$
- - - $\beta = 8650$

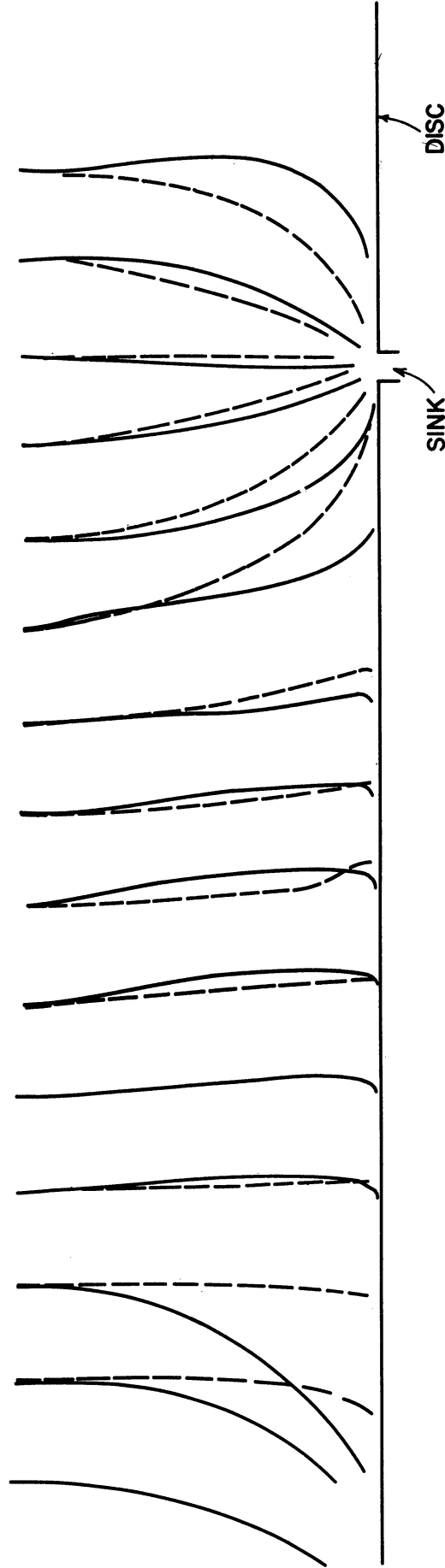


Figure 5.2. Superposition of the Streamlines (Experimental.)
for $\beta = 8650$ ($\omega = 2.5$ rad/sec, $Q_0 = 5$ scfm)
and $\beta = 5470$ ($\omega = 4.0$ rad/sec, $Q_0 = 2.5$ scfm).
The Streamlines are 2 inches Apart at the Top.

dimensionality of the system, the dividing streamlines are difficult to detect, but the qualitative effect is immediately apparent.

Now in the experiment

$$1.5 \leq Q_0 \leq 5.0 \text{ scfm} \quad (5.1)$$

$$2.5 \leq \omega \leq 5.5 \text{ rad/sec} \quad (5.2)$$

and

$$v \simeq 1.8 \times 10^{-4} \text{ ft}^2/\text{sec} \quad (5.3)$$

Using (4.30) along with (2.29) one finds

$$r_0 = 1.468 \left(\frac{Q_0}{2\pi\omega} \right)^{1/3} \text{ ft} = 17.6 \left(\frac{Q_0}{2\pi\omega} \right)^{1/3} \text{ in} \quad (5.4)$$

(One notes here that r_0 is independent of the fluid used, i.e., the results should be the same for any fluid.) Thus from (5.1), (5.2), and (5.4)

$$1.99 \leq r_0 \leq 3.08 \text{ in} \quad (5.5)$$

is the predicted range for the experiment. However, the experiment shows that (see Figure 5.2)

$$6 \leq r_0 \leq 10 \text{ in} , \quad (5.6)$$

indicating that indeed (5.4) is valid only for small β .

Similarly, from the von Kármán results computed by Cochran one sees that the boundary layer thickness (based on the fact that the radial and tangential velocities are very small) is approximately of the dimensionless height

$$Z \simeq 6.0 \quad (5.7)$$

or

$$0.413 \leq z \leq 0.61 \text{ in} \quad (5.8)$$

is the predicted range of the boundary layer thickness. However, as can be seen from Figure 5.3, the effect of the rotational motion of the disc affects the flow at considerably larger distances of the order of two or more inches.

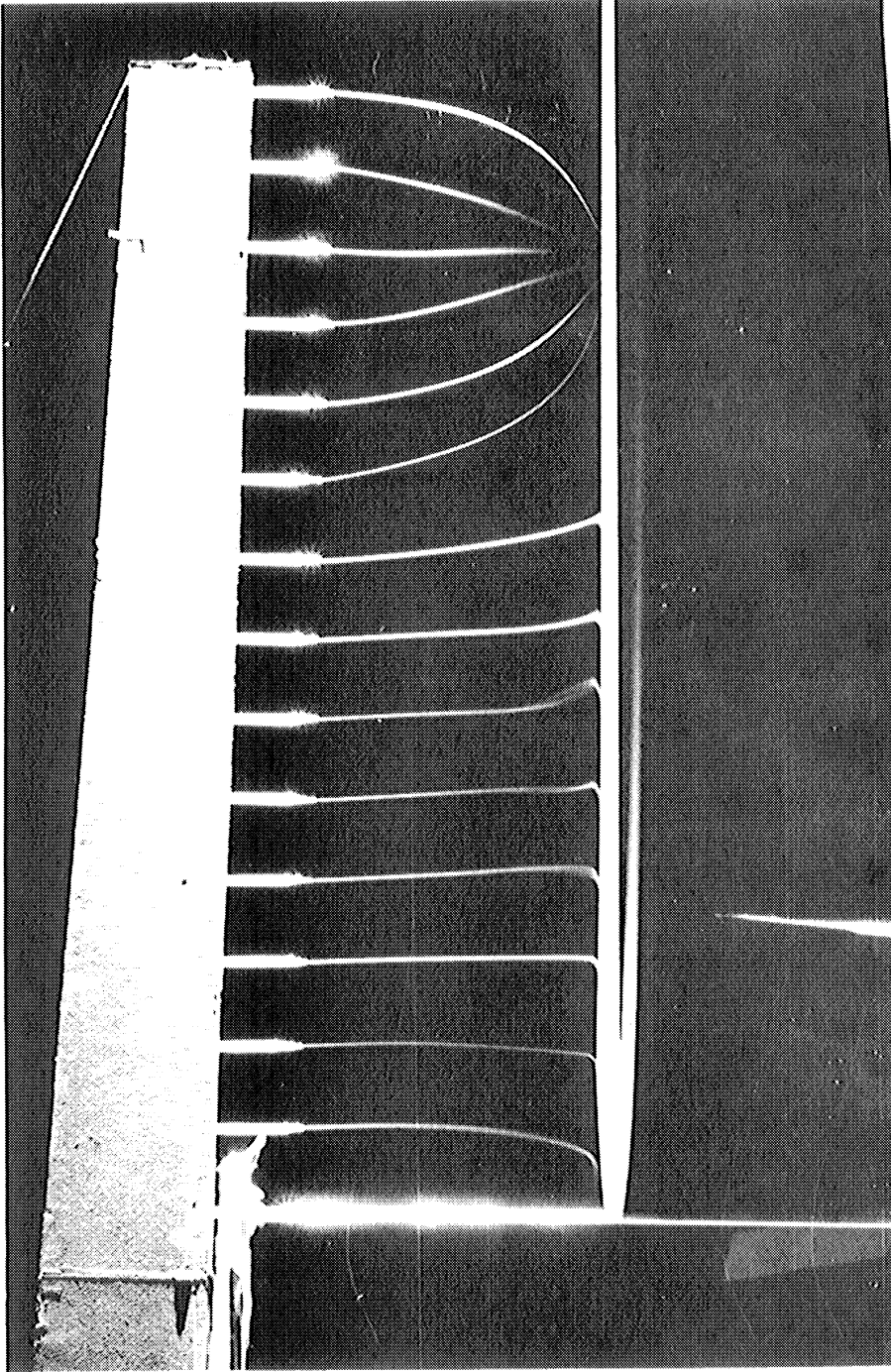


Figure 5.3. Photograph of the Streamlines for $\omega = 2.5$ rad/sec
and $Q_0 = 5.0$ scfm.

CHAPTER 6

CONCLUSIONS

Summarizing the results, it is found that (1) the numerical study indicates that for small values of β the non-dimensional radial distance of the dividing streamline from the axis of rotation is proportional to the cube root of the parameter β , which is a measure of the ratio of rotational and sink attractive forces to the viscous force; (2) the flow fairly far away from the sink at rather large heights above the disc is still influenced somewhat by the sink as evidenced by the streamlines curving slightly toward the sink in this region; (3) the dividing streamline intersects the disc at right angles; and (4) the location of the minimum pressure gradient along the disc appears to be at the intersection of the dividing streamline and the disc.

A phenomenon best described as a tendency to preserve circulation is demonstrated both experimentally and numerically, although the effect is diminished near the disc by viscosity. The circumferential velocity of a fluid particle located between the axis of symmetry and the dividing streamline first increases due to the viscous effects as it approaches the disc. This gives rise to a circulation. As the particle is drawn towards the sink, its radial distance from the axis of rotation decreases. Then, due to the predominance of the convection effects over the viscous effects, the circumferential velocity increases.

CHAPTER 7

SUGGESTIONS FOR FUTURE WORK

The results presented in the present work are indicative of the general behavior of the flow but the fine structure has not been obtained. A finer grid spacing would improve the accuracy of the solution and would serve as an indication as to whether the method converges to the correct solution (i.e., if decreasing the grid spacing by an order of magnitude gives the same significant figures, one would be optimistic about the correctness).

Also, the problem of the rotating disc with a center source can be very easily investigated with no additional experimental equipment required and using the present computer program.

As mentioned previously, the computer program is also set up to include vortex chamber problems. Specifically, it is possible to consider a cylindrical chamber in which the wall is stationary or rotating, the top is stationary or rotating, and the bottom is stationary or rotating and has a source or sink at its center. Each of these conditions may or may not be present independently of the others.

It appears from the results of the experimental program that the use of a much larger room to better ensure a quiescent atmosphere would be very desirable. A stronger pump would enable increasing the range of β . Also, a better method of measuring the position of the dividing streamline should be devised. One might try finer streams of smoke more closely spaced and use a telephoto lens on the camera. The main difficulty seems to stem from the

fact that the air velocities are very small and hence any disturbances, even though small, affect the flow considerably.

A suggestion prompted by Equation (5.4) is to use a different fluid, say water, because the location of the dividing streamline is independent of the fluid used. A small diameter disc, say about 12 inches, could be immersed in a very large diameter tank, say 10-12 feet, such as is available in the Fluids Laboratory on the North Campus. This would allow use of better flow visualization techniques, but would still require long waits between runs, and would still be dependent on room temperature variations.

APPENDIX A

GRAPHS OF STREAMLINES AND VELOCITY PROFILES

Only the graphs of the velocity components for $\beta = 3.0$ are shown here. For other values of β , the graphs have the same general shape.

The graphs of the streamlines for all values of β are also shown.

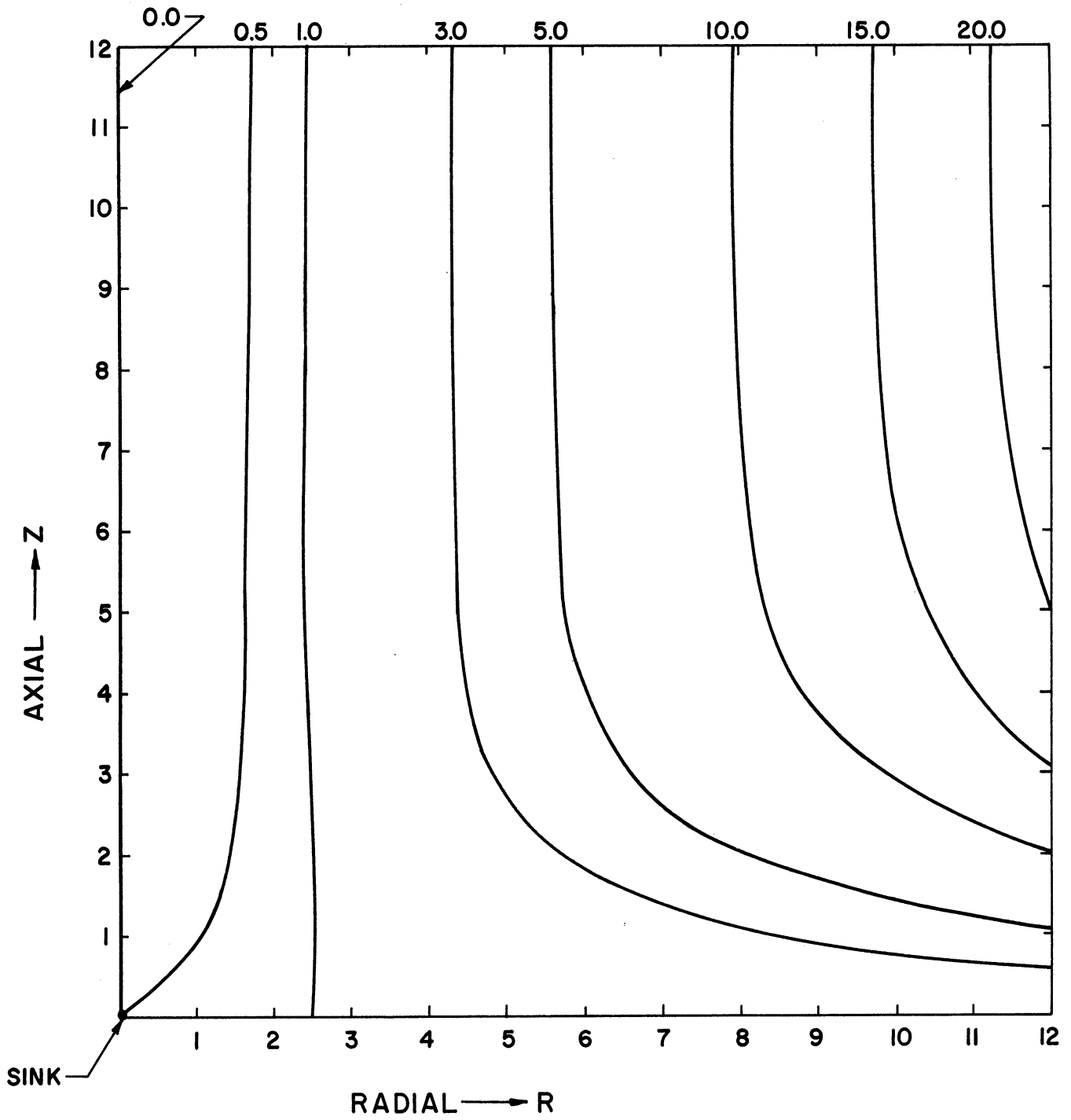


Figure A-1. Streamlines for $\beta = 1.0$.

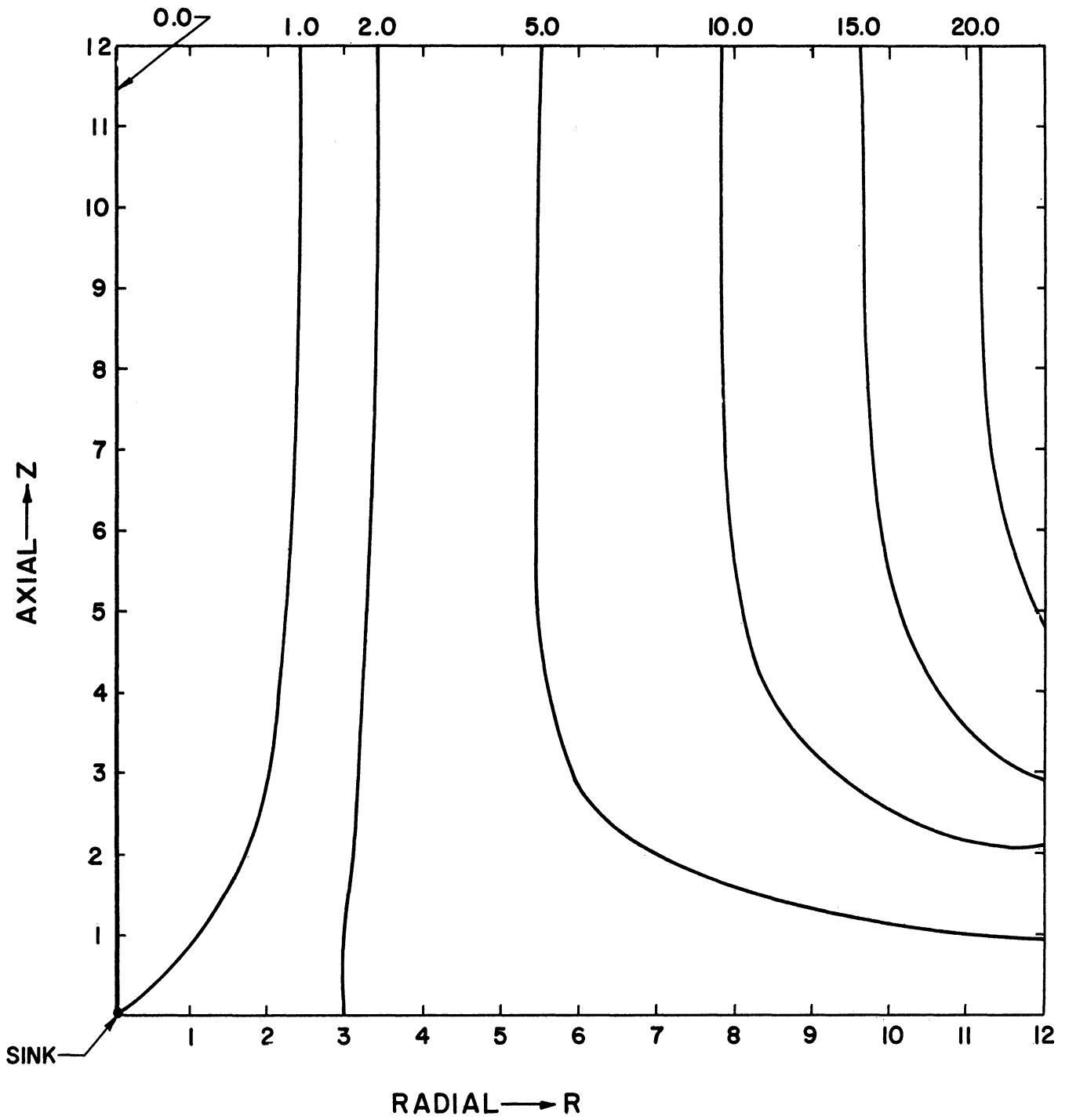


Figure A-2. Streamlines for $\beta = 2.0$.

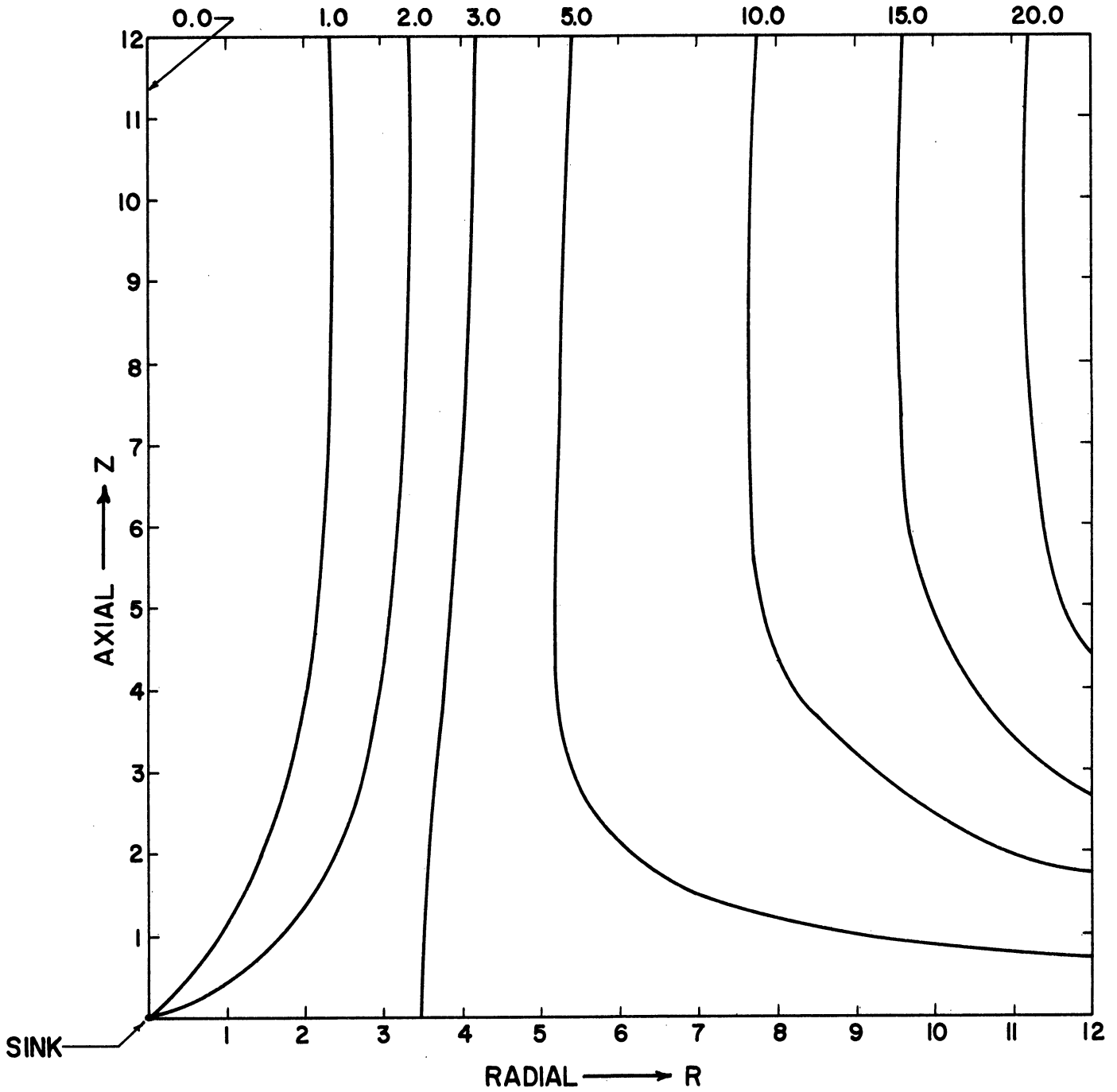


Figure A-3. Streamlines for $\beta = 3.0$.

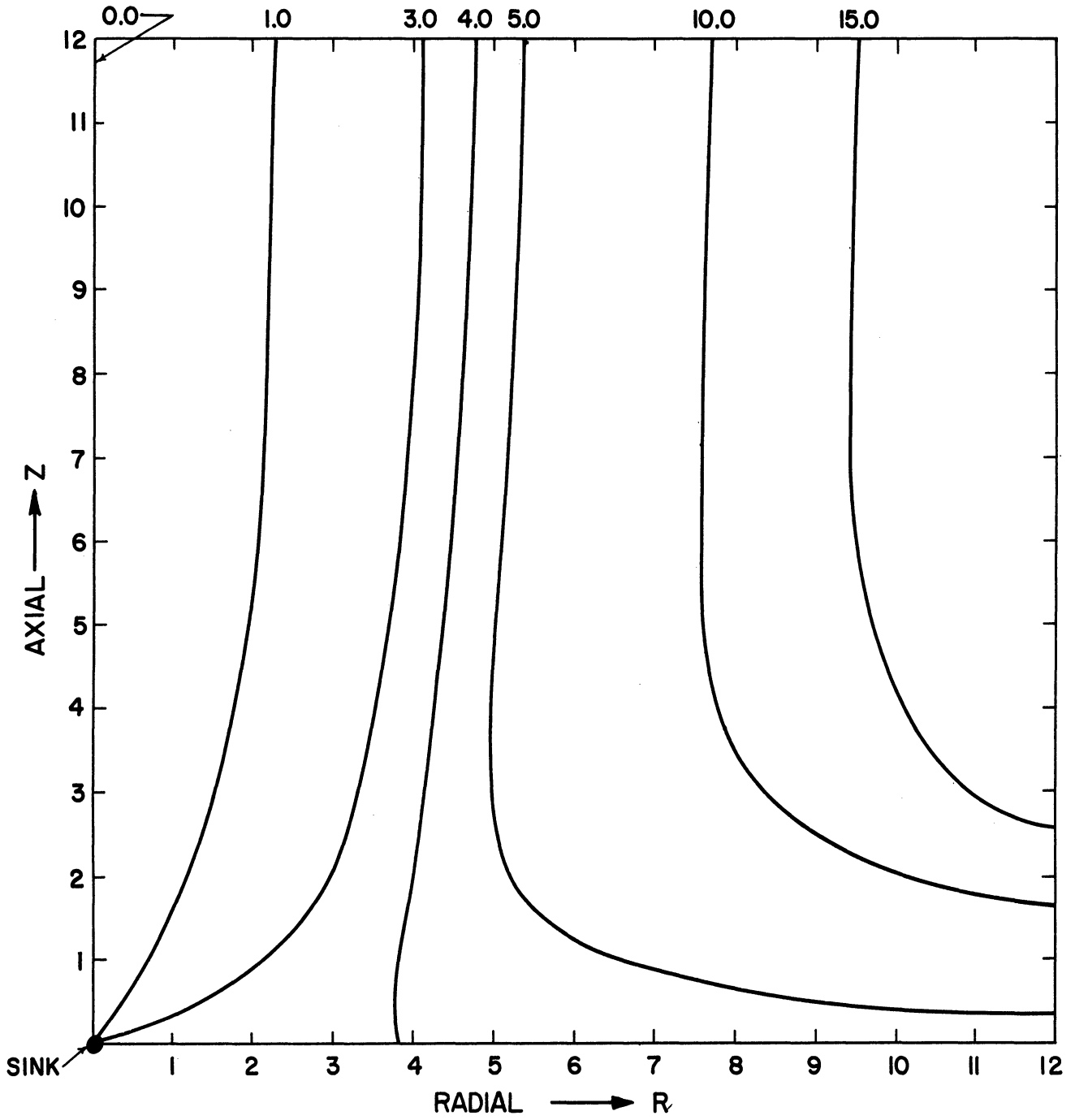


Figure A-4. Streamlines for $\beta = 4.0$.

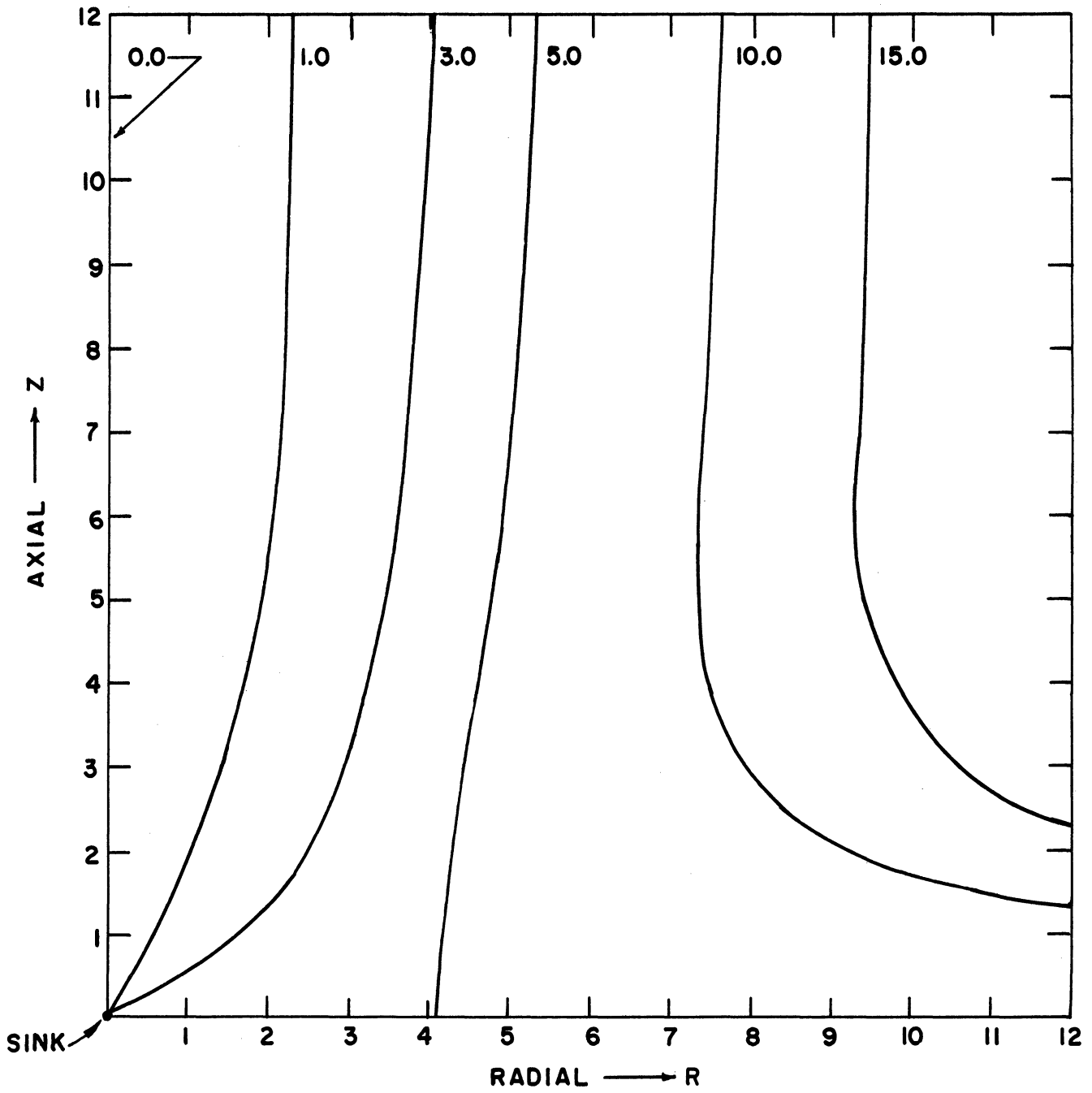


Figure A-5. Streamlines for $\beta = 5.0$.

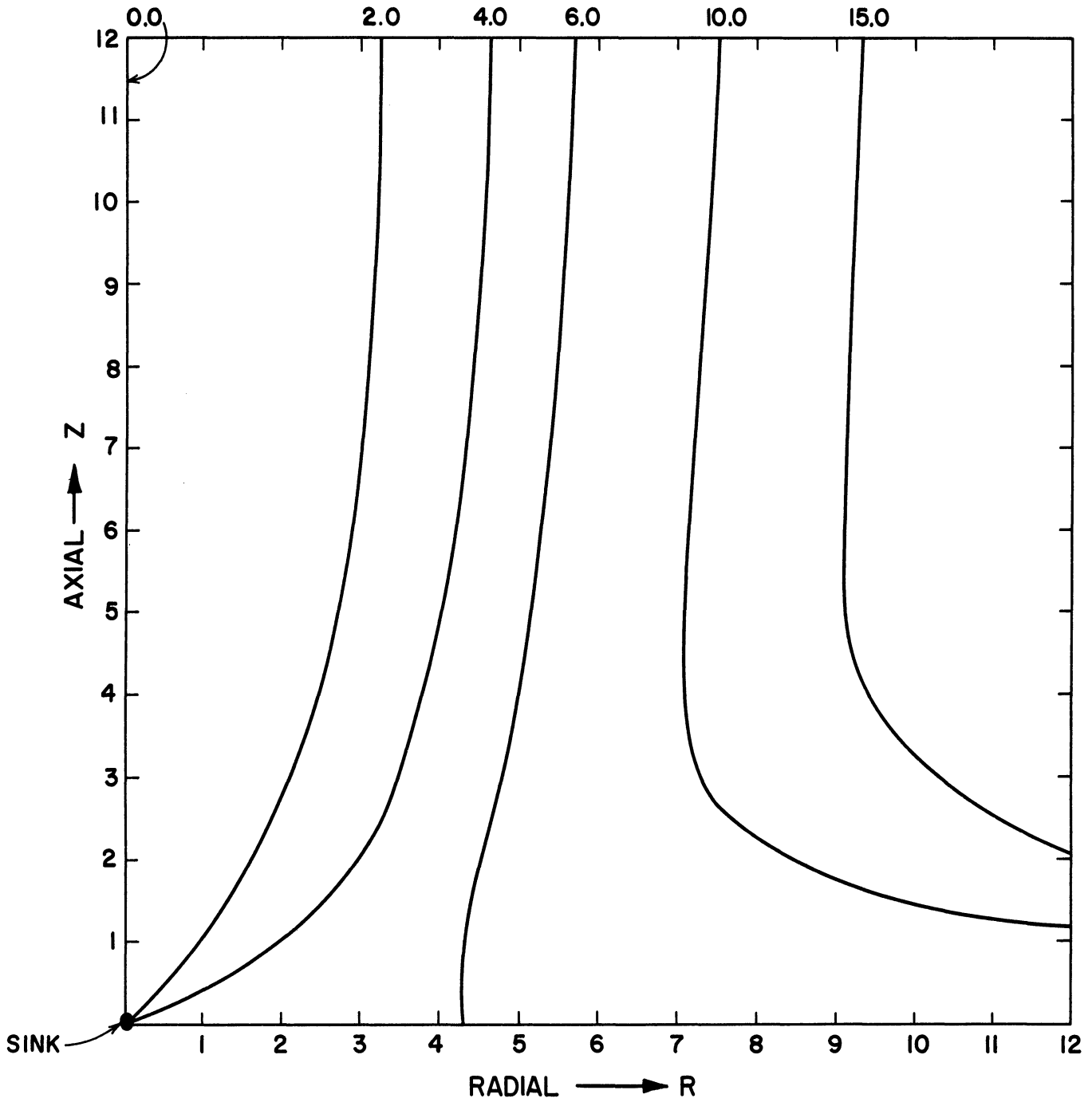


Figure A-6. Streamlines for $\beta = 6.0$.

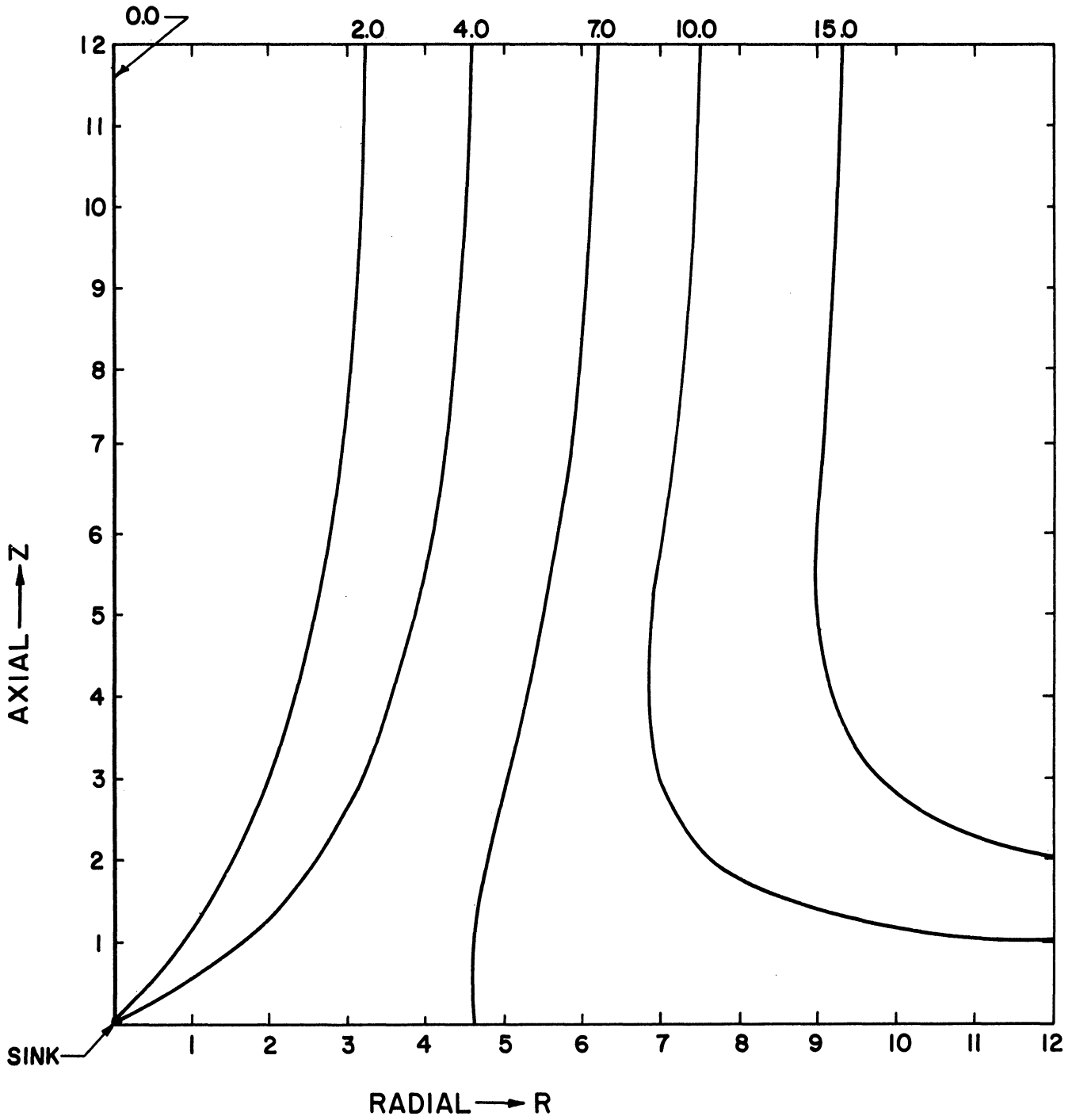


Figure A-7. Streamlines for $\beta = 7.0$.

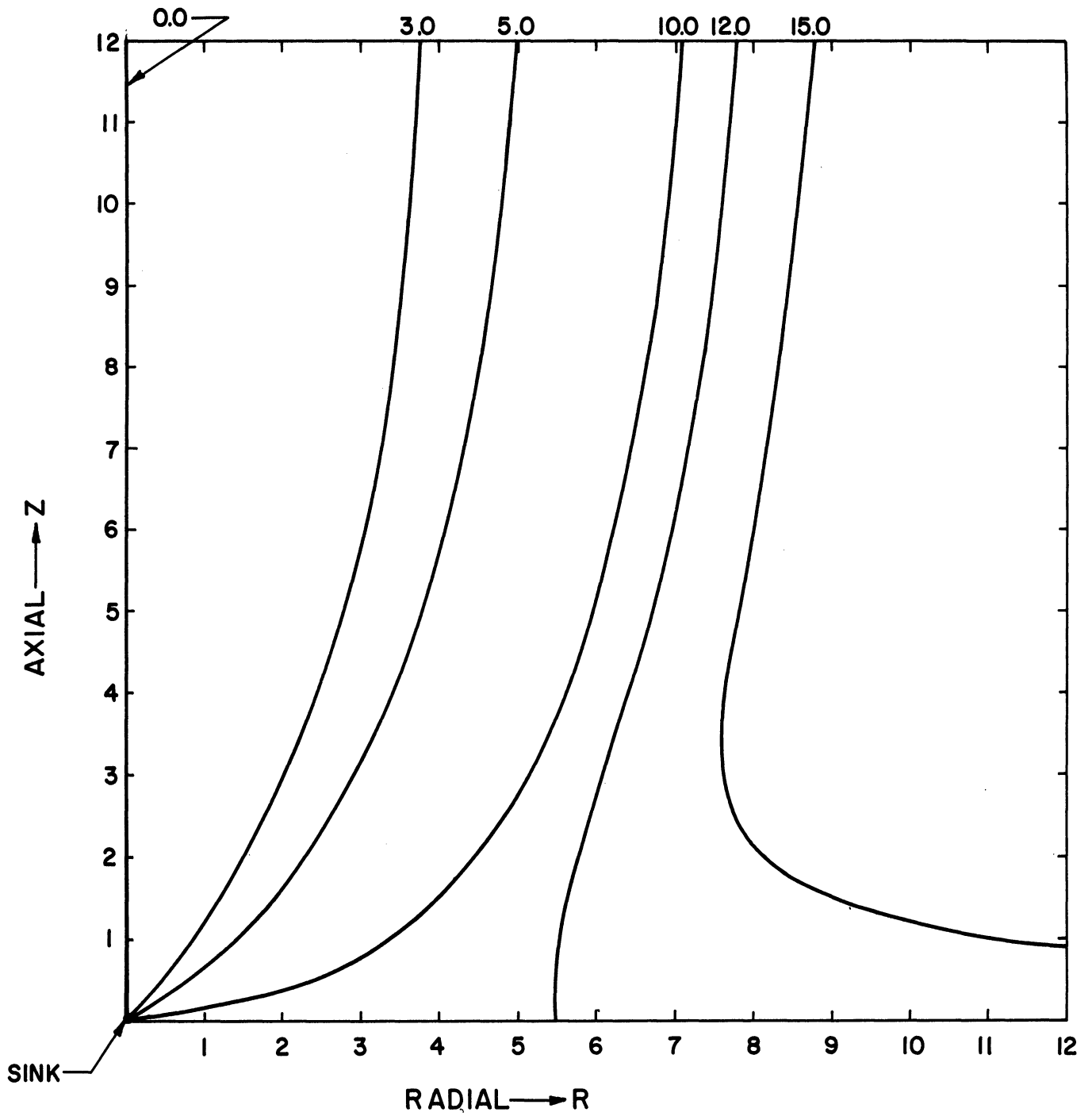


Figure A-8. Streamlines for $\beta = 12.0$.

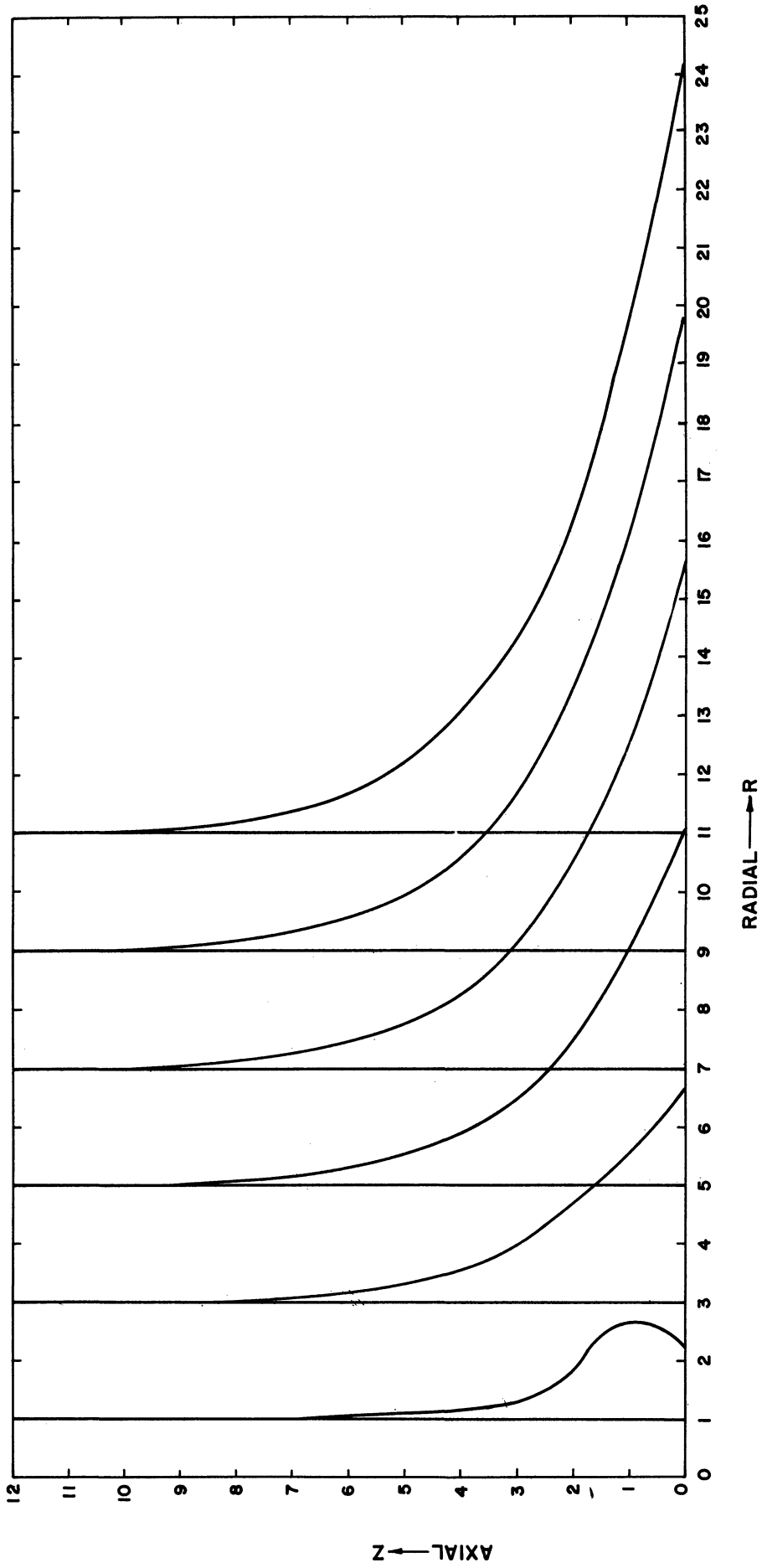


Figure A-9. Tangential Velocities (V) for $\beta = 3.0$.

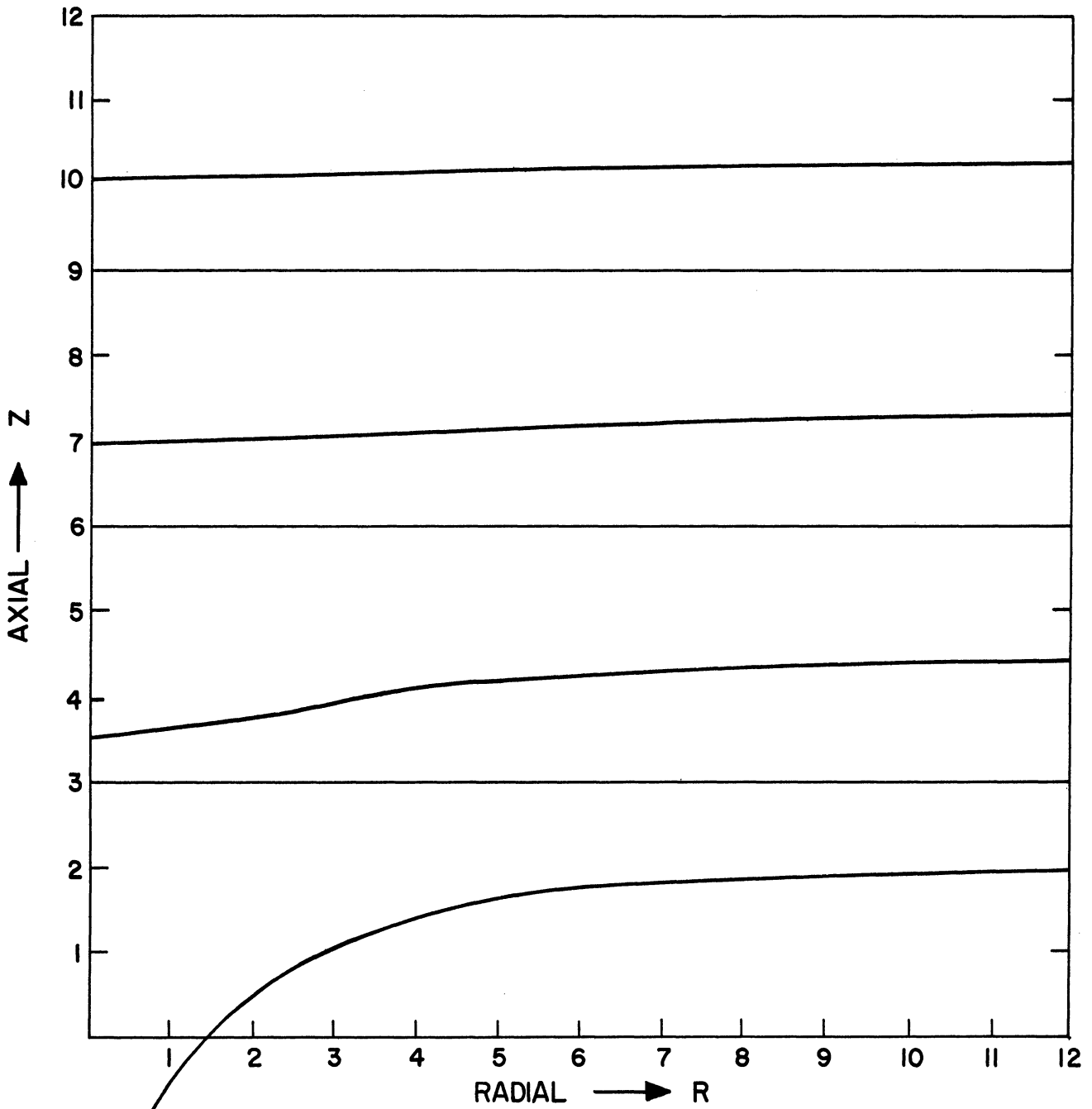


Figure A-10. Vertical Velocities (W) for $\beta = 3.0$.

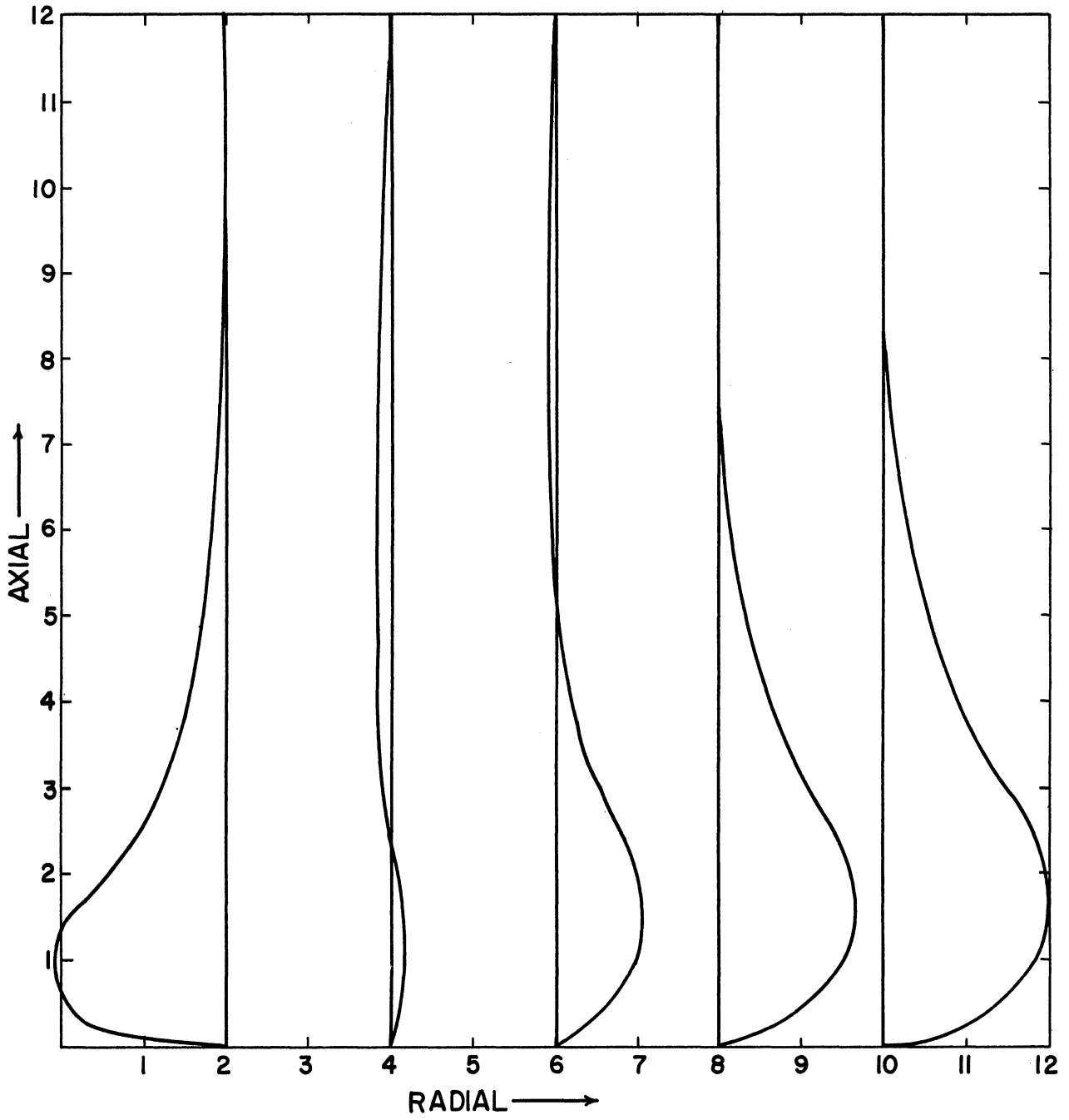


Figure A-11. Radial Velocities (U) for $\beta = 3.0$.

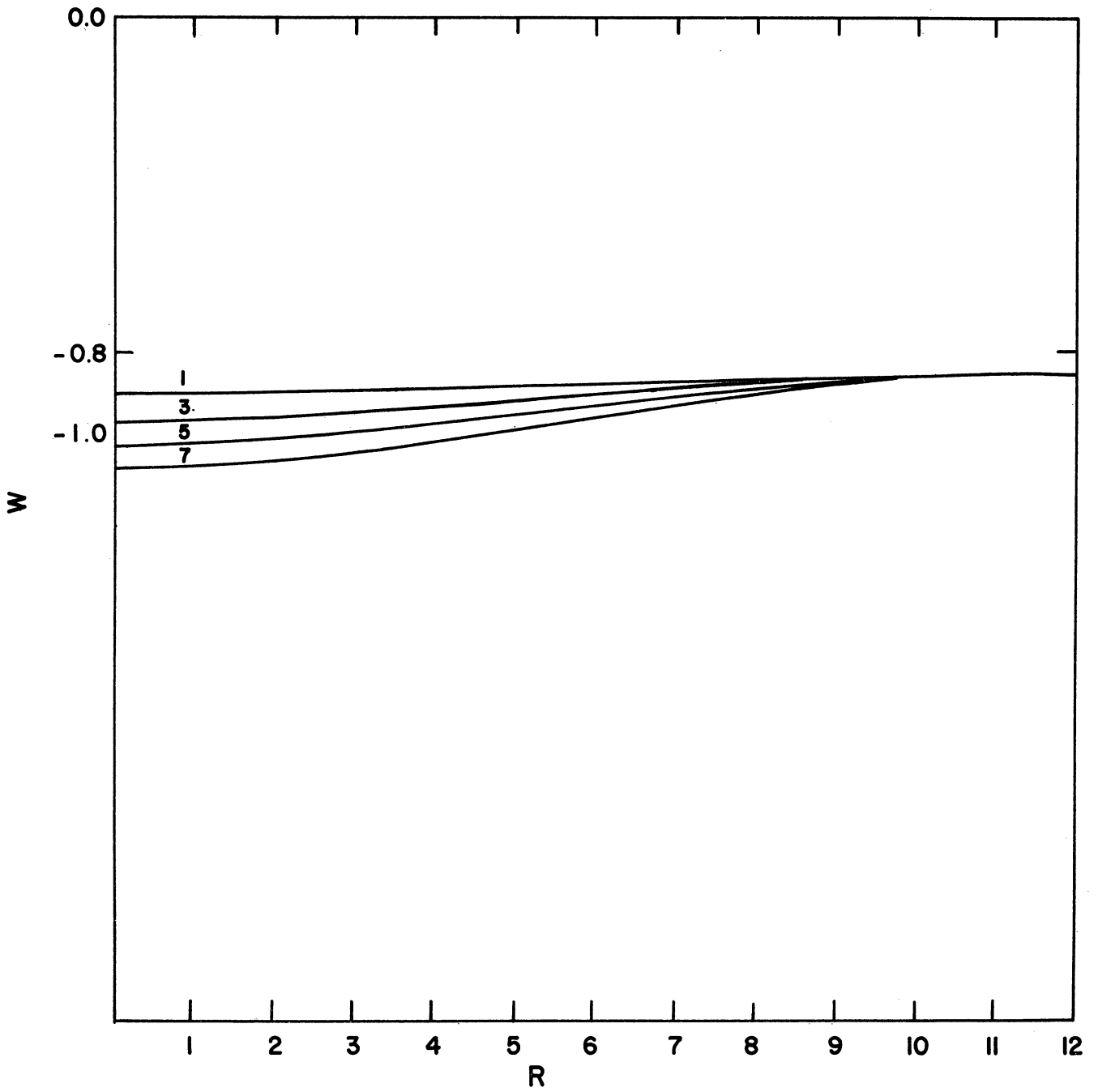


Figure A-12. Axial Velocity (W) Profiles for Various Values of β at $Z = 7.2$.

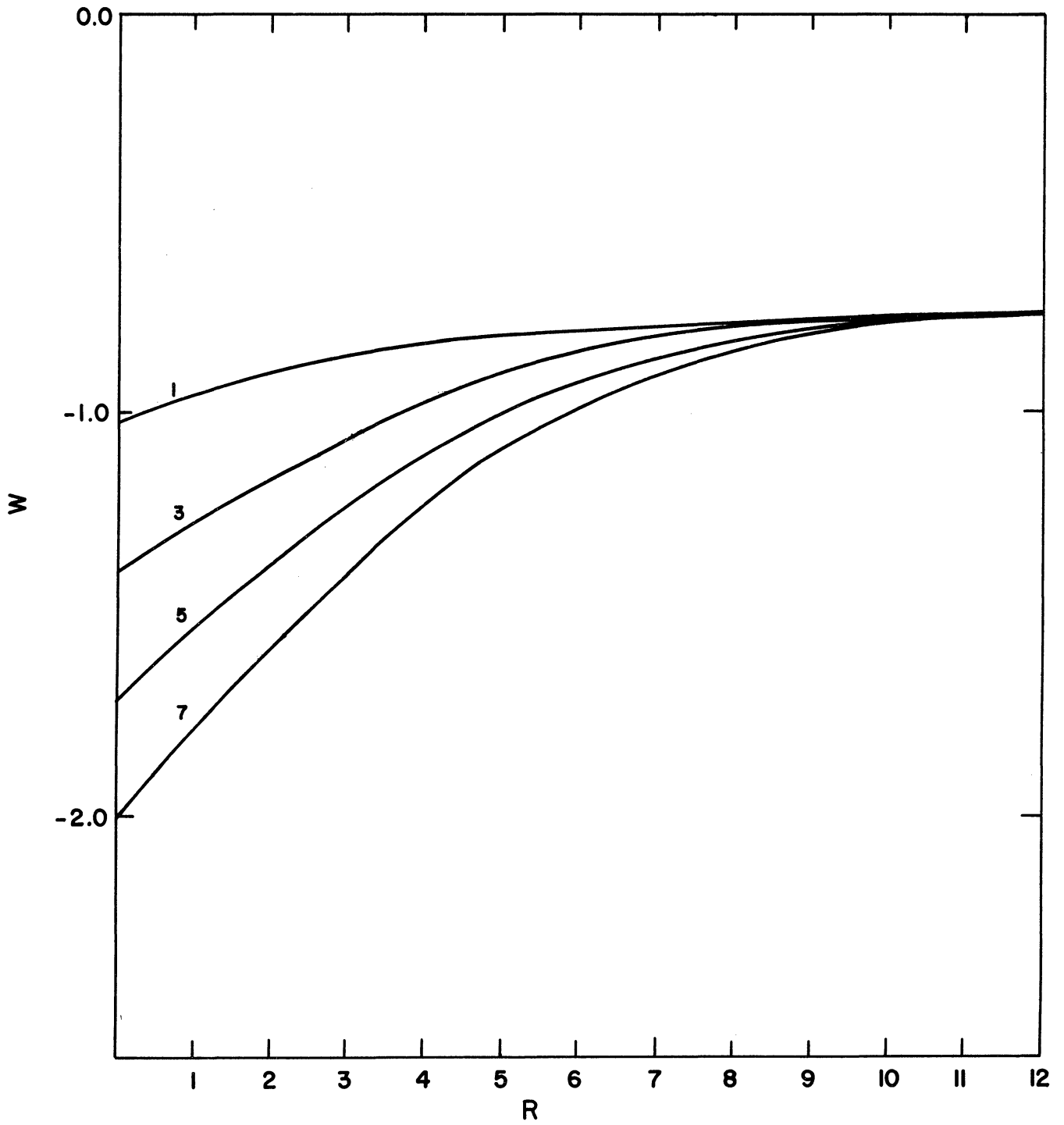


Figure A-13. Axial Velocity (W) Profiles for Various Values of β at $Z = 3.0$.

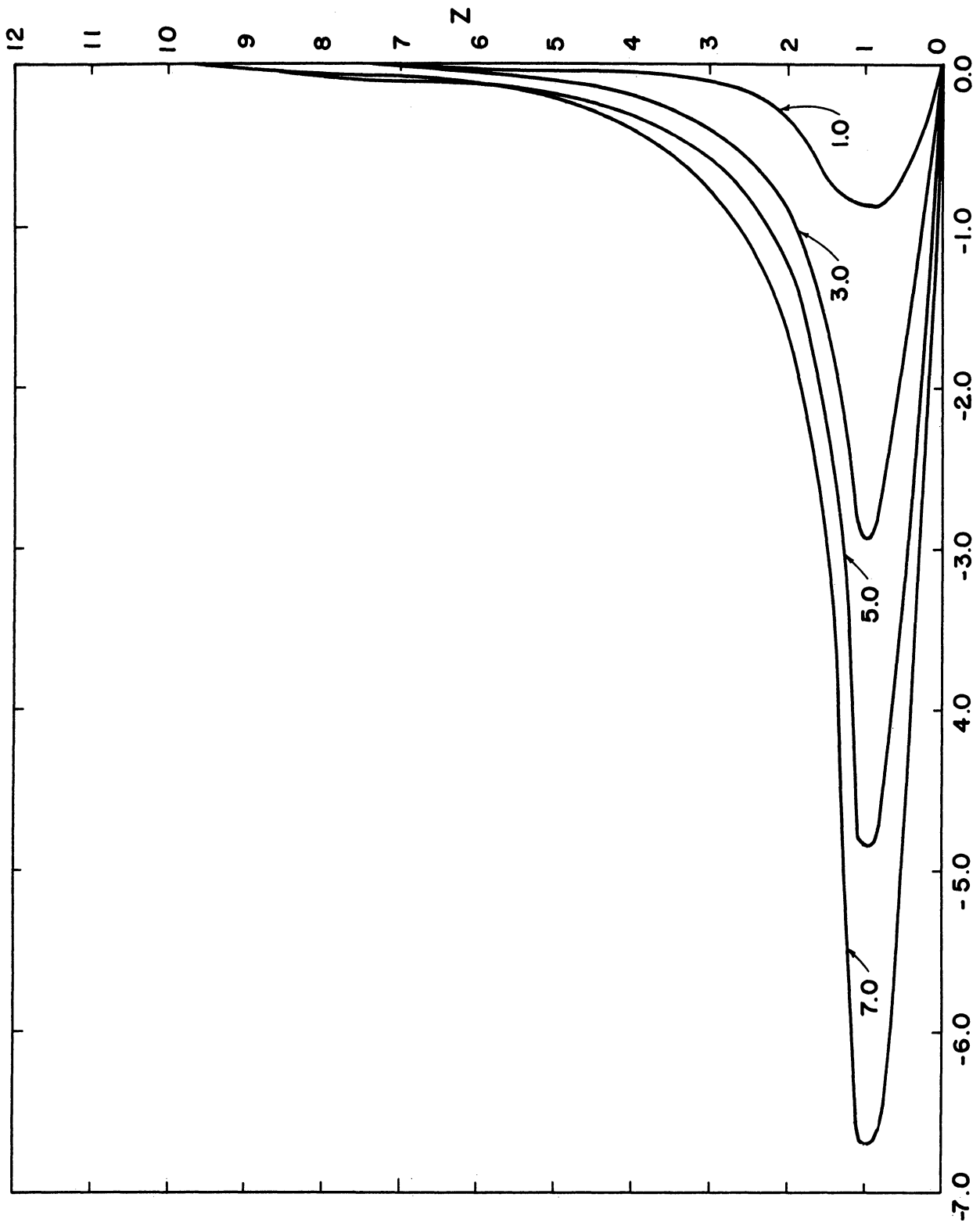


Figure A-14. Radial Velocity (U) Profiles Various Values of β at $R = 0.6$.

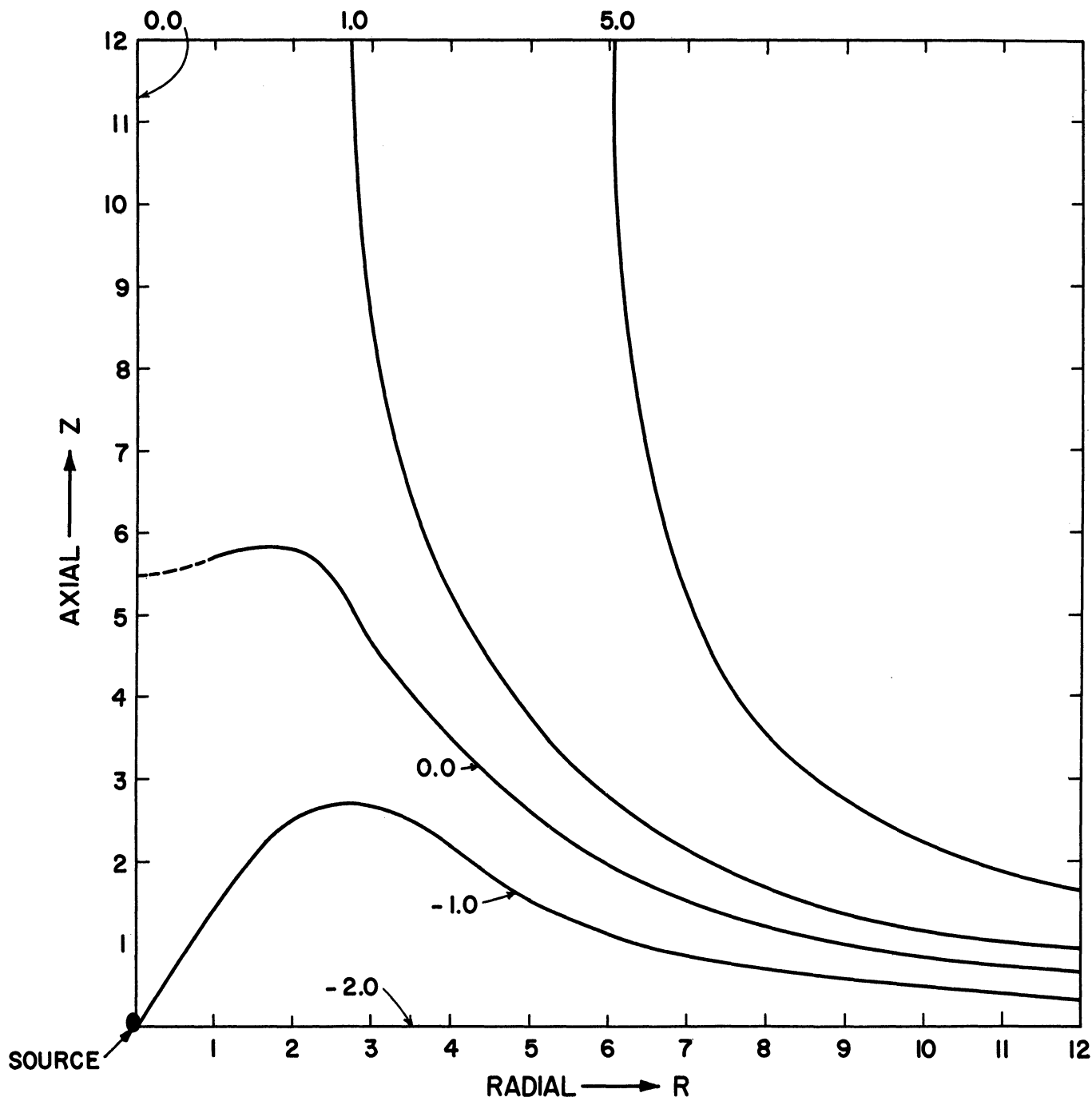


Figure A-15. Streamlines for $\beta = -2.0$.

APPENDIX B

COMPUTER PROGRAMS

The computer programs are in the MAD language and are given here. The data which must be submitted along with the main program (MAIN.001) and its subroutines is as follows:

Boolean Symbols

BB	Sets the value for BB1 and BB3 after the first time step.
BB1	Prints the current values of GAMMAS and GAMMAP.
BB2	Transfers to START and transfers to NINTH.
BB3	Prints the current values of VSTAR and VPRIME.
BB4	Prints the current values of A, PSI, and DELTA for each iteration.
BB5	Transfers to FIRST.
BB6	Increases the value of ITMAX and calculates PSI for a more accurate estimate.
BB7	Prints current values of U and W.
BB8	Transfers to NINTH. Reads and prints previously computed values of BETA, PSI, U, V, W, and GAMMA from a punched deck obtained from a previous run.
BB9	Prints U, V, W, GAMMA, PSI every DIT time step.
BBFINE	Changes to a finer grid.
BBFIX	Prints I, J, PSI, U, V, W, and GAMMA for fixed increments of I and J at intermediate time steps.
BBMAIN	Prints and punches I, J, PSI, U, V, W, and GAMMA for steady state.
BBPSI	Prints PSI and DELTA for each time step.
BBSLCT	Prints I, J, PSI, U, V, W, and GAMMA for selected values of I and J.

BBSKIP Transfers to NINTH and then to SECOND.
BPUNCH Punches steady state values.
BVTOP Sets the values for $V(I, JMAX)$.
BZEROU Sets $U(IMAX, J) = 0$.
BZEROV Sets $V(IMAX, J) = 0$.
BZEROW Sets $W(IMAX, J) = 0$.
GAMTOP Computes $GAMMA(I, JMAX)$.
VSTILL Sets $V(I, 0) = 0$.
VXI Sets the values for $V(IMAX, J)$.

Data

A Optimization parameter for the successive over-relaxation technique.
BETA Value of the stream function on the dividing streamline.
BETMAX Maximum value of BETA.
DBETA Increment of BETA.
DIM(0) = 2, JMAX + 3, JMAX + 1.
DIT Increment for ITER.
DITMAX Increases ITMAX and gives the maximum value for ITER.
DTAU Increment for time.
DXI Radial grid spacing.
DZETA Vertical grid spacing.
EPSI = 0.002
G Values of G from the von Kármán problem.
H Values of H from the von Kármán problem.

IEND	Last value of I for which intermediate values are printed.
IFOUR	Selected value of I for which intermediate values are printed.
IMAX	Number of grid spacings in the radial direction.
IONE	Selected value of I for which intermediate values are printed.
ISPACE	Increment of I for which intermediate values are printed.
ISTART	First value of I for which intermediate values are printed.
ITHREE	Selected value of I for which intermediate values are printed.
ITMAX	Maximum number of iterations for the successive over-relaxation technique.
ITONE	First value for ITER used in selecting the time step for which the intermediate values are to be printed.
ITWO	Selected value of I for which the intermediate values are printed.
JEND	Same as IEND, only for J.
JFOUR	Same as IFOUR, only for J.
JMAX	Same as IMAX, only for J.
JONE	Same as IONE, only for J.
JSPACE	Same as ISPACE, only for J.
JSTART	Same as ISTART, only for J.
JTWO	Same as ITWO, only for J.
RE	Inverse of the Reynolds number for the problem.
TAUMAX	Time for which steady state is reached.


```
$ COMPILE MAD, PRINT OBJECT, PUNCH OBJECT                                MAIN.001
RFLOW DUE TO A ROTATING DISC WITH A SINK
PROGRAM COMMON U,V,VSTAR,VPRIME,W,GAMMA,VSTILL, RE, PSI,AAA
1,CEE,DEE,CAPB,CAPC,DXI2I,IDXISQ,IDXZ,IDXICU,OVER2I,MINUSI,PL
2US2I,OIDXI,OIDXIS, H,G,A,IDXI,BB,DTAUD2,DXISQ,DXISQ2,DZE
3TSQ,DZETA2,DZETS2,DZSQI,DZETS4,PL2ARE,AOARE,DZETA6,DZET12,DXI
412,DXISQ1,DXI2,DXISQH,ARE,EPSI,BETA,DXI,DZETA,I,J,ITMAX,ITER
5,BB1,BB2,BB3,BBFINE,ISTART,JSTART,IEND,JEND
6,BB4,BB5,BB6,BB7,BB8,BB9
7,DIM,ANSW1,ANSW2,ANSW3,BETMAX,DBETA,DTAU,OLDATA,TAU,TAUMAX,DI
8TMAX,K,BEE,IMAX,JMAX,LIMAX,LJMAX,ENDBET
9,BBPSI,ENDTAU,SPACE
DIMENSION U(1900,DIM),V(1900,DIM),VSTAR(1900,DIM),VPRIME(1900
1,DIM),W(1900,DIM),GAMMA(1900,DIM),GAMMAS(1900,DIM),GAMMAP(190
20,DIM),PSI(1900,DIM),DELTA(1900,DIM),AAA(250),CEE(250),DEE(25
30),CAPB(250),CAPC(250),DXI2I(250),IDXISQ(250),IDXZ(250),IDXI
4CU(250),OVER2I(250),MINUSI(250),PLUS2I(250),OIDXI(250),OIDXIS
5(250),H(50),G(50),A(11),IDXI(250)
6,DIM(3)
EQUIVALENCE (VSTAR(0),GAMMAS(0)),(VPRIME(0),GAMMAP(0)),
1(GAMMAP(0),DELTA(0))
INTEGER IMAX,JMAX,DITMAX,LIMAX,LJMAX
BOOLEAN BPUNCH
BOOLEAN BZEROW,VXI,BZEROV,BZEROU,GAMTOP,BVTOP
BOOLEAN BBFINE
BOOLEAN BBSKIP
INTEGER IEND,JEND
INTEGER IONE,ITWO,ITHREE,IFOUR
INTEGER JONE,JTWO,JTHREE,JFOUR
INTEGER DIT,ITONE
INTEGER ISTART,JSTART,ISPACE,JSPACE
INTEGER I,J,K,ITMAX,ITER
VECTOR VALUES SPACE=$5HDXI= E13.6,7HDZETA= E13.6*$
VECTOR VALUES ENDTAU=$5HTAU= E13.6,6HDTAU= E13.6*$
VECTOR VALUES OLDDATA=$(2I3,5E13.6)*$
VECTOR VALUES ENDBET=$6HBETA= E13.6*$
VECTOR VALUES ANSW1=$(S2,I3,S1,I3,5E16.6)*$
VECTOR VALUES ANSW2=$(2I3,5E13.6)*$
VECTOR VALUES ANSW3=$1H6,S3,1HI,S3,1HJ,S10,3HPSI,S13,1HU,S14,
11HV,S15,1HW,S14,5HGAMMA//*$
BOOLEAN BB,BB1,BB2,BB3,BB4,BB5,BB6,BB7,BB8,BB9
BOOLEAN VSTILL
BOOLEAN BBMAIN,BBFIX,BBSLCT
BOOLEAN BBPSI
FIRST READ AND PRINT DATA
WHENEVER BB8
READ FORMAT ENDBET, BETA
READ FORMAT ENDTAU,TAU,DTAU
READ FORMAT SPACE,DXI,DZETA
PRINT RESULTS BETA
PRINT RESULTS TAU,DTAU,DXI,DZETA
THROUGH OLDA, FOR I=0,1,I.G.IMAX
THROUGH OLDA, FOR J=0,1,J.G.JMAX
OLDA READ FORMAT OLDDATA,I,J,PSI(I,J),U(I,J),V(I,J),W(I,J),GAMMA(I,
1J)
PRINT FORMAT ANSW3
THROUGH OLD, FOR I=0,1,I.G.IMAX
THROUGH OLD, FOR J=0,1,J.G.JMAX
OLD PRINT FORMAT ANSW1,I,J,PSI(I,J),U(I,J),V(I,J),W(I,J),GAMMA(I,
```

```
1J)
  END OF CONDITIONAL
RCOMPUTE CONSTANTS
  WHENEVER BBFINE
  DTAU=DTAU/4.0
  DXI=DXI/2.0
  DZETA=DZETA/2.0
  END OF CONDITIONAL
  DTAUD2=2.0/DTAU
  DXISQ=DXI*DXI
  DZETSQ=DZETA*DZETA
RCOMPUTE VALUES FOR A FINER GRID
  WHENEVER BBFINE
  EXECUTE BEGIN.
  PRINT FORMAT ANSW3
  THROUGH FINE, FOR I=0,1,I.G.IMAX
  THROUGH FINE, FOR J=0,1,J.G.JMAX
FINE  PRINT FORMAT ANSW1,I,J,PSI(I,J),U(I,J),V(I,J),W(I,J),
1GAMMA(I,J)
  TRANSFER TO SKIP
  END OF CONDITIONAL
  IDXI(0)=0.0
  DXI2I(0)=0.0
  IDXISQ(0)=0.0
  IDXDZ(0)=0.0
  IDXICU(0)=0.0
  OVER2I(0)=0.0
  MINUSI(0)=0.0
  PLUS2I(0)=0.0
  OIDXI(0)=0.0
  OIDXIS(0)=0.0
  THROUGH REPEAT, FOR I=1,1,I.G.IMAX
  IDXI(I)=I*DXI
  DXI2I(I)=1.0/(2.0*IDXI(I)*DXI)
  IDXISQ(I)=IDXI(I)*IDXI(I)
  IDXDZ(I)=IDXI(I)*DZETA
  IDXICU(I)=IDXI(I)*DXISQ
  OVER2I(I)=1.0/(2.0*I)
  MINUSI(I)=1.0-OVER2I(I)
  PLUS2I(I)=1.0+OVER2I(I)
  OIDXI(I)=1.0/IDXI(I)
REPEAT OIDXIS(I)=OIDXI(I)*OIDXI(I)
SKIP  DXISQ2=2.0/DXISQ
  DZETA2=2.0*DZETA
  DZETS2=2.0*DZETSQ
  DZSQI=1.0/DZETSQ
  DZETS4=4.0/DZETS2
  ARE=DXISQ/DZETSQ
  PL2ARE=2.0*(1.0+ARE)
  DZETA6=6.0*DZETA
  DZET12=12.0*DZETA
  DXI12=12.0*DXI
  DXISQ1=DXISQ2/2.0
  DXI2=2.0*DXI
  DXISQH=DXISQ1/2.0
  DXI1=1.0/DXI
  LIMAX=IMAX-1
  LJMAX=JMAX-1
  WHENEVER BBFINE
```

```
      TAU=0.0
      TRANSFER TO NINTH
      END OF CONDITIONAL
      WHENEVER BBSKIP,TRANSFER TO NINTH
R COMPUTE PSI, V, OR VALUES FOR A FINER GRID
      EXECUTE BEGIN.
      WHENEVER BVTOP
      THROUGH TOPV,FOR I=1,1,I.E.IMAX
TOPV      V(I,JMAX)=IDXI(I)
      END OF CONDITIONAL
      WHENEVER BZEROW
      THROUGH WWALL,FOR J=1,1,J.G.JMAX
WWALL    W(IMAX,J)=0.0
      END OF CONDITIONAL
      WHENEVER VXI
      THROUGH BVXI,FOR J=1,1,J.G.JMAX
BVXI     V(IMAX,J)=IDXI(IMAX)
      OR WHENEVER BZEROV
      THROUGH VEZERO,FOR J=1,1,J.G.JMAX
VEZERO   V(IMAX,J)=0.0
      OTHERWISE
      CONTINUE
      END OF CONDITIONAL
      WHENEVER BZEROU
      THROUGH UEZERO,FOR J=1,1,J.G.JMAX
UEZERO   U(IMAX,J)=0.0
      END OF CONDITIONAL
FOURTH   TAU=0.0
      WHENEVER BB2, TRANSFER TO START
NINTH    BB2=0B
      WHENEVER BBSKIP,TRANSFER TO SECOND
      THROUGH EIGHTH,FOR I=0,1,I.G.IMAX
EIGHTH   PSI(I,0)=BETA
      WHENEVER BZEROW.AND.BZEROU
      THROUGH ZEROW,FOR J=1,1,J.G.JMAX
ZEROW    PSI(IMAX,J)=BETA
      OTHERWISE
      JMAXSQ=1.0/(JMAX*JMAX)
      THROUGH ENDPSI,FOR J=1,1,J.G.JMAX
      DELTA(IMAX,J)=PSI(IMAX,J)+(1.0-J*J*JMAXSQ)*BETA
      WHENEVER PSI(IMAX,J+1).G.DELTA(IMAX,J)
      PSI(IMAX,J)=DELTA(IMAX,J)
      OTHERWISE
      TRANSFER TO SECOND
      END OF CONDITIONAL
ENDPSI   CONTINUE
      END OF CONDITIONAL
      BBSKIP=1B
SECOND   TAU=TAU+DTAU
      PRINT RESULTS TAU
      RCOMPUTE OPTIMUM VALUE OF A
      EXECUTE AOPT.
      WHENEVER BB5,TRANSFER TO FIRST
      WHENEVER BBFINE,TRANSFER TO START
      WHENEVER BZEROU,TRANSFER TO ENDU
      THROUGH UEND,FOR J=1,1,J.E.JMAX
UEND     U(IMAX,J)=OIDXI(IMAX)*(PSI(IMAX,J+1)-PSI(IMAX,J-1))/DZETA2
      1*RE.P.1.5
ENDU     CONTINUE
```

```

        THROUGH PSITOP, FOR I=1,1,I.G.IMAX
PSITOP  PSI(I,JMAX)=(4.0*PSI(I,LJMAX)-PSI(I,JMAX-2))/3.0
        WHENEVER BZEROW.AND.BZEROU, TRANSFER TO SOLID
        THROUGH PSIEND, FOR VALUES OF I=IMAX
        THROUGH PSIEND, FOR J=1,1,J.E.JMAX
PSIEND  PSI(I,J)=0.5*(5.0*PSI(I-1,J)-4.0*PSI(I-2,J)
        1+PSI(I-3,J)+(3.0*PSI(I,J)-4.0*PSI(I-1,J)+PSI(I-2,J))*0.5/I)
SOLID   CONTINUE
        THROUGH GWTOP, FOR VALUES OF J=JMAX
        THROUGH GWTOP, FOR I=1,1,I.E.IMAX
        WHENEVER I.E.1
        W(1,J)=-OIDXI(I)*(-2.0*PSI(0,J)-3.0*PSI(1,J)+6.0*PSI(2,J)-PSI
        1(3,J))/(6.0*DXI)
        2*RE.P.1.5
        OR WHENEVER I.G.1.AND.I.L.LIMAX
        W(I,J)=-OIDXI(I)*(PSI(I-2,J)-8.0*PSI(I-1,J)+8.0*PSI(I+1,J)-PS
        1I(I+2,J))/DXI12
        2*RE.P.1.5
        OTHERWISE
        W(I,J)=-OIDXI(I)*(2.0*PSI(I+1,J)+3.0*PSI(I,J)-6.0*PSI(I-1,J)+
        1PSI(I-2,J))/(6.0*DXI)
        2*RE.P.1.5
        END OF CONDITIONAL
        WHENEVER GAMTOP
        GAMMA(I,J)=((PSI(I+1,J)-2.0*PSI(I,J)+PSI(I-1,J))/IDXICU(I)-
        1(PSI(I+1,J)-PSI(I-1,J))*DXI2I(I)/IDXI(I)+0.5*DZSQI*(
        28.0*PSI(I,J-1)-7.0*PSI(I,J)-PSI(I,J-2))
        3*OIDXI(I)
        4)*RE.P.1.5
        END OF CONDITIONAL
GWTOP   CONTINUE
        THROUGH CORNER , FOR VALUES OF I=IMAX
        THROUGH CORNER , FOR VALUES OF J=JMAX
        WHENEVER GAMTOP
        GAMMA(I,J)=((2.*PSI(I,J)-5.0*PSI(I,J-1)+4.0*PSI(I,J-2)-PSI(I,
        1J-3))*OIDXI(I)*DZSQI+
        2          0.5*(PSI(I,J)-PSI(I-1,J)-PSI(I-2,J)+PSI(I-3,J))/
        3IDXICU(I)-DXI2I(I)*(2.0*PSI(I,J)-PSI(I-1,J)-2.0*PSI(I-2,J)+PS
        4I(I-3,J))*OIDXI(I)
        5)*RE.P.1.5
        END OF CONDITIONAL
CORNER  CONTINUE
START   CONTINUE
        R COMPUTE NEW U AND W VALUES AND NEW GAMMA(I,0) (I.E. DISC) VA
        RLUES
        EXECUTE SUBUWG.
        WHENEVER BBFINE, TRANSFER TO EXVEE
        WHENEVER BZEROW, TRANSFER TO WENDO
        THROUGH WEND, FOR J=1,1,J.G.JMAX
WEND    W(IMAX,J)=W(LIMAX,J)
WENDO   CONTINUE
        THROUGH NGAM, FOR VALUES OF I=IMAX
        THROUGH NGAM, FOR J=1,1,J.E.JMAX
NGAM    GAMMA(I,J)=OIDXI(I)*(RE.P.1.5)*(PSI(I,J+1)-2.0*PSI(I,J)+
        1PSI(I,J-1))*DZSQI
        WHENEVER BB2, TRANSFER TO NINTH
        R COMPUTE NEW V VALUES
        WHENEVER BB3, PRINT COMMENT$1 VSTAR(0,0)...VSTAR(IMAX,JMAX)
        1 FOLLOWED BY VPRIME(0,0)...VPRIME(IMAX,JMAX)$

```

```
EXVEE    EXECUTE SUBV.
          WHENEVER BBFINE,TRANSFER TO EXGAM
          WHENEVER VXI,TRANSFER TO EXGAM
          WHENEVER BZEROV,TRANSFER TO EXGAM
          THROUGH VEND, FOR VALUES OF I=IMAX
          THROUGH VEND, FOR J=1,1,J.E.JMAX
VEND     V(I,J)=(3.0*DXI*OIDXI(I)*V(I,J)+9.0*V(I-1,J)-4.5*V(I-2,J)+
          1V(I-3,J))/5.5
          R COMPUTE NEW GAMMA VALUES
          WHENEVER BB1, PRINT COMMENT$1 GAMMAS(0,0)...GAMMAS(IMAX,JMAX)
          1 FOLLOWED BY GAMMAP(0,0)...GAMMAP(IMAX,JMAX)$
EXGAM    EXECUTE SUBG.
          WHENEVER BB9
          THROUGH SIXTH, FOR ITER=ITONE,DIT,ITER.G.DITMAX
          WHENEVER TAU .G. ITER*DTAU-EPSI .AND. TAU .L. ITER*DTAU+EPSI
          PRINT RESULTS TAU,DTAU,DXI,DZETA
          PRINT FORMAT ANSW3
          WHENEVER BBSLCT
          THROUGH TENTH, FOR VALUES OF I=IONE,ITWO,ITHREE,IFOUR
          THROUGH TENTH, FOR VALUES OF J=JONE,JTWO,JTHREE,JFOUR
TENTH    PRINT FORMAT ANSW1,I,J,PSI(I,J),U(I,J),V(I,J),W(I,J),GAMMA(I,
          1J)
          END OF CONDITIONAL
          WHENEVER BBFIX
          THROUGH THIRD, FOR I=ISTART,ISPACE,I.G.IEND
          THROUGH THIRD, FOR J=JSTART,JSPACE,J.G.JEND
THIRD    PRINT FORMAT ANSW1,I,J,PSI(I,J),U(I,J),V(I,J),W(I,J),GAM
          1MA(I,J)
          END OF CONDITIONAL
          TRANSFER TO SEVEN
          END OF CONDITIONAL
SIXTH    CONTINUE
          END OF CONDITIONAL
SEVEN    WHENEVER TAU.L.TAUMAX, TRANSFER TO SECOND
          WHENEVER BBMAIN
          PRINT COMMENT$1 STEADY STATE VALUES $
          PRINT RESULTS TAU,DTAU,DXI,DZETA
          PRINT RESULTS BETA
          WHENEVER BPUNCH
          PUNCH FORMAT ENDBET,BETA
          PUNCH FORMAT ENDTAU,TAU,DTAU
          PUNCH FORMAT SPACE,DXI,DZETA
          THROUGH PUNCH, FOR I=0,1,I.G.IMAX
          THROUGH PUNCH, FOR J=0,1,J.G.JMAX
PUNCH    PUNCH FORMAT ANSW2,I,J,PSI(I,J),U(I,J),V(I,J),W(I,J),GAMM
          1A(I,J)
          END OF CONDITIONAL
          PRINT FORMAT ANSW3
          THROUGH FINAL, FOR I=0,1,I.G.IMAX
          THROUGH FINAL, FOR J=0,1,J.G.JMAX
FINAL    PRINT FORMAT ANSW1,I,J,PSI(I,J),U(I,J),V(I,J),W(I,J),GAM
          1MA(I,J)
          END OF CONDITIONAL
          WHENEVER .ABS.BETA .G. BETMAX, TRANSFER TO FIFTH
          BETA=BETA+DBETA
          BBSKIP=0B
          TRANSFER TO FOURTH
FIFTH    TRANSFER TO FIRST
          END OF PROGRAM
```

```
$COMPILE MAD, PRINT OBJECT, PUNCH OBJECT                                COEFF001
    DIMENSION RZERO(100),A(2000,DIM),BETA(100),BETA1(100),BETA2(
    1100),SMALLA(100),DUMMY(100),DIM(3)
    INTEGER I,J,M,N
    VECTOR VALUES TITLE=$S3,1HI,S5,6HSMALLA*$
    VECTOR VALUES ANSWER=$S2,I2,E13.6*$
START   READ AND PRINT DATA
        N=DIM(2)
        M=DIM(2)
        THROUGH NEWR, FOR I=1,1,I.G.N
NEWR    RZERO(I)=RZERO(I)+DEL R*(BETA(I)-BETA1(I))/(BETA2(I)-BETA1(I))
        THROUGH ONE, FOR I=1,1,I.G.N
        THROUGH ONE, FOR J=1,1,J.G.N
ONE     A(I,J)=RZERO(I).P.J
        R=SLE.(N,M,A(1,1),SMALLA(1),BETA(1),DUMMY(1),0)
        PRINT RESULTS R
        PRINT RESULTS M,N,RZERO(1)...RZERO(N),BETA(1)...BETA(N)
        PRINT FORMAT TITLE
        THROUGH END, FOR J=1,1,J.G.N
END     PRINT FORMAT ANSWER,J,SMALLA(J)
        TRANSFER TO START
        END OF PROGRAM
```

```
$COMPILE MAD, PRINT OBJECT, PUNCH OBJECT                                EXPON001
    INTEGER I,IMAX
    DIMENSION RZERO(100),BETA(100),BETA1(100),BETA2(100),ALPHA(10
    10),C(100)
    VECTOR VALUES VALUE=$(S2,I3,S4,4E16.6)*$
    VECTOR VALUES LABEL=$1H6,S3,1HI,S13,4HBETA,S11,5HRZERO,S10,5H
    1ALPHA,S13,1HC//*$
    VECTOR VALUES TITLE=$S46,40HCOMPUTED VALUES FOR THE EXPONENT
    10F BETA//*$
    READ AND PRINT DATA
    THROUGH NEWR, FOR I=1,1,I.G.IMAX
NEWR    RZERO(I)=RZERO(I)+DEL R*(BETA(I)-BETA1(I))/(BETA2(I)-BETA1(I))
        THROUGH ALPHAC, FOR I=1,1,I.E.IMAX
        ALPHA(I)=(ELOG.(RZERO(I+1))-ELOG.(RZERO(I)))/(ELOG.(BETA(I+1)
        1)-ELOG.(BETA(I)))
ALPHAC C(I)=RZERO(I)*(BETA(I).P.-ALPHA(I))
        PRINT FORMAT TITLE
        PRINT FORMAT LABEL
        THROUGH ANSWER, FOR I=1,1,I.E.IMAX
ANSWER PRINT FORMAT VALUE,I,BETA(I),RZERO(I),ALPHA(I),C(I)
        END OF PROGRAM
```

```
$ COMPILE MAD, PRINT OBJECT, PUNCH OBJECT
```

```
RCOMPUTE INITIAL VALUES OF PSI, V, AND GAMMA
EXTERNAL FUNCTION
PROGRAM COMMON U,V,VSTAR,VPRIME,W,GAMMA,VSTILL, RE, PSI,AAA
1,CEE,DEE,CAPB,CAPC,DXI2I,IDXISQ,IDXIDZ,IDXICU,OVER2I,MINUSI,PL
2US2I,OIDXI,OIDXIS, H,G,A,IDX1,BB,DTAUD2,DXISQ,DXISQ2,DZE
3TSQ,DZETA2,DZETS2,DZSQI,DZETS4,PL2ARE,AOARE,DZETA6,DZET12,DXI
412,DXISQ1,DXI2,DXISQH,ARE,EPSI,BETA,DXI,DZETA,I,J,ITMAX,ITER
5,BB1,BB2,BB3,BBFINE,ISTART,JSTART,IEND,JEND
6,BB4,BB5,BB6,BB7,BB8,BB9
7,DIM,ANSW1,ANSW2,ANSW3,BETMAX,DBETA,DTAU,OLDATA,TAU,TAUMAX,DI
8TMAX,K,BEE,IMAX,JMAX,LIMAX,LJMAX,ENDBET
9,BBPSI,ENDTAU,SPACE
DIMENSION U(1900,DIM),V(1900,DIM),VSTAR(1900,DIM),VPRIME(1900
1,DIM),W(1900,DIM),GAMMA(1900,DIM),GAMMAS(1900,DIM),GAMMAP(190
20,DIM),PSI(1900,DIM),DELTA(1900,DIM),AAA(250),CEE(250),DEE(25
30),CAPB(250),CAPC(250),DXI2I(250),IDXISQ(250),IDXIDZ(250),IDXI
4CU(250),OVER2I(250),MINUSI(250),PLUS2I(250),OIDXI(250),OIDXIS
5(250),H(50),G(50),A(11),IDX1(250)
6,DIM(3)
EQUIVALENCE (VSTAR(0),GAMMAS(0)),(VPRIME(0),GAMMAP(0)),
1(GAMMAP(0),DELTA(0))
INTEGER IMAX,JMAX,DITMAX,LIMAX,LJMAX
INTEGER ISTART, JSTART, IEND, JEND
INTEGER I,J,K,ITMAX,ITER
VECTOR VALUES SPACE=$5HDXI= E13.6,7HDZETA= E13.6*$
VECTOR VALUES ENDTAU=$5HTAU= E13.6,6HDTAU= E13.6*$
VECTOR VALUES OLDDATA=$(2I3,5E13.6)*$
VECTOR VALUES ENDBET=$6HBETA= E13.6*$
VECTOR VALUES ANSW1=$(S2,I3,S1,I3,5E16.6)*$
VECTOR VALUES ANSW2=$(2I3,5E13.6)*$
VECTOR VALUES ANSW3=$1H6,S3,1HI,S3,1HJ,S10,3HPSI,S13,1HU,S14,
11HV,S15,1HW,S14,5HGAMMA//*$
BOOLEAN BB,BB1,BB2,BB3,BB4,BB5,BB6,BB7,BB8,BB9
BOOLEAN BBPSI
BOOLEAN VSTILL
BOOLEAN BBFINE
ENTRY TO BEGIN.
THROUGH ONE, FOR J=0,1,J.G.JMAX
V(0,J)=0.0
U(0,J)=0.0
W(IMAX,J)=-H(J)
W(0,J)=0.0
U(IMAX,J)=0.0
GAMMA(0,J)=0.0
PSI(0,J)=0.0
THROUGH TWO, FOR I=0,1,I.G.IMAX
V(I,JMAX)=0.0
GAMMA(I,JMAX)=0.0
PSI(I,JMAX)=IDXISQ(I)*H(JMAX)/2.0
V(I,0)=IDX1(I)
WHENEVER VSTILL,V(I,0)=0.0
PSI(I,0)=0.0
U(I,0)=0.0
U(I,JMAX)=0.0
W(I,JMAX)=-0.886
W(I,0)=0.0
THROUGH THREE, FOR J=1,1,J.E.JMAX
THROUGH THREE, FOR I=1,1,I.G.IMAX
PSI(I,J)=IDXISQ(I)*H(J)/2.0
```

ONE

TWO

```

THREE      V(I,J)=IDXI(I)*G(J)
            THROUGH FOUR, FOR J=1,1,J.E.JMAX
            THROUGH FOUR, FOR I=1,1,I.E.IMAX
FOUR       GAMMA(I,J)=(PSI(I+1,J)-2.0*PSI(I,J)+PSI(I-1,J))/IDXICU(I)
            1-(PSI(I
            2+1,J)-PSI(I-1,J))*DXI2I(I)/IDXI(I)+(PSI(I,J+1)-2.0*PSI(I,J)+P
            3SI(I,J-1))*DZSQI/IDXI(I)
            THROUGH UIMAX, FOR VALUES OF I=IMAX
            THROUGH UIMAX, FOR J=1,1,J.E.JMAX
            WHENEVER J.E.1
            U(I,1)=OIDXI(I)*(-2.0*PSI(I,0)-3.0*PSI(I,1)+6.0*PSI(I,2)-PSI(
            1I,3))/DZETA6
            OR WHENEVER J.G.1.AND.J.L.LJMAX
            U(I,J)=OIDXI(I)*(PSI(I,J-2)-8.0*PSI(I,J-1)+8.0*PSI(I,J+1)-PSI
            1(I,J+2))/DZET12
            OTHERWISE
            U(I,J)=OIDXI(I)*(2.0*PSI(I,J+1)+3.0*PSI(I,J)-6.0*PSI(I,J-1)+P
            1SI(I,J-2))/DZETA6
UIMAX      END OF CONDITIONAL
            WHENEVER BB2, PRINT RESULTS PSI(0,0)...PSI(IMAX,JMAX)
            1,V(0,0)...V(IMAX,JMAX)
            FUNCTION RETURN
            END OF FUNCTION

```

```

$COMPILE MAD, PRINT OBJECT, PUNCH OBJECT                                AOPT.001
R COMPUTE A OPTIMUM
EXTERNAL FUNCTION
PROGRAM COMMON U,V,VSTAR,VPRIME,W,GAMMA,VSTILL,RE, PSI,AAA
1,CEE,DEE,CAPB,CAPC,DXI2I,IDXISQ,IDXIDZ,IDXICU,OVER2I,MINUSI,PL
2US2I,OIDXI,OIDXIS, H,G,A,IDXI,BB,DTAUD2,DXISQ,DXISQ2,DZE
3TSQ,DZETA2,DZETS2,DZSQI,DZETS4,PL2ARE,AOARE,DZETA6,DZET12,DXI
412,DXISQ1,DXI2,DXISQH,ARE,EPSI,BETA,DXI,DZETA,I,J,ITMAX,ITER
5,BB1,BB2,BB3,BBFINE,ISTART,JSTART,IEND,JEND
6,BB4,BB5,BB6,BB7,BB8,BB9
7,DIM,ANSW1,ANSW2,ANSW3,BETMAX,DBETA,DTAU,OLDDATA,TAU,TAUMAX,DI
8TMAX,K,BEE,IMAX,JMAX,LIMAX,LJMAX,ENDBET
9,BBPSI,ENDTAU,SPACE
DIMENSION U(1900,DIM),V(1900,DIM),VSTAR(1900,DIM),VPRIME(1900
1,DIM),W(1900,DIM),GAMMA(1900,DIM),GAMMAS(1900,DIM),GAMMAP(190
20,DIM),PSI(1900,DIM),DELTA(1900,DIM),AAA(250),CEE(250),DEE(25
30),CAPB(250),CAPC(250),DXI2I(250),IDXISQ(250),IDXIDZ(250),IDXI
4CU(250),OVER2I(250),MINUSI(250),PLUS2I(250),OIDXI(250),OIDXIS
5(250),H(50),G(50),A(11),IDXI(250)
6,DIM(3)
EQUIVALENCE (VSTAR(0),GAMMAS(0)),(VPRIME(0),GAMMAP(0)),
1(GAMMAP(0),DELTA(0))
INTEGER IMAX,JMAX,DITMAX,LIMAX,LJMAX
INTEGER I,J,K,ITMAX,ITER
INTEGER ISTART, JSTART, IEND, JEND
BOOLEAN VSTILL
BOOLEAN BBFINE
VECTOR VALUES ENDDTAU=$5HTAU= E13.6,6HDTAU= E13.6*$
VECTOR VALUES SPACE=$5HDXI= E13.6,7HDZETA= E13.6*$
VECTOR VALUES OLDDATA=$(2I3,5E13.6)*$
VECTOR VALUES ENDBET=$6HBETA= E13.6*$

```



```
VECTOR VALUES ANSW1=$(S2,I3,S1,I3,5E16.6)*$
VECTOR VALUES ANSW2=$(2I3,5E13.6)*$
VECTOR VALUES ANSW3=$1H6,S3,1HI,S3,1HJ,S10,3HPSI,S13,1HU,S14,
11HV,S15,1HW,S14,5HGAMMA//*$
BOOLEAN BB,BB1,BB2,BB3,BB4,BB5,BB6,BB7,BB8,BB9
BOOLEAN BBPSI
ENTRY TO AOPT.
K=0
AOARE=A(K)/PL2ARE
THROUGH KZERO , FOR ITER=1,1,ITER.G.ITMAX
THROUGH KZERO,FORJ=1,1,J.E.JMAX
THROUGH KZERO, FOR I=1,1,I.G.LIMAX
DELTA(I,J)=AOARE*(-IDXICU(I)*GAMMA(I,J)*RE.P.-1.5+PSI(I+1,J)
1*MINUSI(I)+
2PSI(I-1,J)*PLUS2I(I)+ARE*(PSI(I,J+1)+PSI(I,J-1))-PL2ARE*PSI(I
3,J))
KZERO PSI(I,J)=PSI(I,J)+DELTA(I,J)
FUNCTION RETURN
END OF FUNCTION
```

```
$COMPILE MAD, PRINT OBJECT, PUNCH OBJECT AOPT.101
R COMPUTE A OPTIMUM
EXTERNAL FUNCTION
PROGRAM COMMON U,V,VSTAR,VPRIME,W,GAMMA,VSTILL, RE, PSI,AAA
1,CEE,DEE,CAPB,CAPC,DXI2I,IDXISQ,IDXIDZ,IDXICU,OVER2I,MINUSI,PL
2US2I,OIDXI,OIDXIS, H,G,A,IDX1,BB,DTAUD2,DXISQ,DXISQ2,DZE
3TSQ,DZETA2,DZETS2,DZSQI,DZETS4,PL2ARE,AOARE,DZETA6,DZET12,DXI
412,DXISQ1,DXI2,DXISQH,ARE,EPSI,BETA,DXI,DZETA,I,J,ITMAX,ITER
5,BB1,BB2,BB3,BBFINE,ISTART,JSTART,IEND,JEND
6,BB4,BB5,BB6,BB7,BB8,BB9
7,DIM,ANSW1,ANSW2,ANSW3,BETMAX,DBETA,DTAU,OLDDATA,TAU,TAUMAX,DI
8TMAX,K,BEE,IMAX,JMAX,LIMAX,LJMAX,ENDBET
9,BBPSI,ENDTAU,SPACE
DIMENSION U(1900,DIM),V(1900,DIM),VSTAR(1900,DIM),VPRIME(1900
1,DIM),W(1900,DIM),GAMMA(1900,DIM),GAMMAS(1900,DIM),GAMMAP(190
20,DIM),PSI(1900,DIM),DELTA(1900,DIM),AAA(250),CEE(250),DEE(25
30),CAPB(250),CAPC(250),DXI2I(250),IDXISQ(250),IDXIDZ(250),IDXI
4CU(250),OVER2I(250),MINUSI(250),PLUS2I(250),OIDXI(250),OIDXIS
5(250),H(50),G(50),A(11),IDX1(250)
6,DIM(3)
EQUIVALENCE (VSTAR(0),GAMMAS(0)),(VPRIME(0),GAMMAP(0)),
1(GAMMAP(0),DELTA(0))
INTEGER IMAX,JMAX,DITMAX,LIMAX,LJMAX
INTEGER I,J,K,ITMAX,ITER
INTEGER ISTART, JSTART, IEND, JEND
BOOLEAN BBFINE
VECTOR VALUES ENDTAU=$5HTAU= E13.6,6HDTAU= E13.6*$
VECTOR VALUES SPACE=$5HDXI= E13.6,7HDZETA= E13.6*$
VECTOR VALUES OLDDATA=$(2I3,5E13.6)*$
VECTOR VALUES ENDBET=$6HBETA= E13.6*$
VECTOR VALUES ANSW1=$(S2,I3,S1,I3,5E16.6)*$
VECTOR VALUES ANSW2=$(2I3,5E13.6)*$
VECTOR VALUES ANSW3=$1H6,S3,1HI,S3,1HJ,S10,3HPSI,S13,1HU,S14,
11HV,S15,1HW,S14,5HGAMMA//*$
```

```

      BOOLEAN BB, BB1, BB2, BB3, BB4, BB5, BB6, BB7, BB8, BB9
      BOOLEAN VSTILL
      BOOLEAN BBPSI
      ENTRY TO AOPT.
      THROUGH STORE, FOR I=0,1,I.G.IMAX
      THROUGH STORE, FOR J=0,1,J.G.JMAX
STORE   VSTAR(I,J)=PSI(I,J)
      THROUGH AFTER, FOR K=0,1,K.G.10
      AOARE=A(K)/PL2ARE
      THROUGH CHANGE, FOR I=0,1,I.G.IMAX
CHANGE  THROUGH CHANGE, FOR J=0,1,J.G.JMAX
      PSI(I,J)=VSTAR(I,J)
      THROUGH NEXTIT, FOR ITER=1,1,ITER.G.ITMAX
      THROUGH NEXTX, FOR I=1,1,I.G.LIMAX
      THROUGH NEXTX, FOR J=1,1,J.E.JMAX
      DELTA(I,J)=AOARE*(-IDXICU(I)*GAMMA(I,J)*RE.P.-1.5+PSI(I+1,J)
1*MINUSI(I)+
2PSI(I-1,J)*PLUS2I(I)+ARE*(PSI(I,J+1)+PSI(I,J-1))-PL2ARE*PSI(I
3,J))
NEXTX   PSI(I,J)=PSI(I,J)+DELTA(I,J)
NEXTIT  WHENEVER BB4, PRINT RESULTS ITER,A(K),PSI(0,0)...PSI(IMAX,
1JMAX),DELTA(0,0)...DELTA(IMAX,JMAX)
AFTER   PRINT RESULTS A(K),PSI(0,0)...PSI(IMAX,JMAX),DELTA(0,0)...
1DELTA(IMAX,JMAX)
      WHENEVER BBPSI, PRINT RESULTS A(K),PSI(0,0)...PSI(IMAX,JMAX),
1DELTA(0,0)...DELTA(IMAX,JMAX)
      WHENEVER BB6
      THROUGH MANYIT, FOR I=0,1,I.G.IMAX
      THROUGH MANYIT, FOR J=0,1,J.G.JMAX
MANYIT  PSI(I,J)=VSTAR(I,J)
      THROUGH AFTERA, FOR VALUES OF K=5
      AOARE=A(K)/PL2ARE
      ITMAX=ITMAX+DITMAX
      THROUGH NEXTXA, FOR ITER=1,1,ITER.G.ITMAX
      THROUGH NEXTXA, FOR I=1,1,I.E.IMAX
      THROUGH NEXTXA, FOR J=1,1,J.E.JMAX
      DELTA(I,J)=AOARE*(-IDXICU(I)*GAMMA(I,J)*RE.P.-1.5+PSI(I+1,J)
1*MINUSI(I)+
2PSI(I-1,J)*PLUS2I(I)+ARE*(PSI(I,J+1)+PSI(I,J-1))-PL2ARE*PSI(I
3,J))
NEXTXA  PSI(I,J)=PSI(I,J)+DELTA(I,J)
AFTERA  PRINT RESULTS A(K),PSI(0,0)...PSI(IMAX,JMAX),DELTA(0,0)...
1DELTA(IMAX,JMAX)
      END OF CONDITIONAL
      FUNCTION RETURN
      END OF FUNCTION
```

```

$COMPILE MAD, PRINT OBJECT, PUNCH OBJECT                                SUBUW001
      RCOMPUTE NEW U AND W VALUES, COMPUTE NEW GAMMA(I,0) VALUES
      EXTERNAL FUNCTION
      PROGRAM COMMON U,V,VSTAR,VPRIME,W,GAMMA,VSTILL, RE,  PSI,AAA
1,CEE,DEE,CAPB,CAPC,DXI2I,IDXISQ,IDXIDZ,IDXICU,OVER2I,MINUSI,PL
2US2I,OIDXI,OIDXIS,      H,G,A,IDX I, BB,DTAUD2,DXISQ,DXISQ2,DZE
3TSQ,DZETA2,DZETS2,DZSQI,DZETS4,PL2ARE,AOARE,DZETA6,DZET12,DXI
412,DXISQ1,DXI2,DXISQH,ARE,EPSI,BETA,DXI,DZETA,I,J,ITMAX,ITER
5, BB1, BB2, BB3, BBFINE, ISTART, JSTART, IEND, JEND
6, BB4, BB5, BB6, BB7, BB8, BB9
```

```
7,DIM,ANSW1,ANSW2,ANSW3,BETMAX,DBETA,DTAU,OLDATA,TAU,TAUMAX,DI
8TMAX,K,BEE,IMAX,JMAX,LIMAX,LJMAX,ENDBET
9,BBPSI,ENDTAU,SPACE
  DIMENSION U(1900,DIM),V(1900,DIM),VSTAR(1900,DIM),VPRIME(1900
1,DIM),W(1900,DIM),GAMMA(1900,DIM),GAMMAS(1900,DIM),GAMMAP(190
20,DIM),PSI(1900,DIM),DELTA(1900,DIM),AAA(250),CEE(250),DEE(25
30),CAPB(250),CAPC(250),DXI2I(250),IDXISQ(250),IDXZ(250),IDXI
4CU(250),OVER2I(250),MINUSI(250),PLUS2I(250),OIDXI(250),OIDXIS
5(250),H(50),G(50),A(11),IDXI(250)
6,DIM(3)
  EQUIVALENCE (VSTAR(0),GAMMAS(0)),(VPRIME(0),GAMMAP(0)),
1(GAMMAP(0),DELTA(0))
  INTEGER IMAX,JMAX,DITMAX,LIMAX,LJMAX
  INTEGER ISTART, JSTART, IEND, JEND
  INTEGER I,J,K,ITMAX,ITER
  VECTOR VALUES SPACE=$5HDXI= E13.6,7HDZETA= E13.6*$
  VECTOR VALUES ENDTAU=$5HTAU= E13.6,6HDTAU= E13.6*$
  VECTOR VALUES OLDDATA=$(2I3,5E13.6)*$
  VECTOR VALUES ENDBET=$6HBETA= E13.6*$
  VECTOR VALUES ANSW1=$(S2,I3,S1,I3,5E16.6)*$
  VECTOR VALUES ANSW2=$(2I3,5E13.6)*$
  VECTOR VALUES ANSW3=$1H6,S3,1HI,S3,1HJ,S10,3HPSI,S13,1HU,S14,
11HV,S15,1HW,S14,5HGAMMA//*$
  BOOLEAN VSTILL
  BOOLEAN BB,BB1,BB2,BB3,BB4,BB5,BB6,BB7,BB8,BB9
  BOOLEAN BBFINE
  BOOLEAN BBPSI
  ENTRY TO SUBUWG.
  WHENEVER BBFINE,TRANSFER TO SKIP
  THROUGH ORIGIN, FOR I=1,1,I.G.IMAX
ORIGIN  GAMMA(I,0)=OIDXI(I)*(8.0*PSI(I,1)-7.0*PSI(I,0)-PSI(I,2))/DZET
1S2
2*RE.P.1.5
SKIP  THROUGH NEXT1, FOR I=1,1,I.E.IMAX
  THROUGH NEXT1, FOR J=1,1,J.E.JMAX
  WHENEVER J.E.1
    U(I,1)=OIDXI(I)*(-2.0*PSI(I,0)-3.0*PSI(I,1)+6.0*PSI(I,2)-PSI(
1I,3))/DZETA6
  2*RE.P.1.5
    OR WHENEVER J.G.1.AND.J.L.LJMAX
    U(I,J)=OIDXI(I)*(PSI(I,J-2)-8.0*PSI(I,J-1)+8.0*PSI(I,J+1)-PSI
1(I,J+2))/DZET12
  2*RE.P.1.5
    OTHERWISE
    U(I,J)=OIDXI(I)*(2.0*PSI(I,J+1)+3.0*PSI(I,J)-6.0*PSI(I,J-1)+P
1SI(I,J-2))/DZETA6
  2*RE.P.1.5
    END OF CONDITIONAL
  WHENEVER I.E.1
    W(1,J)=-OIDXI(I)*(-2.0*PSI(0,J)-3.0*PSI(1,J)+6.0*PSI(2,J)-PSI
1(3,J))/(6.0*DXI)
  2*RE.P.1.5
    OR WHENEVER I.G.1.AND.I.L.LIMAX
    W(I,J)=-OIDXI(I)*(PSI(I-2,J)-8.0*PSI(I-1,J)+8.0*PSI(I+1,J)-PS
1I(I+2,J))/DXI12
  2*RE.P.1.5
    OTHERWISE
    W(I,J)=-OIDXI(I)*(2.0*PSI(I+1,J)+3.0*PSI(I,J)-6.0*PSI(I-1,J)+
1PSI(I-2,J))/(6.0*DXI)
```

```
2*RE.P.1.5
NEXT1   END OF CONDITIONAL
        THROUGH WZERO, FOR J=1,1,J.G.JMAX
WZERO   W(0,J)=(PSI(3,J)-2.0*PSI(2,J)-11.0*PSI(1,J))*DXISQ1/5.0
1*RE.P.1.5
        WHENEVER BB2, PRINT RESULTS U(0,0)...U(IMAX,JMAX),W(0,0)...
1W(IMAX,JMAX),GAMMA(0,0)...GAMMA(IMAX,JMAX)
        WHENEVER TAU .G.0.0
        WHENEVER BB7
        PRINT RESULTS U(0,0)...U(IMAX,JMAX),W(0,0)...W(IMAX,JMAX)
        END OF CONDITIONAL
        END OF CONDITIONAL
        FUNCTION RETURN
        END OF FUNCTION
```

```
$ COMPILE MAD, PRINT OBJECT, PUNCH OBJECT                                SUBV.001
RCOMPUTE VSTAR AND VPRIME
EXTERNAL FUNCTION
PROGRAM COMMON U,V,VSTAR,VPRIME,W,GAMMA,VSTILL, RE, PSI,AAA
1,CEE,DEE,CAPB,CAPC,DXI2I,IDXISQ,IDXZ,IDXICU,OVER2I,MINUSI,PL
2US2I,OIDX,OIDXIS, H,G,A,IDX,BB,DTAUD2,DXISQ,DXISQ2,DZE
3TSQ,DZETA2,DZETS2,DZSQI,DZETS4,PL2ARE,AOARE,DZETA6,DZET12,DXI
412,DXISQ1,DXI2,DXISQH,ARE,EPSI,BETA,DXI,DZETA,I,J,ITMAX,ITER
5,BB1,BB2,BB3,BBFINE,ISTART,JSTART,IEND,JEND
6,BB4,BB5,BB6,BB7,BB8,BB9
7,DIM,ANSW1,ANSW2,ANSW3,BETMAX,DBETA,DTAU,OLDATA,TAU,TAUMAX,DI
8TMAX,K,BEE,IMAX,JMAX,LIMAX,LJMAX,ENDBET
9,BBPSI,ENDTAU,SPACE
DIMENSION U(1900,DIM),V(1900,DIM),VSTAR(1900,DIM),VPRIME(1900
1,DIM),W(1900,DIM),GAMMA(1900,DIM),GAMMAS(1900,DIM),GAMMAP(190
20,DIM),PSI(1900,DIM),DELTA(1900,DIM),AAA(250),CEE(250),DEE(25
30),CAPB(250),CAPC(250),DXI2I(250),IDXISQ(250),IDXZ(250),IDXI
4CU(250),OVER2I(250),MINUSI(250),PLUS2I(250),OIDX(250),OIDXIS
5(250),H(50),G(50),A(11),IDX(250)
6,DIM(3)
EQUIVALENCE (VSTAR(0),GAMMAS(0)),(VPRIME(0),GAMMAP(0)),
1(GAMMAP(0),DELTA(0))
INTEGER IMAX,JMAX,DITMAX,LIMAX,LJMAX
INTEGER I,J,K,ITMAX,ITER
VECTOR VALUES SPACE=$5HDXI= E13.6,7HDZETA= E13.6*$
VECTOR VALUES ENDTAU=$5HTAU= E13.6,6HDTAU= E13.6*$
VECTOR VALUES OLDDATA=$(2I3,5E13.6)*$
VECTOR VALUES ENDBET=$6HBETA= E13.6*$
VECTOR VALUES ANSW1=$(S2,I3,S1,I3,5E16.6)*$
VECTOR VALUES ANSW2=$(2I3,5E13.6)*$
VECTOR VALUES ANSW3=$1H6,S3,1HI,S3,1HJ,S10,3HPSI,S13,1HU,S14,
11HV,S15,1HW,S14,5HGAMMA//*$
BOOLEAN VSTILL
BOOLEAN BB,BB1,BB2,BB3,BB4,BB5,BB6,BB7,BB8,BB9
INTEGER ISTART, JSTART, IEND, JEND
BOOLEAN BBFINE
BOOLEAN BBPSI
ENTRY TO SUBV.
THROUGH REPEAT, FOR I=0,1,I.G.IMAX
THROUGH REPEAT, FOR J=0,1,J.G.JMAX
VSTAR(IMAX,J)=V(IMAX,J)
```

```

VSTAR(I,0)=V(I,0)
VSTAR(I,JMAX)=V(I,JMAX)
REPEAT
VSTAR(0,J)=V(0,J)
  THROUGH VEE1, FOR J=1,1,J.G.LJMAX
  THROUGH VEE3, FOR I=1,1,I.G.LIMAX
  WHENEVER I.E.1
    CAPB(1)=DTAUD2+DXISQ2*RE
    CAPC(1)=(V(1,J-1)*(W(1,J)/DZETA2+DZSQI*RE)+V(1,J)*(DTAUD2-
1U(1,J)/DXI-(DZETS4+DXISQ1)*RE)+V(1,J+1)*(-W(1,J)/DZETA2+DZSQI
2*RE))/CAPB(1)
    CEE(1)=U(1,J)/DXI2-(DXISQ1+DXISQH)*RE
    OR WHENEVER I.L.LIMAX .AND. I.G.1
    AAA(I)=-U(I,J)/DXI2-(DXISQ1-DXI2I(I))*RE
    CEE(I)=U(I,J)/DXI2-(DXISQ1+DXI2I(I))*RE
    DEE(I)=V(I,J-1)*(W(I,J)/DZETA2+DZSQI*RE)+V(I,J)*(DTAUD2-
1U(I,J)/DXI(I)-(DZETS4+1.0/IDXISQ(I))*RE)+V(I,J+1)*(-W(I,J)/
2DZETA2+DZSQI*RE)
    OTHERWISE
    AAA(I)=-U(I,J)/DXI2-(DXISQ1-DXI2I(I))*RE
    DEE(I)=-V(I+1,J)*(U(I,J)/DXI2-(DXISQ1+DXI2I(I))*RE)+V(I,J-1)*
1(W(I,J)/DZETA2+DZSQI*RE)+V(I,J)*(DTAUD2-U(I,J)/DXI(I)-(DZETS
24+1.0/IDXISQ(I))*RE)+V(I,J+1)*(-W(I,J)/DZETA2+DZSQI*RE)
    END OF CONDITIONAL
    BEE=DTAUD2+DXISQ2*RE
    WHENEVER I.NE.1
    CAPB(I)=BEE-AAA(I)*CEE(I-1)/CAPB(I-1)
    CAPC(I)=(DEE(I)-AAA(I)*CAPC(I-1))/CAPB(I)
VEE3
    END OF CONDITIONAL
    THROUGH VEE1, FOR I=LIMAX,-1,I.L.1
    WHENEVER I.E.LIMAX,VSTAR(I,J)=CAPC(I)
VEE1
    WHENEVER I.L.LIMAX,VSTAR(I,J)=CAPC(I)-(CEE(I)*VSTAR(I+1,J))/
1CAPB(I)
    WHENEVER BB3, PRINT RESULTS VSTAR(0,0)...VSTAR(IMAX,JMAX)
    THROUGH REPEAT, FOR I=0,1,I.G.IMAX
    THROUGH REPEAT, FOR J=0,1,J.G.JMAX
    VPRIME(I,0)=V(I,0)
    VPRIME(I,JMAX)=V(I,JMAX)
    VPRIME(0,J)=V(0,J)
REPEAT
    VPRIME(IMAX,J)=VSTAR(IMAX,J)
    THROUGH VEE2, FOR I=1,1,I.G.LIMAX
    THROUGH VEE4, FOR J=1,1,J.G.LJMAX
    WHENEVER J.E.1
    CAPB(J)=DTAUD2+DZETS4*RE
    CAPC(1)=(-V(I,0)*(-W(I,1)/DZETA2-DZSQI*RE)+VSTAR(I-1,1)*(U(I,
11)/DXI2+(DXISQ1-DXI2I(I))*RE)+VSTAR(I,1)*(DTAUD2-DXISQ2*RE)
2+VSTAR(I+1,1)*(-U(I,1)/DXI2+(DXISQ1+DXI2I(I))*RE))/CAPB(1)
    CEE(1)=W(I,1)/DZETA2-DZSQI*RE
    OR WHENEVER J.L.LJMAX .AND. J.G.1
    AAA(J)=-W(I,J)/DZETA2-DZSQI*RE
    CEE(J)=W(I,J)/DZETA2-DZSQI *RE
    DEE(J)=VSTAR(I-1,J)*(U(I,J)/DXI2+(DXISQ1-DXI2I(I))*RE)
1+VSTAR(I,J)*(DTAUD2-RE*D
2XISQ2)+VSTAR(I+1,J)*(-U(I,J)/DXI2+(DXISQ1+DXI2I(I))*RE)+V(I,J
3)*(-U(I,J)/DXI(I)-RE/IDXISQ(I))
    OTHERWISE
    AAA(J)=-W(I,J)/DZETA2-DZSQI*RE
    DEE(J)=-V(I,J+1)*(W(I,J)/DZETA2-DZSQI*RE)+VSTAR(I-1,J)*(U(I,J
1)/DXI2+(DXISQ1-DXI2I(I))*RE)+VSTAR(I,J)*(DTAUD2-DXISQ2*RE)+
2VSTAR(I+1,J)*(-U(I,J)/DXI2+(DXISQ1+DXI2I(I))*RE)+V(I,J)*(-U(I

```

```
3,J)/IDXI(I)-OIDXIS(I)*RE)
  END OF CONDITIONAL
  BEE=DTAUD2+DZETS4*RE
  WHENEVER J.NE.1
  CAPB(J)=BEE-AAA(J)*CEE(J-1)/CAPB(J-1)
  CAPC(J)=(DEE(J)-AAA(J)*CAPC(J-1))/CAPB(J)
VEE4  END OF CONDITIONAL
      THROUGH VEE2, FOR J=LJMAX,-1,J.L.1
      WHENEVER J.E.LJMAX, VPRIME(I,J)=CAPC(J)
VEE2  WHENEVER J.L.LJMAX, VPRIME(I,J)=CAPC(J)-CEE(J)*VPRIME(I,J+1)/
1CAPB(J)
      WHENEVER BB3, PRINT RESULTS VPRIME(0,0)...VPRIME(IMAX,JMAX)
      BB3=BB
      THROUGH VEEF, FOR I=0,1,I.G.IMAX
      THROUGH VEEF, FOR J=0,1,J.G.JMAX
VEEF  V(I,J)=VPRIME(I,J)
      FUNCTION RETURN
      END OF FUNCTION
```

```
$COMPILE MAD,PRINT OBJECT, PUNCH OBJECT                                SUBG.001
RCOMPUTE GAMMAS AND GAMMAP
EXTERNAL FUNCTION
PROGRAM COMMON U,V,VSTAR,VPRIME,W,GAMMA,VSTILL, RE,  PSI,AAA
1,CEE,DEE,CAPB,CAPC,DXI2I,IDXISQ,IDXIDZ,IDXICU,OVER2I,MINUSI,PL
2US2I,OIDXI,OIDXIS,      H,G,A,IDX I,BB,DTAUD2,DXISQ,DXISQ2,DZE
3TSQ,DZETA2,DZETS2,DZSQI,DZETS4,PL2ARE,AOARE,DZETA6,DZET12,DXI
4I2,DXISQ1,DXI2,DXISQH,ARE,EPSI,BETA,DXI,DZETA,I,J,ITMAX,ITER
5,BB1,BB2,BB3,BBFINE,ISTART,JSTART,IEND,JEND
6,BB4,BB5,BB6,BB7,BB8,BB9
7,DIM,ANSW1,ANSW2,ANSW3,BETMAX,DBETA,DTAU,OLDATA,TAU,TAUMAX,DI
8TMAX,K,BEE,IMAX,JMAX,LIMAX,LJMAX,ENDBET
9,BBPSI,ENDTAU,SPACE
  DIMENSION U(1900,DIM),V(1900,DIM),VSTAR(1900,DIM),VPRIME(1900
1,DIM),W(1900,DIM),GAMMA(1900,DIM),GAMMAS(1900,DIM),GAMMAP(190
20,DIM),PSI(1900,DIM),DELTA(1900,DIM),AAA(250),CEE(250),DEE(25
30),CAPB(250),CAPC(250),DXI2I(250),IDXISQ(250),IDXIDZ(250),IDXI
4CU(250),OVER2I(250),MINUSI(250),PLUS2I(250),OIDXI(250),OIDXIS
5(250),H(50),G(50),A(11),IDX I(250)
6,DIM(3)
  EQUIVALENCE (VSTAR(0),GAMMAS(0)),(VPRIME(0),GAMMAP(0)),
1(GAMMAP(0),DELTA(0))
  INTEGER IMAX,JMAX,DITMAX,LIMAX,LJMAX
  INTEGER I,J,K,ITMAX,ITER
  INTEGER ISTART, JSTART, IEND, JEND
  BOOLEAN BBFINE
  VECTOR VALUES SPACE=$5HDXI= E13.6,7HDZETA= E13.6*$
  VECTOR VALUES ENDTAU=$5HTAU= E13.6,6HDTAU= E13.6*$
  VECTOR VALUES OLDDATA=$(2I3,5E13.6)*$
  VECTOR VALUES ENDBET=$6HBETA= E13.6*$
  VECTOR VALUES ANSW1=$(S2,I3,S1,I3,5E16.6)*$
  VECTOR VALUES ANSW2=$(2I3,5E13.6)*$
  VECTOR VALUES ANSW3=$1H6,S3,1HI,S3,1HJ,S10,3HPSI,S13,1HU,S14,
11HV,S15,1HW,S14,5HGAMMA//*$
  BOOLEAN VSTILL
  BOOLEAN BB,BB1,BB2,BB3,BB4,BB5,BB6,BB7,BB8,BB9
```

```

BOOLEAN BBPSI
ENTRY TO SUBG.
THROUGH REPEAT, FOR I=0,1,I.G.IMAX
THROUGH REPEAT, FOR J=0,1,J.G.JMAX
GAMMAS(0,J)=GAMMA(0,J)
GAMMAS(IMAX,J)=GAMMA(IMAX,J)
GAMMAS(I,JMAX)=GAMMA(I,JMAX)
REPEAT GAMMAS(I,0)=GAMMA(I,0)
THROUGH GEE1, FOR J=1,1,J.G.LJMAX
THROUGH GEE3, FOR I=1,1,I.G.LIMAX
WHENEVER I.E.1
CAPB(1)=DTAUD2+DXISQ2*RE
CAPC(1)=(GAMMA(1,J-1)*(W(1,J)/DZETA2+DZSQI*RE)+GAMMA(1,J)*(
1DTAUD2+U(1,J)/DXI-(DZETS4+DXISQ1)*RE)+GAMMA(1,J+1)*(-W(1,J)/
2DZETA2+DZSQI*RE)+(VPRIME(1,J)/IDXDZ(I))*(VPRIME(1,J+1)-VPRIME
3(1,J-1)))/CAPB(1)
CEE(1)=U(1,J)/DXI2-(DXISQ1+DXISQH)*RE
OR WHENEVER I.L.LIMAX .AND. I.G.1
AAA(I)=-U(I,J)/DXI2-(DXISQ1-DXI2I(I))*RE
CEE(I)=U(I,J)/DXI2-(DXISQ1+DXI2I(I))*RE
DEE(I)=GAMMA(I,J-1)*(W(I,J)/DZETA2+DZSQI*RE)+GAMMA(I,J)*(DTAU
1D2+U(I,J)/IDXI(I)-(DZETS4+OIDXIS(I))*RE)+GAMMA(I,J+1)*(-W(I,J
2)/DZETA2+DZSQI*RE)+(VPRIME(I,J)/IDXDZ(I))*(VPRIME(I,J+1)-VPRI
3ME(I,J-1))
OTHERWISE
AAA(I)=-U(I,J)/DXI2-(DXISQ1-DXI2I(I))*RE
DEE(I)=-GAMMA(I+1,J)*(U(I,J)/DXI2-(DXISQ1+DXI2I(I))*RE)+
1GAMMA(I,J-1)*(W(I,J)/DZETA2+DZSQI*RE)+GAMMA(I,J)*(DTAUD2+U(
2I,J)*OIDXI(I)-(DZETS4+OIDXIS(I))*RE)+GAMMA(I,J+1)*(-W(I,J)/
3DZETA2+DZSQI*RE)+(VPRIME(I,J)/IDXDZ(I))*(VPRIME(I,J+1)
4-VPRIME(I,J-1))
END OF CONDITIONAL
BEE=DTAUD2+DXISQ2*RE
WHENEVER I.NE.1
CAPB(I)=BEE-AAA(I)*CEE(I-1)/CAPB(I-1)
CAPC(I)=(DEE(I)-AAA(I)*CAPC(I-1))/CAPB(I)
GEE3 END OF CONDITIONAL
THROUGH GEE1, FOR I=LIMAX,-1,I.L.1
WHENEVER I.E.LIMAX
GAMMAS(I,J)=CAPC(I)
OR WHENEVER I.L.LIMAX
GAMMAS(I,J)=CAPC(I)-CEE(I)*GAMMAS(I+1,J)/CAPB(I)
GEE1 END OF CONDITIONAL
WHENEVER BB1, PRINT RESULTS GAMMAS(0,0)...GAMMAS(IMAX,JMAX)
THROUGH REPEAT, FOR I=0,1,I.G.IMAX
THROUGH REPEAT, FOR J=0,1,J.G.JMAX
GAMMAP(0,J)=GAMMAS(0,J)
GAMMAP(I,0)=GAMMAS(I,0)
GAMMAP(IMAX,J)=GAMMAS(IMAX,J)
REPEAT GAMMAP(I,JMAX)=GAMMAS(I,JMAX)
THROUGH GEE2, FOR I=1,1,I.G.LIMAX
THROUGH GEE4, FOR J=1,1,J.G.LJMAX
WHENEVER J.E.1
CAPB(1)=DTAUD2+DZETS4*RE
CEE(1)=W(I,1)/DZETA2-DZSQI*RE
CAPC(1)=(GAMMAS(I-1,1)*(U(I,1)/DXI2+(DXISQ1-DXI2I(I))*RE)+
1GAMMAS(I,1)*(DTAUD2-DXISQ2*RE)+GAMMAS(I+1,1)*(-U(I,1)/DXI2+(
2DXISQ1+DXI2I(I))*RE)+GAMMA(I,1)*(U(I,1)/IDXI(I)-OIDXIS(I)*RE)
3+(V(I,1)/IDXDZ(I))*(V(I,2)-V(I,0))+GAMMAP(I,0)*(DZSQI*RE+W(I,

```

```
41)/DZETA2))/CAPB(1)
  OR WHENEVER J.L.LJMAX.AND.J.G.1
  AAA(J)=-W(I,J)/DZETA2-DZSQI*RE
  CEE(J)=W(I,J)/DZETA2-DZSQI*RE
  DEE(J)=GAMMAS(I-1,J)*(U(I,J)/DXI2+(DXISQ1-DXI2I(I))*RE)+
1GAMMAS(I,J)*(DTAUD2-DXISQ2*RE)+GAMMAS(I+1,J)*(-U(I,J)/DXI2+(
2DXISQ1+DXI2I(I))*RE)+GAMMA(I,J)*(U(I,J)/IDXI(I)-OIDXIS(I)*RE)
3+(V(I,J)/IDXZ(I))*(V(I,J+1)-V(I,J-1))
  OTHERWISE
  CEE(J)=W(I,J)/DZETA2-DZSQI*RE
  AAA(J)=-W(I,J)/DZETA2-DZSQI*RE
  DEE(J)=GAMMAS(I-1,J)*(U(I,J)/DXI2+(DXISQ1-DXI2I(I))*RE)+
1GAMMAS(I,J)*(DTAUD2-DXISQ2*RE)+GAMMAS(I+1,J)*(-U(I,J)/DXI2+(
2DXISQ1+DXI2I(I))*RE)+GAMMA(I,J)*(U(I,J)/IDXI(I)-OIDXIS(I)*RE)
3+(V(I,J)/IDXZ(I))*(V(I,J+1)-V(I,J-1))
4-GAMMA(I,J+1)*(W(I,J)/DZETA2-RE*DZSQI)
  END OF CONDITIONAL
  BEE=DTAUD2+DZETS4*RE
  WHENEVER J.NE.1
  CAPB(J)=BEE-AAA(J)*CEE(J-1)/CAPB(J-1)
  CAPC(J)=(DEE(J)-AAA(J)*CAPC(J-1))/CAPB(J)
GEE4  END OF CONDITIONAL
  THROUGH GEE2, FOR J=LJMAX,-1,J.L.1
  WHENEVER J.E.LJMAX
  GAMMAP(I,J)=CAPC(J)
  OR WHENEVER J.L.LJMAX
  GAMMAP(I,J)=CAPC(J)-CEE(J)*GAMMAP(I,J+1)/CAPB(J)
GEE2  END OF CONDITIONAL
  WHENEVER BB1, PRINT RESULTS GAMMAP(0,0)...GAMMAP(IMAX,JMAX)
  BB1=BB
  THROUGH GEEF, FOR I=0,1,I.G.IMAX
  THROUGH GEEF, FOR J=0,1,J.G.JMAX
GEEF  GAMMA(I,J)=GAMMAP(I,J)
  FUNCTION RETURN
  END OF FUNCTION
```


BIBLIOGRAPHY

1. Barua, S. N., "A Source in a Rotating Fluid," Q. Journ. Mech. Appl. Math., 8, (1955) 22.
2. Birkhoff, G., Personal communication.
3. Birkhoff, G., Varga, R. S., Young, D., "Alternating Direction Implicit Methods," Advances in Computers, 3, Academic Press Inc., New York, 1962.
4. Bödewadt, U. T., "Die Drehströmung über festen Grunde," ZAMM, 20, (1940) 241.
5. Cochran, W. G., "The Flow Due to a Rotating Disc," Proc. Cambridge Phil. Soc., 30, (1934) 365.
6. Fromm, J. E., Harlow, F. H., "Numerical Solution of the Problem of Vortex Street Development," Physics of Fluids, 6, (July, 1963) 7.
7. Long, R. R., "A Vortex in an Infinite Viscous Fluid," J. Fluid Mech., 11, 1961.
8. Long, R. R., "Sources and Sink at the Axis of a Rotating Liquid," Q. Journ. Mech. Appl. Math., 9, 1956.
9. Rosenblat, S., "Flow Between Torsionally Oscillating Discs," J. Fluid Mech., 8, July, 1960.
10. Schlichting, H., Boundary Layer Theory, McGraw-Hill, New York, 1960.
11. Stewartson, K., Proc. Camb. Phil. Soc., 49, 333.
12. Stewartson, K., "On Almost Rigid Rotations," J. Fluid Mech., 3, 1957.
13. Taylor, G. I., "The Boundary Layer in the Converging Nozzle of a Swirl Atomizer," Q. Journ. Mech. Appl. Math., 3, 1950.
14. Von Karman, T., "Laminare und Turbulente Reibung," ZAMM, 1, (1921) 233-252; NACA T. M., (1946) 1092.
15. Wilkes, J. O., The Finite Difference Computation of Natural Convection in an Enclosed Rectangular Cavity, Ph.D. Thesis, The University of Michigan, 1963.